12-2015

EFFECTS OF PHARMACOLOGICAL AND GENETIC DISRUPTION OF CHEMOKINE RECEPTOR CXCR4 IN B-CELL ACUTE LYMPHOBLASTIC LEUKEMIA

Shubhchintan Randhawa

EFFECTS OF PHARMACOLOGICAL AND GENETIC DISRUPTION OF CHEMOKINE RECEPTOR CXCR4 IN B-CELL ACUTE LYMPHOBLASTIC LEUKEMIA

by

Shubhchintan Randhawa, M.Sc.

APPROVED:

_____
Jan A. Burger, M.D. Ph.D.
Advisory Professor

_____
Richard E. Davis, M.D.

_____
Zeev Estrov, M.D.

_____
Varsha Gandhi, Ph.D.

_____
Marina Konopleva, M.D. Ph.D.

APPROVED:

_____
Dean, The University of Texas
Graduate School of Biomedical Sciences at Houston

EFFECTS OF PHARMACOLOGICAL AND GENETIC DISRUPTION OF CXCR4 CHEMOKINE RECEPTOR IN B-CELL ACUTE LYMPHOBLASTIC LEUKEMIA

A

DISSERTATION

Presented to the Faculty of
The University of Texas
Health Science Center at Houston
and
The University of Texas
MD Anderson Cancer Center
Graduate School of Biomedical Sciences
in Partial Fulfillment

of the Requirements

for the Degree of

DOCTOR OF PHILOSOPHY

by

Shubhchintan Randhawa, M.Sc.
Houston, Texas

Date of Graduation *(December, 2015)*

Dedication

To my husband who has been so patient

To my mothers who have always been my inspiration

And to my fathers and brother who have always provided comic relief

Acknowledgements

I would like to extend my deepest gratitude towards my Ph.D. advisor, Dr. Jan Burger. I would like to thank him for giving me the opportunity to work in his lab and his support and mentorship through these years. I hold dearly the prospect of helping cancer patients through my time at the bench and Dr. Burger's lab and guidance gave me an ideal opportunity to do valuable translational research that would hopefully, someday, help leukemia patients.

I would also like to thank Dr. Gandhi who has been a constant pillar of support since the day I joined Experimental Therapeutics Academic Department. In addition to being an exceptional academic guide, through ETAP, she has also provided me with ample opportunities to develop my leadership and management skills. I could not have reached this milestone without you.

I would also like to thank all my past and present committee members (Dr. Calin, Dr. Davis, Dr. Estrov, Dr. Gandhi, Dr. McIntyre, Dr. Mehta, Dr. Konopleva, Dr. Vega-Vazquez) for teaching me how to think, which really is the point of the Ph.D. Thank you Dr. Konopleva for the *in vivo* experiments and your clinical insights. Thank you Dr. Davis for genetic knockout experiments and your invaluable input in the project and making me see meaning even in data I thought were worthless.

Thank you so much to all my past and current lab-mates, Stefan Köehrer, Elisa Ten Hacken, Mariela Campbell, Julia Castillo, Ekaterina

Kim, Natalie Rosin, and Qingsong Yin for helping me through countless failed experiments and blunders! I learnt something new with each one.

Thank you Dr. Dipanjan Ghosh for your guidance with the CRSIPR-Cas9 knockout and Dr. Byung-Sik Cho for the *in vivo* experiments.

Thank you Experimental Therapeutics Academic Program for giving me so many opportunities to develop interpersonal and leadership skills and thank you Lidia Vogelsang for such enthusiasm in each task we tried to complete for ETAP. Also, thank you to all my fellow students for making the ride fun all along and making me realize that your experiments were failing too, and that I am not alone.

Thank you Aarthi Goverdhan and Dr. Maitri Shah for always being there. I really cannot imagine how this PhD would have been if you weren't there through the moderately peaking highs and terrifyingly deep lows.

Thank you Kunal for helping me get through the MSc, couldn't have done the PhD without that!

Above all, thank you Gaurav, Ma and Pa for that, which words cannot describe.

EFFECTS OF PHARMACOLOGICAL AND GENETIC DISRUPTION OF CXCR4 CHEMOKINE RECEPTOR IN B-CELL ACUTE LYMPHOBLASTIC LEUKEMIA

Shubhchintan Randhawa, M.Sc

Supervisory Professor: Jan A. Burger, M.D. Ph.D.

The CXCR4 chemokine receptor plays a pivotal role in homing and retention of B-cell Acute Lymphoblastic Leukemia cells to bone marrow niches. The bone marrow stromal cells (BMSCs) constitutively secrete the CXCR4 ligand CXCL12, thus attracting leukemia cells and protecting them from cytotoxic drugs, a mechanism that might be responsible for minimal residual disease after conventional chemotherapy against B-ALL. Indeed, in this study we observed that B-ALL cells that had migrated beneath the BMSCs were highly resistant to chemotherapeutic drugs. Inhibition of CXCR4 to disrupt this interaction presents itself as an attractive target to overcome bone marrow derived drug resistance mechanisms. We observed that not only did pharmacological inhibition of CXCR4 significantly reduce chemotaxis and migration of B-ALL cells beneath BMSCs, it significantly enhanced drug-induced cytotoxicity of Cyclophosphamide, Dexamethasone and Vincristine. Furthermore, we report an *in vitro* and *in vivo* CXCR4 genetic deletion model of B-ALL cells generated using the CRISPR-Cas9 gene editing technology. The CXCR4 Knockout cells display defective chemotaxis and migration

beneath BMSCs. Moreover, the BMSCs fail to rescue the CXCR4 Knockout cells from drug-induced cytotoxicity. Also, non-irradiated NOD/SCID/IL-2rγnull mice injected with CXCR4 Knockout cells displayed significantly lower leukemia burden, bone marrow infiltration and survival as compared to mice injected with CXCR4 wild type cells. Collectively, these findings provide a rationale for clinical targeting of CXCR4 in patients with B-ALL.

TABLE OF CONTENTS

LIST OF ILLUSTRATIONS

LIST OF TABLES

LIST OF ABBREVIATIONS

In order of appearance in text

B-ALL	B-Cell Acute Lymphoblastic Leukemia
CLL	Chronic Lymphoblastic Leukemia
TKI	Tyrosine Kinase Inhibitor
CNS	Central Nervous System
BMSCs	Bone Marrow Stromal Cells
MRD	Minimal Residual Disease
HSC	Hematopoietic Stem Cells
AIEOP-BFM	Associazione Italiana di Ematologia Oncologia Pediatrica and the Berlin-Frankfurt-Münster
NOD/SCID	Non-obese diabetic/Severe combined immunodeficiency
VLA-4	Very Late Antigen – 4
MAPK	Mitogen Activated Protein Kinase
BM	Bone Marrow

HIV	Human Immunodeficiency Virus
ICL	Intra-Cellular Loop
ECL	Extra-Cellular Loop
GDP	Guanosine diphosphate
GTP	Guanosine triphosphate
PI3K	Phosphoinositide-3 Kinase
NRF-1	Nuclear Respiratory Factor-1
YY1	Ying Yang 1
AMP	Adenosine Monophosphate
IL	Interleukin
TNF	Tumor Necrosis Factor
IFN	Interferon
HIF	Hypoxia Inducible Factor
NFκB	Nuclear Factor Kappa B
TGF1	Transforming Growth Factor
FGF	Fibroblast Growth Factor

VEGF	Vascular Endothelial Growth Factor
EGF	Epidermal Growth Factor
VHL	Von Hippel-Lindau Tumor Suppressor
AIP4	Atrophin-1 Interacting Protein 4
SDF1	Stromal cell-Derived Factor 1
CAM-DR	Cell Adhesion Mediated Drug Resistance
FDA	Food and Drug Admnistration
G-CSF	Granulocyte-Colony Stimulating Factor
PE	Phycoerythrin
APC	Allophycocyanin
FITC	Fluoroscein Isothiocyanate
FBS	Fetal Bovine Serum
MEM	Minimal Essential Medium
FACS	Fluorescence Activated Cell Sorting
BSA	Bovine Serum Albumin
$DiOC_6$	3,3'-dihexyloxacarbocyanine iodide

PI	Propidium Iodide
CRISPR	Clustered Regularly Interspaced Short Palindromic Repeats
Cas9	CRISPR Associated Nuclease
MACS	Magnetic Activated Cell Sorting
GFP	Green Fluorescent Protein
BLI	Bio-luminescent Imaging
SEM	Standard Error Mean
PEP	Pseudoemperipolesis
CR	Complete Response
CRp	Complete Response with incomplete platelet recovery
PR	Partial Response
RFS	Relapse Free Survival
OS	Overall Survival
SAS	Statistical Analysis System

MFIR	Mean Fluorescent Intensity Ratio
DNA	Deoxyribonucleic acid
RNA	Ribonucleic Acid
PAM	Protospacer Adjacent Motif
4HC	4-Hydroperoxy Cyclophosphamide
DEX	Dexamethasone
VIN	Vincristine
BM	Bone Marrow
PB	Peripheral Blood
WBC	White Blood Cells
LDH	Lactate Dehydrogenase
AUG BFM	Augmented Berlin-Frankfurt-Münster regimen
HCMAD	Hyper-fractionated Cyclophosphamide, liposomal Vincristine (Marqibor®), Doxorubicin, Dexamethasone
HCVAD	Hyper-fractionated Cyclophosphamide, Vincristine, Doxorubicin, and Dexamethasone

CI	Confidence Interval
Hgb	Hemoglobin
PLT	Platelets
Alb	Albumin

Chapter 1

~ *Introduction* ~

Leukemia represents a group of heterogeneous diseases that can be classified into various groups. There are two major ways that are used to classify the disease. First, it is divided according to the cell type has developed cancer: myeloid or lymphoid. Secondly, it is divided based upon the pathogenesis of the disease: acute or chronic. As the name suggests, leukemias with rapid aggressive onset are grouped as acute and the ones with prolonged asymptomatic development of the disease are grouped as chronic.

Consequently, there are four major groups of leukemia's:

- Acute Lymphoblastic Leukemia
- Acute Myeloid Leukemia
- Chronic Lymphoblastic Leukemia
- Chronic Myeloid Leukemia

The classification shown above, however, is a rather simplistic division of this complex disease and other types of leukemia do exist. Additionally, each of these types is further divided into sub-categories. For example, Acute Lymphoblastic Leukemia can belong to either B cell or T cell lineage. The present study is an investigation into therapeutic agents that may help overcome relapse in patients with B- Cell Acute Lymphoblastic Leukemia.

Acute Lymphoblastic Leukemia

Epidemiology, pathology and morphology

B-cell Acute lymphoblastic Leukemia (B-ALL) is characterized by monoclonal and/or oligoclonal expansion of lymphoid progenitor cells due to somatic mutations(1). Malignant progenitor cells rapidly accumulate in the bone marrow, supersede normal hematopoiesis and result in neutropenia, anemia, thrombocytopenia and dissemination of B-ALL cells into peripheral blood. Majority of diagnosed adult ALL, about 75%, belong to the B-lineage and approximately half of those are pre-B ALL(2). Apart from the bone marrow, the central nervous system (CNS) is a major site of involvement comprising about 8% of adult patients at presentation and relapse of disease(3).

Approximately 6000 new patients are diagnosed annually and about 1400 individuals succumb to the disease in the United States (4). In United States, ALL accounts for about 12% of all leukemias diagnosed. It is the most common type of cancer in patients below 15 years, constituting about 25% of all pediatric cancers and 75% of all pediatric leukemias. Additionally, 20% of all adult acute leukemias are ALL. The disease is characterized by male predominance and bimodal age incidence peaking at 1-4 years and >60 years(4).

ALL cells display lack of differentiation and a diffused chromatin structure. Leukemic cells are also characterized by one or more nucleoli and basophilic cytoplasm. However, it is molecular immunophetyping by flow cytometry that is primarily used to diagnose the disease. For example, ALL cells from the B-lineage typically lack myeloperoxidase (a marker found in myeloid cells).

Genetic Aberrations in B-ALL

Understanding of disturbed gene expression levels and novel gene fusion transcripts has significantly improved our knowledge of ALL progression. Above thirty non-random translocations have been observed in ALL. The pre-dominant mutation in ALL involves the *BCR-ABL* gene re-arrangement that gives rise to the 'Philadelphia chromosome', which is found in about 20% of adult ALL cases. The fusion gene transcript is commonly 190kDa in ALL as compared to 210kDa in Chronic Lymphocytic Leukemia (CLL). The identification of the fusion and gene and its mechanism has allowed development of Tyrosine Kinase Inhibitors (TKI) for Ph+ leukemias (5).

Apart from these structural abnormalities, ALL cells display numerical abnormalities in their chromosomes. Hyperdiploidy is observed in about a third of all pediatric ALLs and is associated with a favorable outcome whereas 15% adult cases present hyperdiploidy and association with a positive outcome is less pronounced. Hypodiploidy is

observed in about 2.8% of ALL cases presented is associated with a worse outcome(1).

Treatment

Treatment for B-ALL typically comprises of three phases, namely, remission-induction, consolidation or intensification and maintenance or continuation therapy. After the induction and consolidation therapies, some high-risk patients are given stem-cell transplantation(2, 3).

The aim of the remission-induction therapy is to eliminate the bulk (99%) of leukemic cell burden from the patient and to restore healthy performance status and normal hematopoiesis. A three-drug induction approach is typically used for standard risk pediatric patients; it contains a glucocorticoid (dexamethasone or prednisone), Vincristine, and a third drug (which can be either asparaginase, Anthracycline or both). For high-risk children and all adult patients, four or more drugs are used as a remission induction therapy. The exception to this treatment regimen is patients with mature B-ALL where the induction therapy includes cytarabine, high-dose methotrexate and cyclophosphamide. Additionally, the rate of remission-induction, disease free survival and overall quality of life of Philadelphia chromosome positive patients has been significantly improved by the addition of Imatinib mesylate to the induction phase. Clinical remission can now be achieved in up to 93% of adult and 99% of pediatric ALL patients.

The aim of the intensification therapy is to eliminate residual drug-resistant cells to decrease the relapse risk. Although the importance of this phase of treatment is widely accepted, there is little unanimity in the duration and regimen. Agents that are commonly used in this phase are Vincristine, high-dose methotrexate with mercaptopurine and corticosteroid with high-dose asparaginase. A re-induction therapy with agents used in the previous phase is also frequently done.

The most intensive phase of treatment is the hematopoietic stem cell transplantation, used only for patients with a high-risk prognosis or poor response to first line therapy owing to significant morbidity and mortality associated with the treatment.

For reasons yet unknown, continuation therapy is required by B-ALL patients to prevent relapse. Therefore, all patients are prescribed chemotherapy for about two years. A daily dose of methotrexate and mercaptopurine is commonly used as the backbone of continuation therapy.

Some studies report up to 30-40% initial relapses owing to Central Nervous System (CNS) involvement, identified primarily by presence of leukemic cells in the cerebrospinal fluid. Other factors such as high-risk genetic abnormalities and hyper-leukocytosis are also associated with

CNS involvement. Cranial irradiation is used in a low percentage of patients due to complications associated with the procedure.

Response rates

Discovery of new drugs and refinement of treatment regimens have led to a 5 year survival rate of 90% in patients below 15 years of age(6). Keeping in view this particular statistic and the fact that a lot these patients will go on to live productive lives as long-term cancer survivors, it is an attractive temptation to classify B-ALL as a cancer that has been cured. The biggest fallacy of this statement would be that it fails to accommodate the poor prognosis of adult patients, the cost, complexity and morbidity associated with current multi-agent therapies in use. Furthermore, our current model of ALL treatment is based primarily on chemotherapeutic agents and does not take into account our rapidly increasing knowledge of and ability to analyze genetic/epigenetic abnormalities in individual patients and translate them into improved diagnostics and targeted therapy. The 5-year survival rate at diagnosis for adults is around 40%(6) and the survival rates for patients with relapsed ALL is a dismal can be as low as 7% (7). Relapse has thus emerged as the primary challenge faced by physicians and new therapeutic targets to prevent relapse and improve Event Free Survival in relapsed patients are urgently required.

Interactions with the bone marrow microenvironment

A crucial chemokine constitutively secreted by BMSCs and essential for directional migration of hematopoietic cells is CXCL12(8-10). In the course of normal B-Cell hematopoiesis, a large proportion of precursor B cells are diverted to programmed cell death to eradicate functionless or harmful cells(11). A critical mechanism used by surviving precursor B cells to evade programmed cell death is their interaction with Bone Marrow Stromal Cells (BMSCs) that provide niches and attachment sites rich in secreted and surface bound survival factors like chemokines and integrins(12). Similarly, B-ALL cells undergo rapid spontaneous apoptosis under in vitro culture conditions that is rescued by bone marrow stroma indicating that microenvironment cues are critical for B-ALL survival(13) and that leukemia cells are not intrinsically resistant to apoptosis. In agreement with the in vitro findings, B-ALL patients consistently show bone marrow infiltration and these interactions with BM microenvironment serve as a primary source of minimal residual disease (MRD) and consequently relapse. Furthermore, the degree of bone marrow infiltration and minimal residual disease are associated with relapse and worse prognosis of the disease(14).

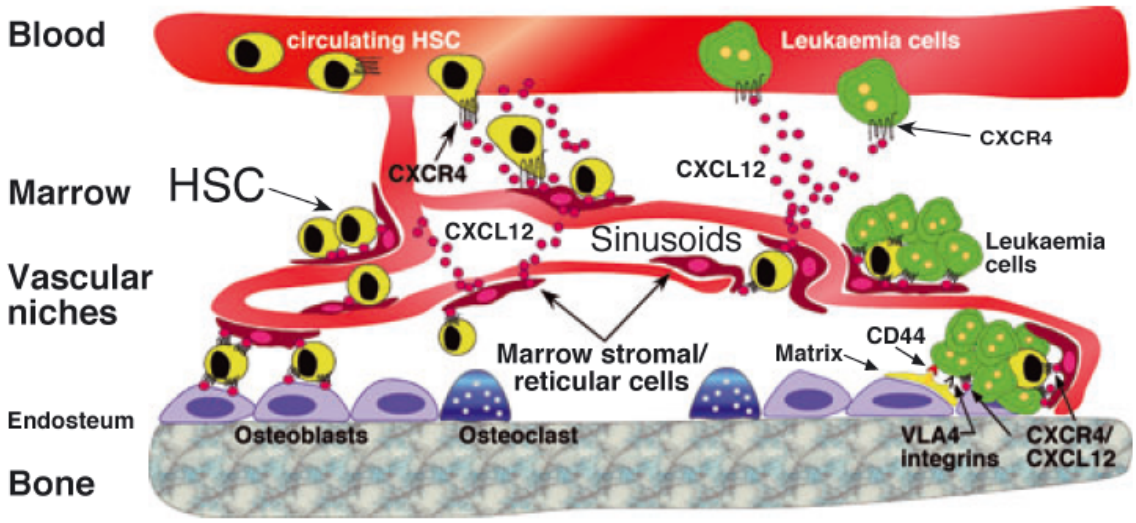
Blood
Marrow
Vascular niches
Endosteum
Bone
circulating HSC
Leukaemia cells
HSC
CXCR4
CXCL12
CXCR4
CXCL12
Sinusoids
Leukaemia cells
Marrow stromal/ reticular cells
Matrix
CD44
Osteoblasts
Osteoclast
VLA4 integrins
CXCR4/ CXCL12

Figure 1

Figure 1. The role of CXCR4 in normal and malignant hematopoietic cell homing to the bone marrow (15). Both normal (HSC, left hand side) and malignant (Leukemia, right hand side) hematopoietic progenitor cells express CXCR4 to home to the bone marrow. Both these cell types follow a CXCL12 gradient that is constitutively secreted by stromal cells in the bone marrow. These intricate netlike stromal cells with excessive CXCL12 secretion are often situated adjoining the vascular network called 'sinusoids'. These sinusoids along with reticular stromal cells form a 'vascular niche' where B-ALL cells migrate with the help of CXCR4.

Figure taken with permission from:

Burger JA, Burkle A. The CXCR4 chemokine receptor in acute and chronic leukaemia: a marrow homing receptor and potential therapeutic target. *Br J Haematol*. 2007;137(4):288-296.

CXCL12 engages its cognate receptor CXCR4 to attract and confine B-ALL cells to BMSCs. Both CXCL12 and CXCR4 knockout mice display severe defects in B lymphopoiesis highlighting the importance of this axis in normal B-Cell development(16, 17). Both normal precursor B-cells (12, 18-20) and leukemia cells(21-23) share this mechanism to home to their bone marrow niches. Precursor-B-cell ALL is characterized by the predisposition to infiltrate extra-medullary sites, for example the central nervous system, liver, spleen and lymph nodes. However, the major site of involvement is in the bone marrow microenvironment. The CXCR4 and integrin mediated interaction between the bone marrow stroma and leukemia cells protects them from chemotherapy induced or spontaneous apoptosis and is a mechanism to account for chemotherapy resistance that eventually leads to minimal residual disease and subsequent relapse.

Minimal residual disease in defined as the remainder of leukemic cells in the bone marrow of ALL patients during or after treatment when the patient is in remission. MRD has immense prognostic value throughout the treatment of leukemia, so much so that it surpasses the impact of other clinical and biological parameters. For instance, the AIEOP-BFM ALL 2000 study reported that for pediatric B-ALL prognostic risk classification based on MRD measurements on treatment days 33 and 78 was better than prior criteria based on age, leukocyte count, genetic subtype and early response to therapy(24). Additionally, a

plethora of independent studies have shown MRD to be a robust prognostic marker in adult ALL as well.

The mouse model with the CXCR4 or CXCL12 gene deletion resulted in early release of B-cells into circulation(19). CXCR4 has also been reported to participate in homing of B-ALL cells to bone marrow in non-obese diabetic severe combined immuno-deficient (NOD/SCID) mice(22, 25). B-ALL cells have been characterized by a distinctive signature of high CXCR4 expression that leads to pertussis toxin sensitive downstream signaling in which VLA-4 integrin has critical important(22). Direct *in vivo* evidence of CXCR4 involvement has also been provided by Sipkins et al (2004)(23) who used *in vivo* confocal microscopy to report that CXCR4 is required for B-ALL cell homing to the murine bone marrow niche. The use of CXCR4 antagonists demonstrated disruption of the leukemia-bone marrow interaction. Additionally, the development of the earliest precursor B cells is highly dependent on CXCL12 and it is also a potent chemo-attractant for pre and pro B cells. CXCR4 has been reported to be expressed and functional in B-ALL cells, causing chemotaxis and spontaneous migration underneath bone marrow stromal cells. B-ALL cell lines like NALM6 and REH require CXCR4 and other adhesion molecules such as CD49D (VLA-4) integrin to undergo migration mentioned above(26, 27) and these data have been also confirmed in patient samples(28, 29). This response of B-ALL cells has been reported to be dependent upon the p38 MAPK signaling

pathway(30). Consequently, inhibition of CXCR4 in B-ALL cells with highly specific antagonists has been reported to block migration of leukemia cells to CXCL12 and partially disrupt stroma mediated drug resistance(31).

Considering the above facts, molecular interactions between B-ALL cells and the BM microenvironment must be identified and effectively targeted in order to improve survival any further.

The CXCR4 Chemokine Receptor

Structure: gene and protein

CXCR4, also known as Fusin or cd184, was first discovered as a co-factor involved in the entry of T-Tropic strain of HIV-1 into CD4 positive T cells. The CXCR4 gene is located at genetic locus 2q21, contains two exons separated by an intron (spanning 2.1 kb) and the cDNA open reading frame is 1659 bp long. A typical upstream promoter region is observed at the 5' flanking region of the CXCR4 open reading frame spanning 2.6 kb with a TATA box 30bp upstream of a transcription start site(32, 33).

The protein is 352 amino acids long and has a molecular weight of about 39kDa containing an N-terminal, seven trans-membrane domains, three intra-cellular loops (ICL), three extra-cellular loops (ECL) and a C terminal. Its structure is represented in Figure 2. It is widely expressed

in different human tissues with particularly high levels of expression in the hematopoietic system. It is a rhodopsin like G-protein coupled receptor that shares 33% homology with other members of the CXC and CC chemokine receptor families, although no functional interactions remain largely exclusive with its ligand CXCL12(34).

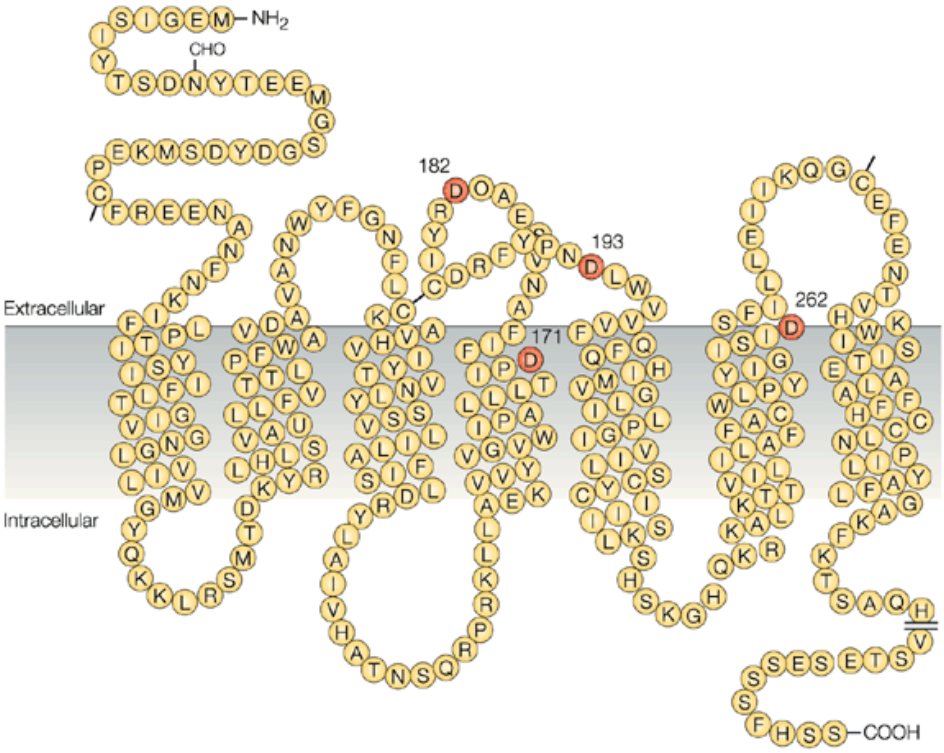

Figure 2

Figure 2. **Structure of CXCR4**. Shown here is protein sequence depicting N-terminal, extracellular, trans-membrane, intracellular and C-terminal domains of CXCR4. The four Aspartate (D) residues involved in the interaction of CXCR4 and Plerixafor (AMD3100) are highlighted in red(35).

Figure reproduced with permission from:

De Clercq E. The bicyclam AMD3100 story. *Nat Rev Drug Discov*. 2003;2(7):581-587.

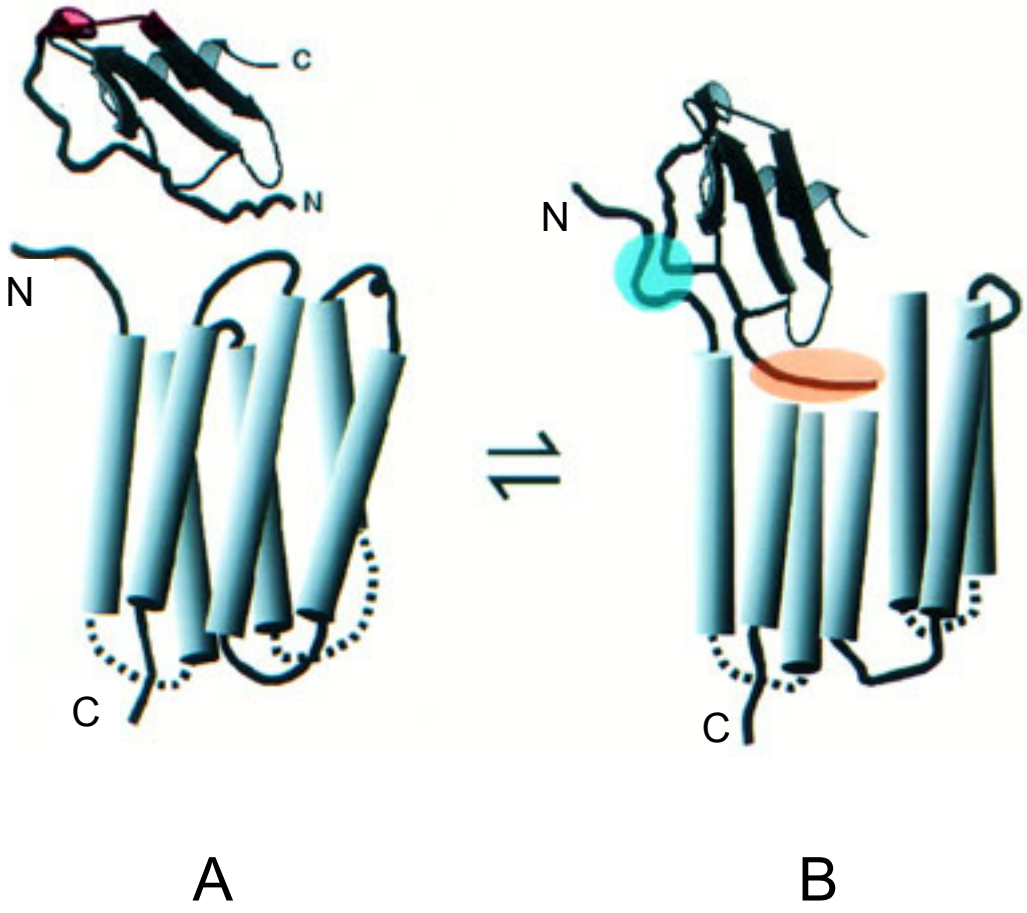

Figure 3

Figure 3. Structure of CXCR4 in complex with its natural ligand CXCL12(36). Schematic shows model of interaction between CXCR4 and its ligand CXCL12 (SDF-1). The seven trans-membrane helix domains are represented as cylinders that are connected to each other by extra and intra cellular loops. CXCL12 is shown above CXCR4 as a ribbon structure (MOLSCRIPT diagram). (A) CXCL12 and CXCR4 are shown separately before any contact between the two. (B) The two contact regions between CXCL12 and CXCR4 are shown blue and orange. The blue region depicts contact between the CXCR4 N-terminal and CXCL12 RFFESH loop both of which are more truncated as compared to the unbound states. The orange region depicts CXCL12 N-terminal binding to the groove above extracellular domains of CXCR4.

Adapted with permission from

Crump, M. P., J. H. Gong, P. Loetscher, K. Rajarathnam, A. Amara, F. Arenzana‐Seisdedos, J. L. Virelizier, M. Baggiolini, B. D. Sykes, and I. Clark‐Lewis. 1997. Solution structure and basis for functional activity of stromal cell‐derived factor‐1; dissociation of CXCR4 activation from binding and inhibition of HIV‐1. *The EMBO journal* 16: 6996-7007.

Mutant studies revealed that the CXCR4 N terminal is essential for CXCL12 binding. Also, CXCL12 interacts with the second extracellular loop to activate downstream signaling pathways and the Asp-Arg-Tyr motif located at the second intracellular loop is required for CXCR4 activation. Additionally, the HIV-1 co-factor function and the signaling function are independent of each other(37).

CXCL12: The CXCR4 ligand

There are two main types of classifications that exist for chemokines. The first type of classification is based on the relative position of the first two of four cysteine residues, giving rise to four subfamilies: CC, CXC, C and CX3C. The second type of classification divides chemokines into two groups, namely, inflammatory or homeostatic(38). Inflammatory chemokines are expressed in an acute and transient manner to attract inflammatory cells to sites of infection or injury. Homeostatic chemokines, on the other hand, are expressed constitutively. CXCL12, also known as Stromal cell-Derived Factor 1 (SDF1) and originally isolated from murine bone marrow, belongs to the 'homeostatic' group of chemokines and was initially discovered as a pre-B-cell growth stimulating factor(39, 40).

The CXCL12 gene displays high degree of evolutionary conservation and is located on chromosome 10q. Various splice variants of CXCL12 (α, β, γ, δ, ε and φ) have been described, with the 89 amino acid α isoform (3 exons) being expressed pre-dominantly(40, 41). CXCL12 β, γ, δ, ε and φ contain 4, 30, 31, 1 and 51 amino acid extension at their C-terminus domain as compared to the α variant(41). The functional significance of these isoforms is poorly understood but it is known that they display differential distribution in various tissues. The present study focused on the α variant owing to lack of γ, δ, ε and φ isoform expression in the bone marrow(41).

CXCL12α is secreted constitutively by the bone marrow stroma and signals through CXCR4. CXCL12 is characterized as a potent inducer of directional migration in a range of cells of hematopoietic origin(9, 42) and along with CXCR4, it plays a critical role in the trafficking of immune and hematopoietic cells to various tissue microenvironments. High continuous expression of CXCL12 by bone marrow stromal cells suggests its important role in the marrow microenvironment. Concurrently, various *in vitro* and *in vivo* studies demonstrate that this chemokine is essential for hematopoietic cell homing and retention in the bone marrow(8, 10). In fact, hematopoietic stem cells selectively migrate to CXCL12 and not to other chemokines(43) and it is required for bone marrow stem cell retention(20, 44, 45).

Mice lacking the CXCL12 gene display phenotypical resemblance to CXCR4 gene deletion mice with deficient myelopoiesis and B-lymphopoiesis, and abnormal development of the heart and neurons(16, 17, 46). This similarity in phenotype had initially suggested that this chemokine and receptor pair is monogamous in nature. However, recent studies by various groups have confirmed that CXCL12 binds to a novel receptor CXCR7 also(47, 48). This receptor is discussed in detail on page 28.

Regulation of CXCR4 signaling

In order to have a clear picture of the role of CXCR4 in human disease it is imperative to have a fundamental understanding of signaling mechanism. The binding of CXCL12 to CXCR4 is proposed to be a 2-step process, the first step involves residues 12-17 of CXCL12 and 2-36 of CXCR4 that cause a conformational change in the receptor. This conformational change exposes a binding pocket in the second and third extracellular loops of CXCR4 that interacts with the first eight amino acids of CXCL12. This constitutes the second step of the interaction(49).

There are two types of CXCR4 signaling that has been discovered; G protein coupled and G protein independent. In its basal state, CXCR4, a G protein coupled receptor has an intracellular heterotrimer of G α, β and γ subunits that are bound to guanine nucleotide GDP. The CXCL12-CXCR4 binding activates the receptor by replacing GDP with GTP, due to

which the βγ dimer is dissociated from the heterotrimer. The Gα subunit can then activate various signaling pathways, for example it activates Src family of kinases. On the other hand, the Gβγ subunit has been shown to activate the phosphoinositide-3 kinase (PI3K) and the JAK/STAT pathways. These pathways ultimately lead to processes like migration, cell adhesion and gene transcription(50).

The basal transcription of CXCR4 is regulated by the contrasting effect of two transcription factors, Nuclear Respiratory Factor-1 (NRF-1) that up-regulates CXCR4 and Ying Yang 1 (YY1) that negatively regulates it. Apart from basal transcription by these two factors, other factors like intracellular calcium, cyclic AMP, various cytokines (IL1-β, IL-2, IL-4, IL-7, IL-10, IL-15, TNF-α and IFN-γ), growth factors (HIF-1, NFκB, TGF-1, bFGF, VEGF, EGF and VHL) regulate CXCR4 expression(50).

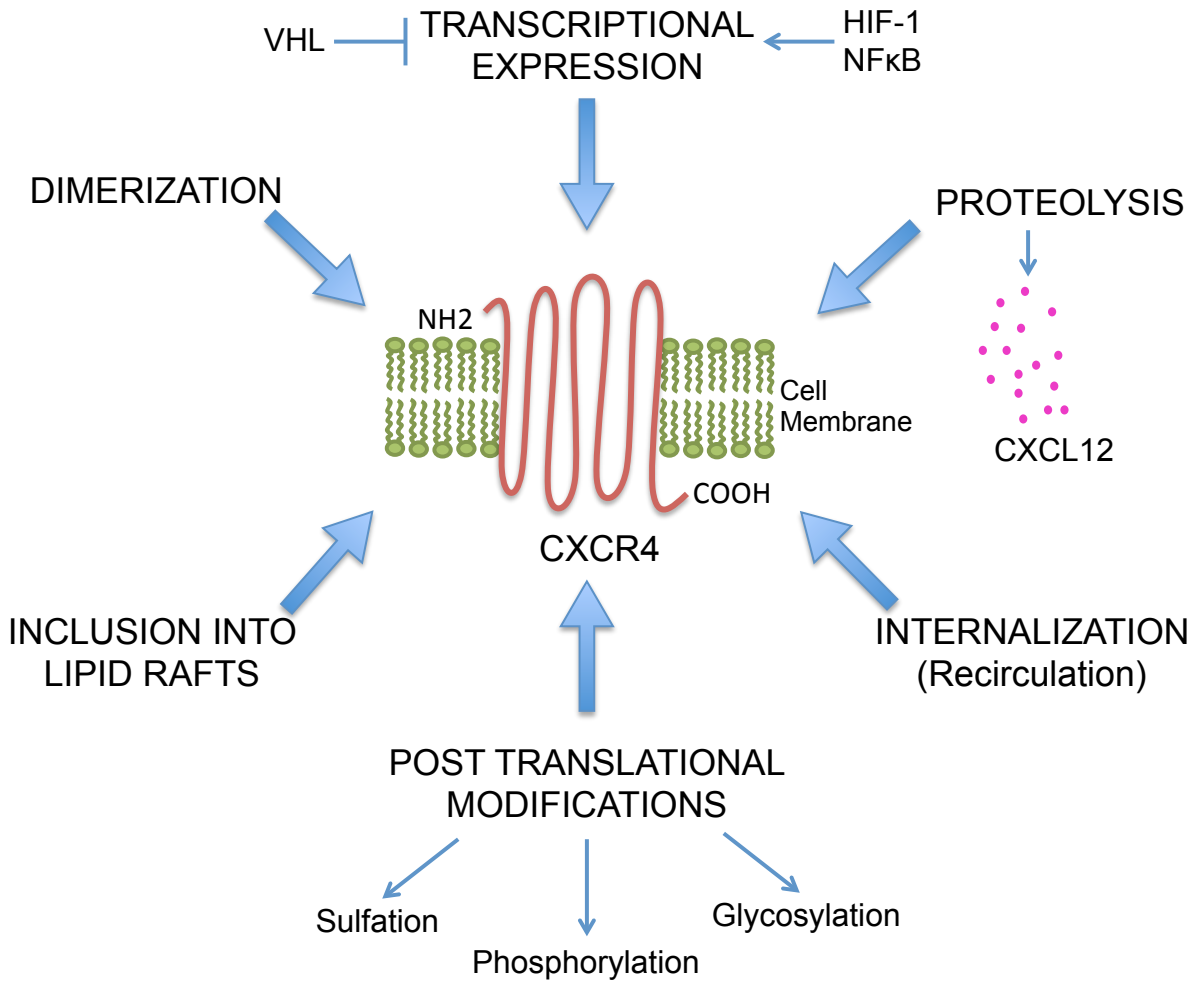
VHL
TRANSCRIPTIONAL EXPRESSION
HIF-1
NFκB
DIMERIZATION
PROTEOLYSIS
NH2
Cell Membrane
CXCL12
COOH
CXCR4
INCLUSION INTO LIPID RAFTS
INTERNALIZATION (Recirculation)
POST TRANSLATIONAL MODIFICATIONS
Sulfation
Phosphorylation
Glycosylation

Figure 4

Figure 4. CXCR4 regulation. Figure depicts different levels of regulation of CXCR4. CXCR4 expression is affected at the transcription level by various processes e.g. inflammation, hypoxia tissue damage through various proteins. For example, CXCR4 expression is up-regulated by HIF-1 and NFκB and down-regulated by VHL. Both CXCR4 and its ligand CXCL12 are susceptible to proteolytic degradation by various proteases in the microenvironment. Upon CXCL12 binding, CXCR4 undergoes rapid and dynamic internalization into endosomal components and CXCL12 depletion has been reported to restore surface CXCR4 expression. Several post translation modifications have been reported for CXCR4 that alter its function. For instance, various phosphorylation sites having positive or negative effects on CXCR4 signaling have been identified. Additionally, glycosylation at Asn11 decreases binding to CD4 positive T cells whereas it is essential for binding to CXCL12. The function of the CXCR4 protein depends upon its inclusion in lipid rafts, which can be regulated by signals from other membrane proteins. Finally, CXCR4 has been shown to undergo dimerization with itself and CXCR7, which has an effect on the downstream signaling pathways (51, 52).

Apart from transcriptional regulation, CXCR4 function is regulated in several other ways. The extracellular domains of CXCR4 have two glycosylation sites, Asn11, that is involved in HIV and CXCL12 binding. Another post-translational modification that regulates ligand binding is tyrosine sulfation at Tyrosines 1, 12 and 21 out of which Tyr 21 accounts for the most sulfation.

Another level of regulation that affects CXCR4 function is its oligomerization. The functional significance of CXCR4 dimerization is not yet understood well, although it has been proposed that homo-dimerization is necessary to enhance response to CXCL12 and stimulate G protein independent stimulation of the JAK/STAT pathway. Additionally, CXCR4 hetero-dimerization with CXCR7 stimulated by CXCL12 has been reported to activate G protein independent β-arrestin signaling. Taken together, these data suggest homo and hetero-dimerization regulates non-canonical signaling in the absence of CXCL12.

Upon CXCL12 binding, CXCR4 is internalized into endosomes, thus reducing surface expression. After internalization, CXCR4 recycles back to the plasma membrane or is sent to lysosomes for proteolytic degradation mediated by E3 ligase AIP4. Phosphorylation may regulate the outcome of the receptor after internalization.

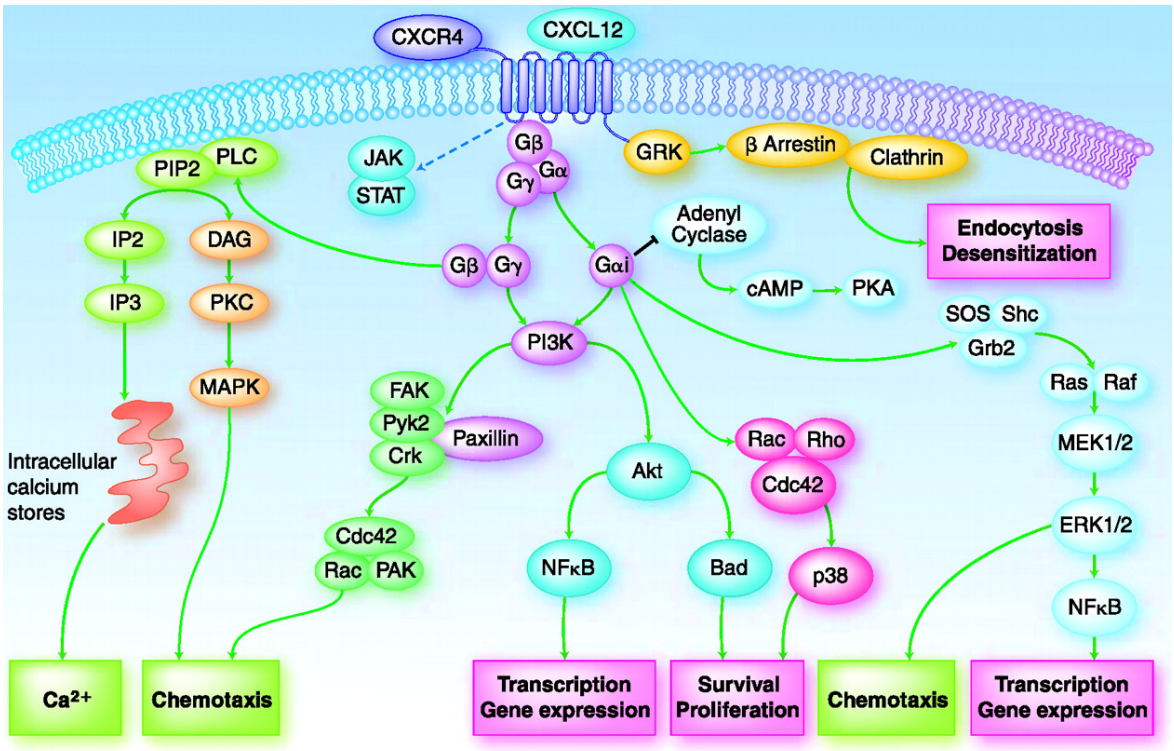
CXCR4
CXCL12
JAK
STAT
Gβ
Gγ
Gα
GRK
β Arrestin
Clathrin
Endocytosis
Desensitization
PIP2
PLC
IP2
DAG
IP3
PKC
MAPK
Gβ Gγ
Gαi
Adenyl
Cyclase
cAMP
PKA
PI3K
SOS Shc
Grb2
Ras Raf
MEK1/2
ERK1/2
NFκB
FAK
Pyk2
Crk
Paxillin
Cdc42
Rac PAK
Akt
Rac Rho
Cdc42
NFκB
Bad
p38
Intracellular
calcium
stores
Ca2+
Chemotaxis
Transcription
Gene expression
Survival
Proliferation
Chemotaxis
Transcription
Gene expression

Figure 5

Figure 5. The CXCR4 signaling network(53). CXCL12 acts through its receptor CXCR4. Engagement of CXCR4 with CXCL12 activates an intricate signaling network that promote calcium mobilization, chemotaxis, survival, proliferation and transcription.

Figure reproduced with permission from

Teicher, B. A., and S. P. Fricker. 2010. CXCL12 (SDF-1)/CXCR4 pathway in cancer. *Clinical cancer research : an official journal of the American Association for Cancer Research* 16: 2927-2931.

CXCR7: the alternate receptor

The identical phenotype displayed by CXCL12 and CXCR4 deficient mice indicated that they have a monogamous interaction, however, recently Burns et al and Balabanian et al (47, 48) have identified a highly conserved alternate receptor for CXC12, called CXCR7. It has been recently de-orphanized and implicated in cell adhesion and survival signaling, but has not found general consensus to its function and expression in various tissues. CXCR7, previously called RDC1, was proposed to be a chemokine receptor based on sequence similarity to CXCR2 and its location in the vicinity of other chemokine receptors (CXCR1, CXCR2 and CXCR4) on chromosome 1 and 2 in mice and humans respectively. It has also been demonstrated to be a co-receptor for immunodeficiency viruses(54). CXCR7 has been termed as an atypical chemokine receptor due to lack of G-protein binding. However, it has been reported to undergo internalization upon CXC12 binding. The main function of CXCR7 has been reported to scavenge CXCL12 away from CXCR4, consequently affecting function of CXCR4 by regulating the amount of ligand available to CXCR4.

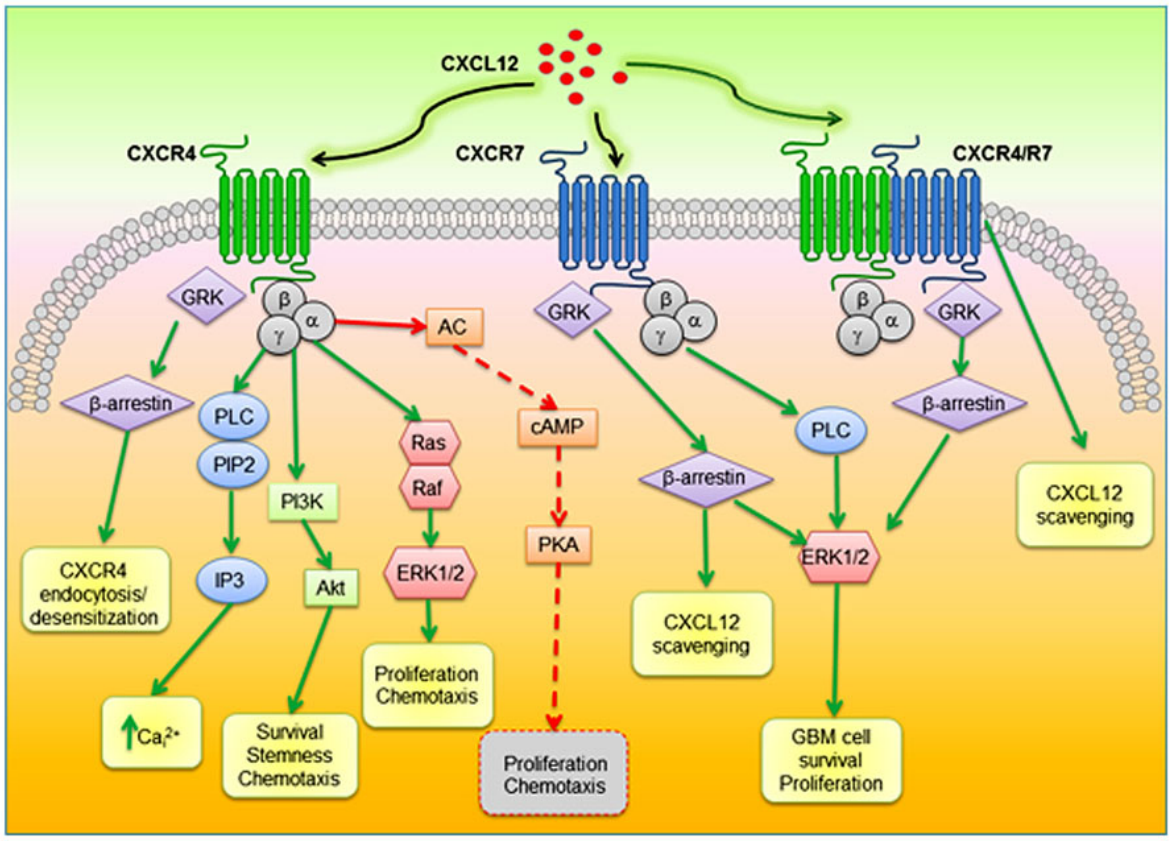
CXCL12
CXCR4
CXCR7
CXCR4/R7
GRK
β
γ
α
AC
β-arrestin
PLC
PIP2
PI3K
Ras
Raf
cAMP
PKA
IP3
Akt
ERK1/2
CXCR4 endocytosis/ desensitization
Proliferation Chemotaxis
Survival Stemness Chemotaxis
Proliferation Chemotaxis
CXCL12 scavenging
GBM cell survival Proliferation

Figure 6

Figure 6. The CXCR4/CXCR7 signaling pathways(55). CXCL12 binds to both CXCR4 and CXCR7 and leads to activation of various signaling pathways dependent upon tissue types. CXCR7 has been mainly shown to sequester CXCL12 away from CXCR4, thus affecting CXCR4 function. However, recent studies have shown that CXCR7 can activate the MAP kinase pathway through β-arrestin in numerous systems tested.

Figure reproduced with permission from

Wurth, R., A. Bajetto, J. K. Harrison, F. Barbieri, and T. Florio. 2014. CXCL12 Modulation of CXCR4 and CXCR7 activity in human glioblastoma stem-like cells and regulation of the tumor microenvironment. *Frontiers in cellular neuroscience* 8.

CXCR4 Inhibition as a Therapeutic Target

Apart from being responsible for chemotaxis of leukemia cells to the bone marrow(56), engagement of CXCR4 also helps in adhesion to BMSCs and activates various signaling cascades providing the cells with direct survival advantage(22). As a result leukemia cells in bone marrow niches may become resistant to chemotherapeutic drugs. This drug resistance mechanism is appropriately known as Cell Adhesion Mediated Drug Resistance (CAM-DR) and accounts for Minimal Residual Disease (MRD) in bone marrow niches and the consequent relapse of ALL. Clinically CXCR4 expression has been shown to be associated with worse outcome in B-ALL patients(57-59). Consequently, inhibition of this axis presents itself as an alluring strategy for prevention of relapse. Indeed, Plerixafor (Mozobil or Previously AMD3100), a reversible small molecule CXCR4 inhibitor, has been FDA approved for stem cell mobilization for Non-Hodgkin lymphoma and Multiple Myeloma(60). It has also been shown to mobilize ALL cells from bone marrow niches to peripheral blood in mice(61). Additionally, Plerixafor is being currently tested in clinical trials as a chemo-sensitizing agent for Acute Myeloid Leukemia(62). In this study, we demonstrate that inhibiting CXCR4 disrupts the ALL-BMSC interaction thus overcoming Cell Adhesion Mediated Drug Resistance provided to ALL cells by BMSCs. Furthermore, apart from the effect of pharmacological inhibition of CXCR4 on

chemotaxis, adhesion and chemo-sensitivity, we report an in vitro and in vivo genetic deletion model of CXCR4 from B-ALL cells.

CXCR4 inhibitors

Plerixafor: the bicyclam story

Plerixafor also known as AMD3100 or Mozobil was derived from an earlier compound, JM1657, which in turn was discovered as an impurity in monocyclam compound commercially prepared for its activity against HIV. The failure in re-synthesis of JM1657 led to development of bicyclam compounds in which two cyclam moieties are tethered through and aromatic bridge (Figure 7). After the synthesis of several bicyclams, a quantum leap was achieved in anti-HIV activity by the synthesis of AMD3100 (AMD stands for AnorMeD, the manufacturer at the time). The viral protein gp120, involved in HIV cell entry was identified as an indirect target and later CXCR4, due to its role as a co-receptor in HIV cell entry, was identified as the direct target for Plerixafor.

Owing to its potential as a potent anti-HIV agent, there was considerable enthusiasm for clinical use. The clinical studies however, showed an increase in white blood cells counts of patients peaking 8 to 10 hours post sub-cutaneous injections. These white blood cells included CD34 positive hematopoietic progenitor cells. Consequently, Broxmeyer et al 2005 (63)demonstrated that plerixafor could effectively mobilize

hematopoietic stem and progenitor cells from their niches, thus giving rise to the concept of plerixafor as a potent mobilizer of HSCs. This mobilization was a clear outcome of CXCR4 inhibition in patients. Consequently, Mozobil or plerixafor, in combination with granulocyte-colony stimulating factor (G-CSF), was approved by the FDA in 2008 as a stem cell mobilizer in patients with Multiple Myeloma or Non-Hodgkin's Lymphoma.

As measured by calcium flux assays, plerixafor inhibited signaling for only CXCR4 but no other chemokine receptors(64). Moreover, CXCR4 failed to internalize upon CXCL12 binding, thereby controlling a critical mechanism of CXCR4 regulation. Certain aspartic residues (as highlighted in Figure 2 have been demonstrated to be essential for the Plerixafor-CXCR4 interaction. Plerixafor has also been shown to block the binding of the 12G5 antibody to the CXCR4 receptor(64). This property has been used to demonstrate that plerixafor has a reversible, but long lasting effect on CXCR4. At the time of treatment, plerixafor occupied 85 to 90% of surface CXCR4, which remained consistent at 24 hours but fell to 60% at 48h, as measured by 12G5 antibody staining(65).

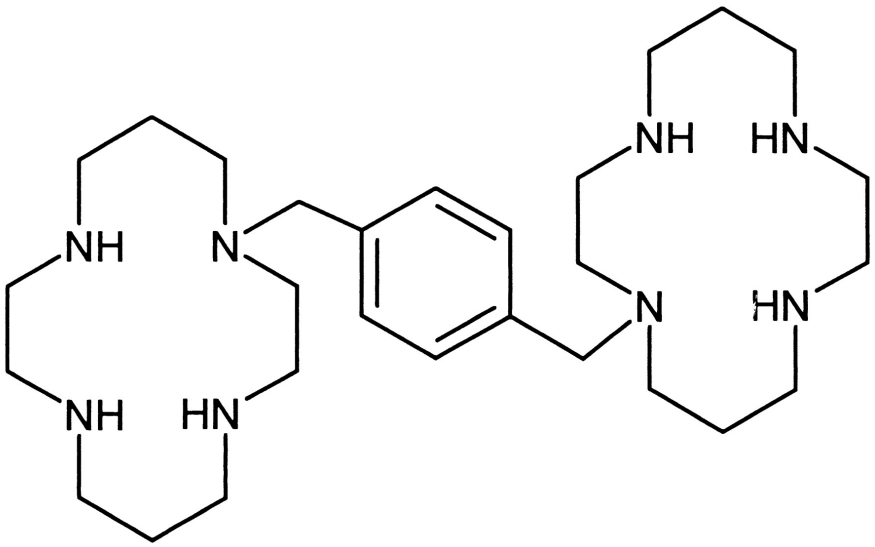

Figure 7

Figure 7. Structure of Plerixafor (66). Plerixafor, also known as AMD3100 and Mozobil, is a bicyclam containing two cyclam (1,4,8,11-tetraazacyclotetradecane) moieties tethered through an aromatic bridge [phenylenebis(methylene)].

Figure reproduced with permission from

Hendrix, C. W., C. Flexner, R. T. MacFarland, C. Giandomenico, E. J. Fuchs, E. Redpath, G. Bridger, and G. W. Henson. 2000. Pharmacokinetics and safety of AMD-3100, a novel antagonist of the CXCR-4 chemokine receptor, in human volunteers. *Antimicrobial agents and chemotherapy* 44: 1667-1673.

BKT140

BKT140, or 4F-benzoyl-TN 14003 is a novel, potent 14-residue synthetic bio-stable peptide which binds selectively to CXCR4 with an affinity of 84 nmol/L as compared to plerixafor which has an affinity of 4 nmol/L. It is a reversible inhibitor that dissociates from CXCR4 with a much slower pace than plerixafor. Additionally, unlike plerixafor that is a weak partial agonist for CXCR4, BKT140 completely shuts down normal signaling cascades downstream of CXCR4. Furthermore, BKT140, unlike plerixafor, does not activate β-arrestin signaling downstream of CXCR7. BKT140 is in clinical trials for patients with acute myeloid leukemia and chronic myeloid leukemia for improving the outcome of chemotherapy.

Summary and Hypothesis

CXCR4 inhibitors Plerixafor (small molecule) and BKT140 (peptide) interfere with CXCR4 activation, signaling and bone marrow homing of leukemia cells. Adhesion of B-ALL cells to bone marrow stromal cell (BMSC) through CXCR4/CXCL12 protects leukemia cells from cytotoxic drugs, and causes cell adhesion-mediated drug resistance (CAM-DR). Due to the critical role of the CXCR4/CXCL12 axis in B-ALL cell adhesion to bone marrow stromal cells (BMSC), we hypothesize that targeting CXCR4 will attenuate CAM-DR in B-ALL.

Chapter 2

~ *Materials & Methods* ~

Reagents and Antibodies

Synthetic human CXCL12 or SDF1α was purchased from R&D Systems (MN, USA). The small molecule CXCR4 inhibitor, Plerixafor, was purchased from SIGMA-ALDRICH (St. Louis, MO, USA) and BKT140 peptide CXCR4 inhibitor was kindly provided by Dr. Amnon Peled (Goldyne Savad Institute of Gene Therapy, Hadassah Hebrew University Hospital, Jerusalem, Israel). Dexamethasone and Vincristine sulfate were purchased from SIGMA-ALDRICH (St. Louis, MO, USA) and 4-Hydroperoxy Cyclophosphamide was purchased from Santa Cruz Biotechnology (Dallas, TX, USA). The anti-CXCR4-phycoerythrin (PE) (12G5) antibody was purchased from BD Pharmingen (San Jose, CA, USA) and the anti-CXCR4-Allophycocyanin (APC) (12G5) antibody was purchased from eBioscience (San Diego, CA, USA). Anti-human/mice-CXCR7-PE antibody clone 8F11-M16 was purchased from Biolegend (San Diego, CA). All the other antibodies used: anti-CD44-fluoroscein isothiocyanate (FITC), anti-CD54-PE, anti-CXCR5-PE, anti-CXCR3-PE, anti-CD62L-FITC, anti-CD49D-PE and CCR7-PE were purchased from BD Pharmingen (San Jose, CA, USA).

Cell culture

Murine bone marrow stromal cell line 9-15C (from C3H/He mouse) and all the B-ALL cell lines were purchased from the RIKEN Cell Bank (Ibaraki, Japan). Cells were cultured in RPMI 1640 medium

supplemented with 10% FBS (Gibco, Grand Island, NY), 2.05 mM L-glutamine and penicillin-streptomycin (Cellgro). B-ALL xenograft cells were a kind gift from the Müschen Laboratory (UCSF, CA) and were maintained in Aplha MEM medium containing 20% FBS, Sodium Pyruvate, GlutaMAX and pencillin-streptomycin.

Chemotaxis assay

The migration of B-ALL cells to CXCL12 was quantified using 24-well transwell plates (Corning Life Sciences, Acton, MA) as described previously(67). In brief, polycarbonate inserts in chemotaxis transwell chambers with a pore size 5µm were used, and $5x10^6$ B-ALL cells, in 100 µL, were added to the top chamber, while CXCL12 (100 ng/ml) was added to the lower wells. The plates were incubated at 37°C after inserts were placed into the wells. RPMI 1640 supplemented with 0.5% bovine serum albumin (assay media) without CXCL12 was used as control. The plate was incubated for 3 hours and assay media in the lower chamber containing migrated was collected and counted in the flow cytometer (FACSCalibur) for 20 seconds at high flow. As a control, a dilution of input cells (1:20) was counted in the same experimental conditions.

Pseudoemperipolesis (in vitro migration of ALL cells under BMSCs)

Pseudoemperipolesis is a CXCR4 dependent *in vitro* phenomenon where leukemia cells spontaneously migrate underneath BMSCs. Briefly,

day before the assay, $9x10^4$ 9-15C murine bone marrow stromal cells were plated per well in 24-well plates. On the day of the experiment, stromal cell layer confluence was examined using phase-contrast microscopy, and $2.5x10^6$ treated or untreated leukemia cells were added to each well. ALL cells were pre-incubated with 10 μg/ml CXCR4 inhibitors (Plerixafor/BKT140) for 1 hour at 37°C. After 4 hours incubation at 37°C, and non-migrated cells in suspension were removed by thorough washing of each well 3 times with RPMI 1640 medium while being careful of not washing away stromal cell layer. Stromal cell layer with migrated leukemia cells was trypsinized and suspended in 500 ml RPMI 1640 supplemented with 10% FCS and counted in a flow cytometer for 20s at high. A lymphocyte gate using the forward and side scatter was set to exclude the stromal cells.

Cell Viability Measurement

Viability was measured using the following protocol. Cells were incubated for 25 minutes in FACS buffer (RPMI 1640 supplemented with 0.5% BSA) containing 40 nM 3,3'-dihexyloxacarbocyanine iodide (DiOC6) and propidium iodide (PI, 10 μg/mL) and the cells were then analyzed by flow cytometry (FACS Calibur, BD Biosciences, San Jose, CA) within 30 minutes. Cells displaying low PI and $DiOC_6$ fluorescence are apoptotic. On the other hand, cells with low high DiOC6 and low PI are viable. Lastly, high PI and low DiOC6 fluorescence in cells is representative of

necrosis.

Cell Adhesion Mediated Drug Resistance (CAM-DR) Experiments

To determine if stromal cells can rescue B-ALL cells from drug induced cytotoxicity and if CXCR4 antagonism can abolish this rescue, ALL-BMSC co-culture experiments were conducted with and without cytotoxic drugs (Dexamethasone, Vincristine and 4-Hydroperoxy cyclophosphamide) and CXCR4 antagonists (Plerixafor and BKT140). Briefly, the day before starting the assay, 9-15C stromal cells were seeded in 24-well plates at a concentration of $2x10^4$ cells/well. After overnight incubation, phase contrast microscopy was used to assess confluence of the stromal cell layer, and treated and untreated leukemia cells were added into each well to a final concentration of $1x10^6$ ALL cells per well. ALL cells were pre-incubated with 10 µg/ml CXCR4 inhibitor (Plerixafor and BKT140) for 1 hour at 37°C. Cytotoxic drugs Dex or Vin were added at the indicated concentrations. For 4-Hydroperoxy Cyclophosphamide, cells were treated with indicated concentrations for 45 minutes and then washed with culture media before plating on stromal cells. ALL cells alone, in co-culture with 9-15C and with the cytotoxic drug were used as controls. Viability of cells in the supernatant was measured at 48-hour time point. Where indicated, viability of ALL cells that migrated under the 9-15C (through PEP) was also measured.

CRISPR-Cas9 based CXCR4 Knockout

CXCR4 knockout cell lines were generated using the CRISPR Cas9 gene editing system. Briefly, a unique 20 bp target sequence located on the second trans-membrane domain of CXCR4 was used to generate the guide CRISPR RNA that was ligated into px330 plasmid (Addgene, MA) under the control of the hU6 promoter. The Cas9 sequence was ligated into the same plasmid under the control of the AmpR promoter. The plasmid was transfected into the ALL cells by electroporation with the Neon Transfection System (Life Technologies, NY) using the conditions 1500 Volts, 20 milliseconds and 1 pulse. After 48 hours the CXCR4 expression was analyzed using FACS analysis. The negative cell population was enriched using two rounds of MACS cell sorting (Miltenyi Biotec, CA). For MACS sorting, the cells were stained with PE conjugated CXCR4 antibody for 15 minutes at 4°C, washed and then stained with anti-PE microbeads for 15 minutes at 4°C before passing through the MACS LD column. The CXCR4 negative cells were collected in the flow through and stained with APC conjugated CXCR4 antibody after 48 hours.

Growth assays

Growth rates of wild type and knockout cell lines were compared by plating 1 x 10^6 cells for each cell line in 24 well plates. Cells were counted for 20 seconds at high at 0, 24, 48 and 72 hours using a flow

cytometer (BD FACS Calibur).

GFP transfection

HEK293T cells were transfected with (5µg) lentiviral plasmid and packaging plasmids pMD2.G (5µg) and pPAX (5µg) using Jet prime transfection reagents according to the manufacturers protocol. The medium containing the virus was collected at 48 hours, centrifuged at 1500 rpm for 5 minutes and supernatant filtered through a 0.45 µm filter. NALM6 WT and NALM6-CXCR4-KO were re-suspended in 5ml viral supernatant and incubated overnight at 37°C. Viral media was replaced with fresh media the next day and GFP expression was analyzed after 48 hours.

***In vivo* experiments**

All mice experiments were performed in accordance with a protocol approved by the Institutional Animal Care and Use Committee of MD Anderson cancer center. To investigate the *in vivo* effects of CXCR4 in NALM6 cells, non-irradiated NOD/SCID/IL-2rγnull (NSG) mice (The Jackson Laboratory, Bar Harbor, ME) were injected via tail vein with $1x10^6$ GFP positive NALM6 wild type or GFP positive NALM6 CXCR4 Knock out cells. Bioluminescence imaging (BLI) was performed on days 6, 10, 14 and 17 to evaluate tumor burden. Briefly, mice were anesthetized and imaged noninvasively with an in vivo imaging system (IVIS-200; Xenogen, Hopkinton, MA) after injection with luciferase

substrate coelenterazine (Biotium, Heyward, CA). Total body bioluminescence was quantified in a region of interest drawn around each mouse. Three mice per group were sacrificed on day 17 to measure GFP positive leukemic cells in different organs and femurs. The expression of surface CXCR4 protein was analyzed by using a Gallios flow cytometer (Beckman Coulter, Brea, CA), and harvested cells were stained with antibodies against CXCR4-allophycocyanin (12G5). Overall survival and mean group survival times were estimated by the Kaplan-Meier method and compared with the log-rank test.

Data Analysis and Statistics

Results have depicted as mean ± standard error about the mean (SEM), of at least three experiments each. PEP were conducted twice in duplicates. Statistical analysis was done with GraphPad Prism 6.0 for Macintosh (GraphPad Software, San Diego, CA, USA). Two-tailed students' *t*-test was used for statistical comparison between groups and the *P* values were assigned as follows (*$P < 0.05$; **$P < 0.01$; ***$P < 0.001$). Flow Cytometry data were analyzed using FLOWJO 9.4.11 software (TreeStar Inc.).

Patient data set analysis

Patient characteristics are summarized in Table S1. CXCR4 and CD49D surface levels on B-ALL cells were quantified by flow cytometry in bone

marrow specimen from 137 patients with newly diagnosed with B-ALL at MD Anderson Cancer Center (Houston, Texas). Overall survival (OS) was defined as the time between treatment start and date of death due to any cause. Patients who were alive were censored at the last follow-up date. For patients who achieved CR, CRp or PR, relapse-free survival (RFS) was defined as time between the date of response and date of disease relapse or death due to any cause, whichever occurred first. Patients who were alive without disease relapse were censored at the last follow-up date. The probabilities of OS and RFS were estimated using the method of Kaplan and Meier. Cox proportional hazards regression models were fit to assess the association between OS or RFS and patient characteristics. In addition, logistic regression analyses were performed to assess the association between patient characteristics and the binary outcome of overall response (i.e., CR, CRp or PR). All statistical analysis were conducted in SAS and Splus.

Chapter 3

~ *Results* ~

CXCR4 is highly expressed in B-ALL cells

A panel of ALL cell lines and xenograft-expanded primary cells were screened for surface expression of various chemokine receptors and adhesion molecules using flow cytometry (Figure 8, 9, 10 and 11). A Mean Fluorescence Intensity Ratio (MFIR) was used to express the data; it is the ratio of mean fluorescence intensity of analyzed marker to the mean fluorescence intensity of respective isotype control. It was observed that all the cell lines and xenograft expanded cells tested were positive for CXCR4, with cell lines showing higher average MFIR than xenograft expanded primary cells (Figure 12). All cell lines and xenografts had high CD49D levels with xenografts showing higher average MFIR. Low or absent levels of other chemokine receptors indicate that CXCR4 is the receptor involved in the homing of ALL cells to the bone marrow. CXCR7, the alternate receptor for CXCL12, was found to be negative for all cell lines tested. Surface expression of other adhesion molecules was variable across cell line.

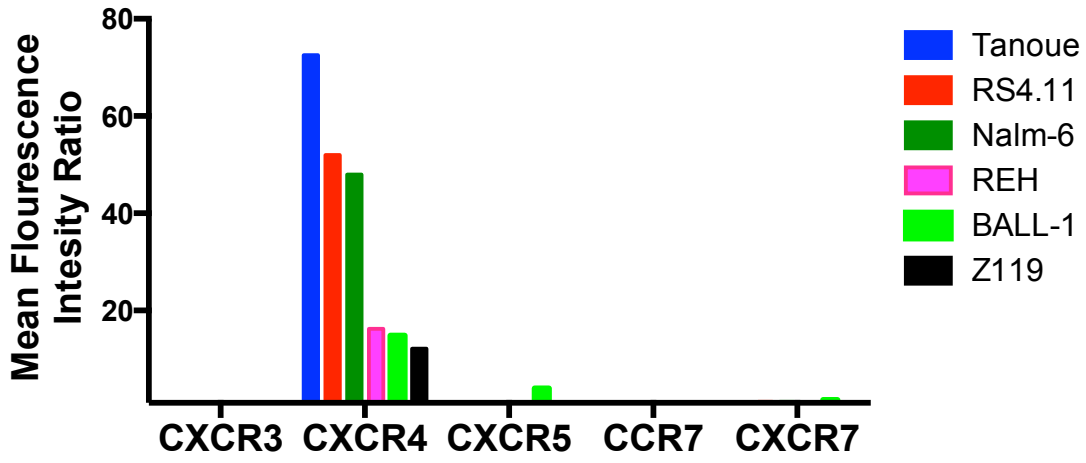
Mean Flourescence Intesity Ratio
80
60
40
20
CXCR3
CXCR4
CXCR5
CCR7
CXCR7
Tanoue
RS4.11
Nalm-6
REH
BALL-1
Z119

Figure 8

Figure 8. CXCR4 is highly expression in B-ALL cell lines. Expression of chemokine receptors in a panel of B-ALL cell lines was measured using flow cytometry surface staining. Y-axis (Mean Fluorescent Intensity Ratio, MFIR) depicts the ratio of the respective marker assessed and the isotype control.

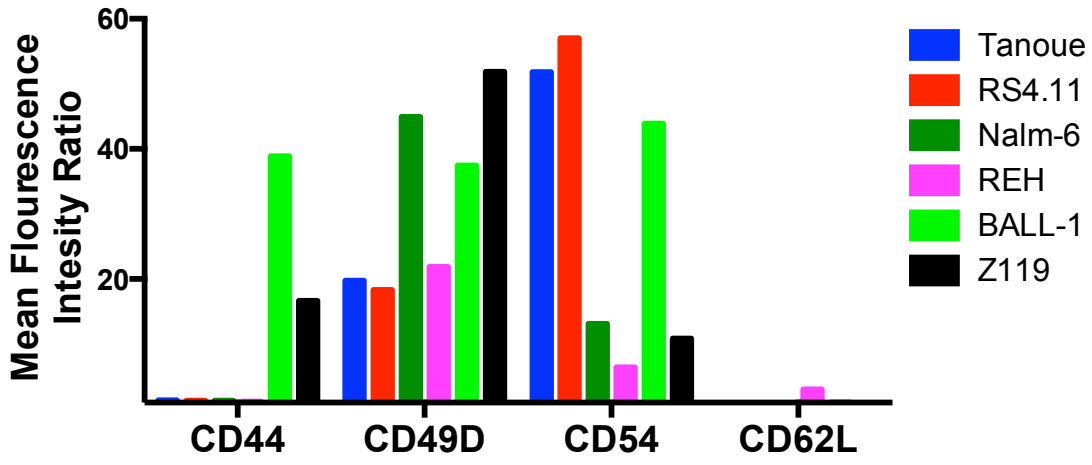
Mean Flourescence Intesity Ratio
60
40
20
CD44
CD49D
CD54
CD62L
Tanoue
RS4.11
Nalm-6
REH
BALL-1
Z119

Figure 9

Figure 9. B-ALL cell lines display variable expression of adhesion molecules. Expression of various adhesion molecules in a panel of B-ALL cell lines was measured using flow cytometry surface staining. Y-axis (Mean Fluorescent Intensity Ratio, MFIR) depicts the ratio of the respective marker assessed and the isotype control.

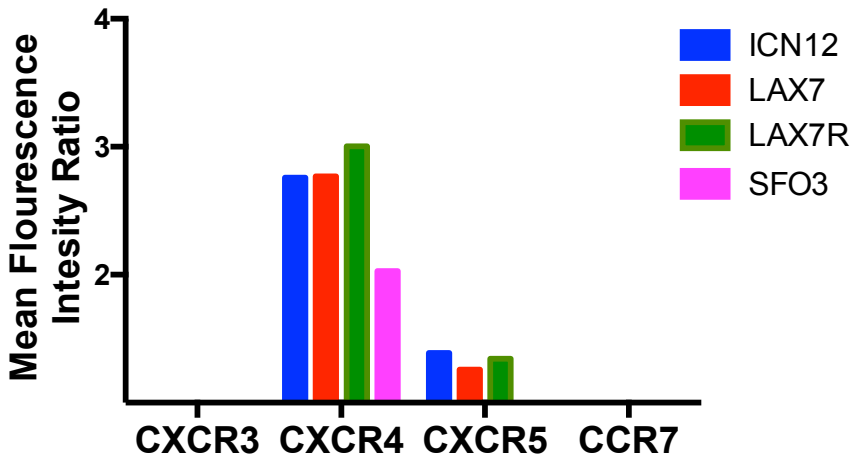
Mean Flourescence Intesity Ratio
4
3
2
CXCR3
CXCR4
CXCR5
CCR7
ICN12
LAX7
LAX7R
SFO3

Figure 10

Figure 10. Xenograft expanded primary B-ALL cells express CXCR4. Expression of chemokine receptors in a panel of xenograft-expanded primary cells was measured using flow cytometry surface staining. Y-axis (Mean Fluorescent Intensity Ratio, MFIR) depicts the ratio of the respective marker assessed and the isotype control.

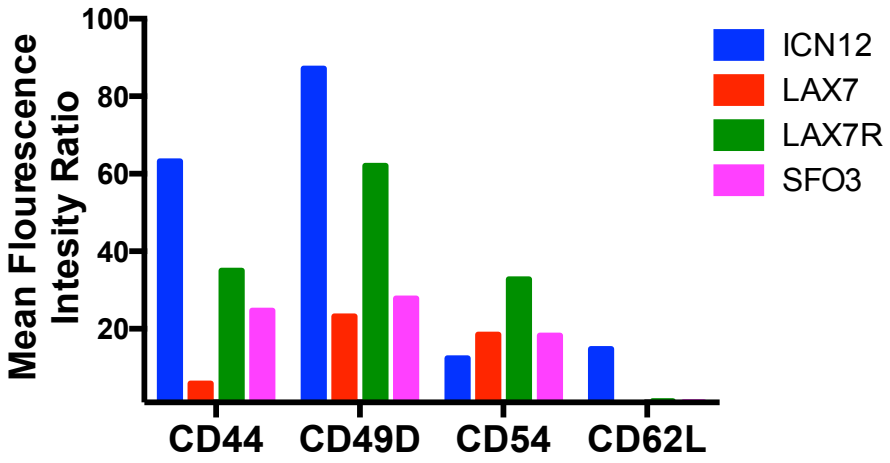
Mean Flourescence Intesity Ratio
100
80
60
40
20
CD44
CD49D
CD54
CD62L
ICN12
LAX7
LAX7R
SFO3

Figure 11

Figure 11. Xenograft expanded primary B-ALL cells display variable expression of adhesion molecules. Expression of adhesion in a panel of xenograft-expanded primary cells was measured using flow cytometry surface staining. Y-axis (Mean Fluorescent Intensity Ratio, MFIR) depicts the ratio of the respective marker assessed and the isotype control.

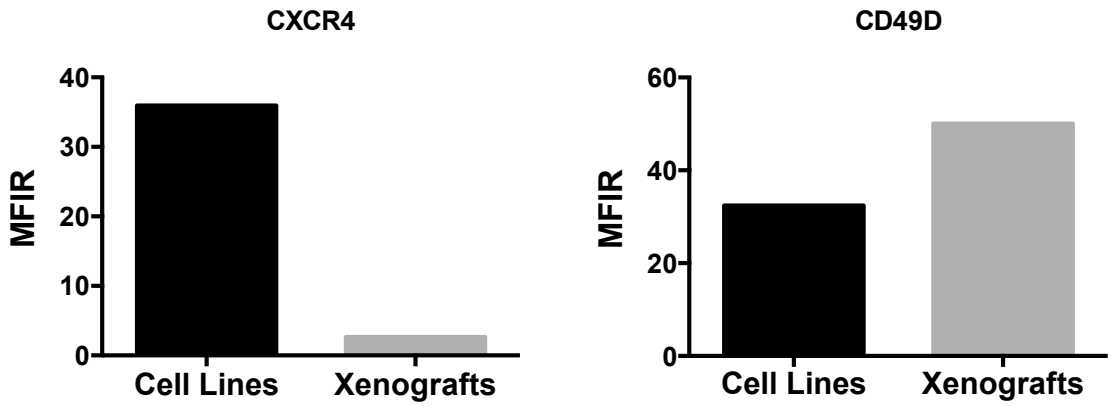
CXCR4
MFIR
40
30
20
10
0
Cell Lines
Xenografts
CD49D
MFIR
60
40
20
0
Cell Lines
Xenografts

Figure 12

Figure 12. Comparison of CXCR4 and CD49D expression in cell lines and xenograft expanded primary B-ALL cells. Cell lines express higher levels of CXCR4 than xenograft expanded primary B-ALL cells. In contrast, xenograft expanded primary B-ALL cells express higher CD49D levels. Y-axis (Mean Fluorescent Intensity Ratio, MFIR) depicts the ratio of the respective marker assessed and the isotype control.

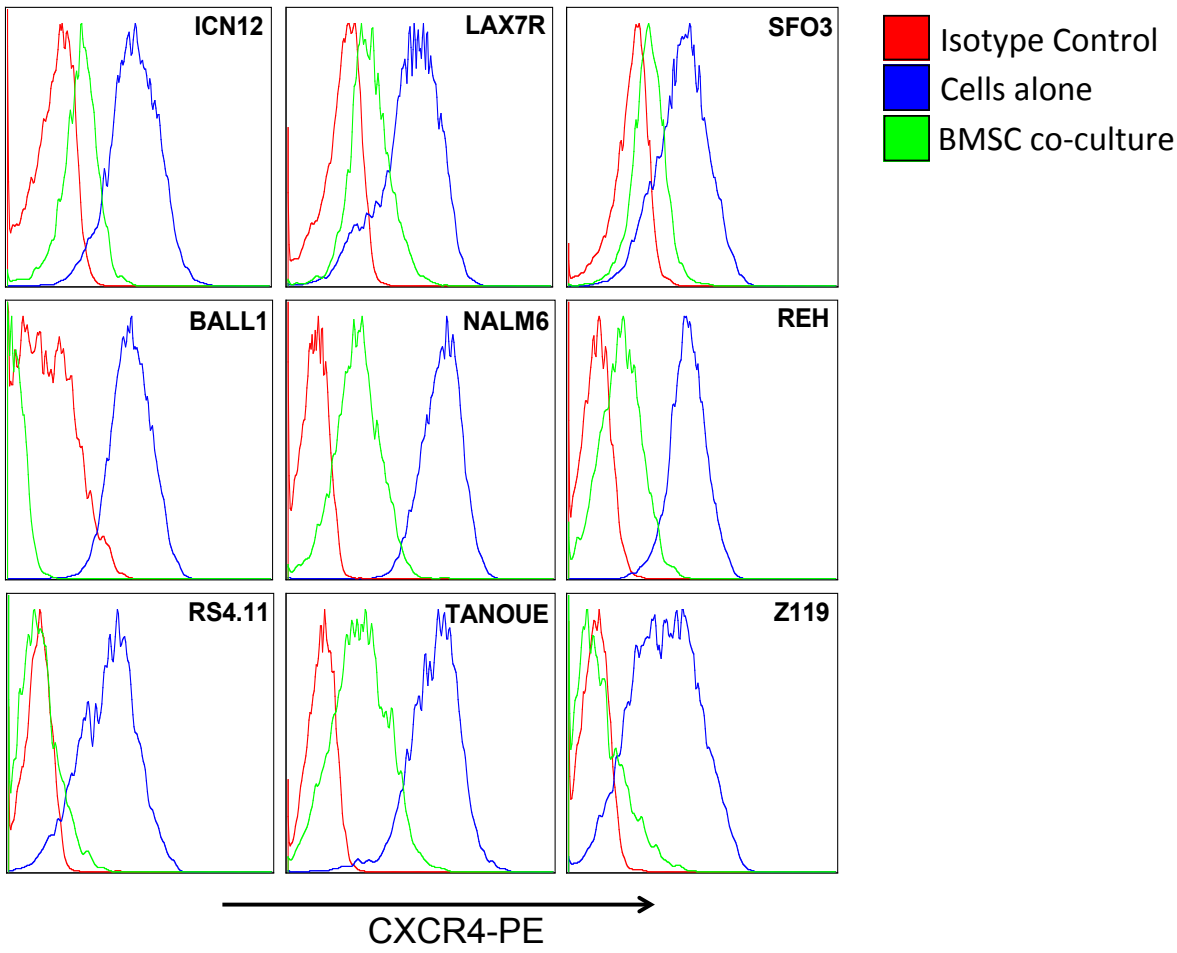
ICN12
LAX7R
SFO3
BALL1
NALM6
REH
RS4.11
TANOUE
Z119
Isotype Control
Cells alone
BMSC co-culture
CXCR4-PE

Figure 13

Figure 13. CXCR4 is down-regulated after co-culture with BMSC. Histograms depict CXCR4 expression of B-ALL cells in the presence or absence of BMSC (OP9 or 9-15C cells) after 48 hours. Compared to B-ALL cells alone (blue lines), co-culture with BMSC (green lines) resulted in a substantial down-regulation of surface CXCR4, due to CXCL12-induced receptor internalization.

Xenograft expanded B-ALL cells displayed drastically lower CXCR4 levels than cell lines. This could be possible due to continuous internalization of CXCR4 because xenograft expanded primary cells are routinely co-cultured with OP9 bone marrow stromal cells that constitutively express CXCL12. To test this hypothesis xenograft expanded primary cells were cultured without stromal cells for 48 hours and then CXCR4 expression quantified. Indeed, the CXCR4 levels increased upon culturing the cells alone. To confirm these results, B-ALL cell lines were cultured with and without stromal cells. As expected, CXCR4 levels on B-ALL cell lines decreased considerably upon exposure to bone marrow stromal cells corroborating the internalization hypothesis (Figure 13).

CXCR4 antagonists inhibit B-ALL cell migration and adhesion

Chemotaxis of ALL cell lines and xenograft cells towards CXCL12 chemokine was tested by the trans-well assay as previously explained(67). The concentration of CXCL12 to be used for chemotaxis experiments was determined through a CXCL12 dose titration using REH cell line. The doses used were 50, 100, 200, 400 and 100 ng/mL (Figure 14). A dose of 100ng/mL was found to be optimal for B-ALL cell lines. Pre-incubation with 10µg/mL Plerixafor or BKT140 for one-hour abrogated chemotaxis to CXCR4 ligand CXCL12 (100ng/ml) in all cell lines and xenograft expanded primary cells tested (Figure 15 and 16). For example, pre-treatment of NALM6 cell line with Plerixafor and

BKT140 significantly reduced chemotaxis to 59.75 ± 5.62% and 13.43 ± 3.73% (mean ± SEM, $p<0.05$) of control respectively. Similarly, SFO3 xenograft chemotaxis was significantly reduced to 22.43 ± 1.92% and 20.85 ± 1.59% (mean ± SEM, $p<0.05$) in response to Plerixafor and BKT140 pre-treatment respectively.

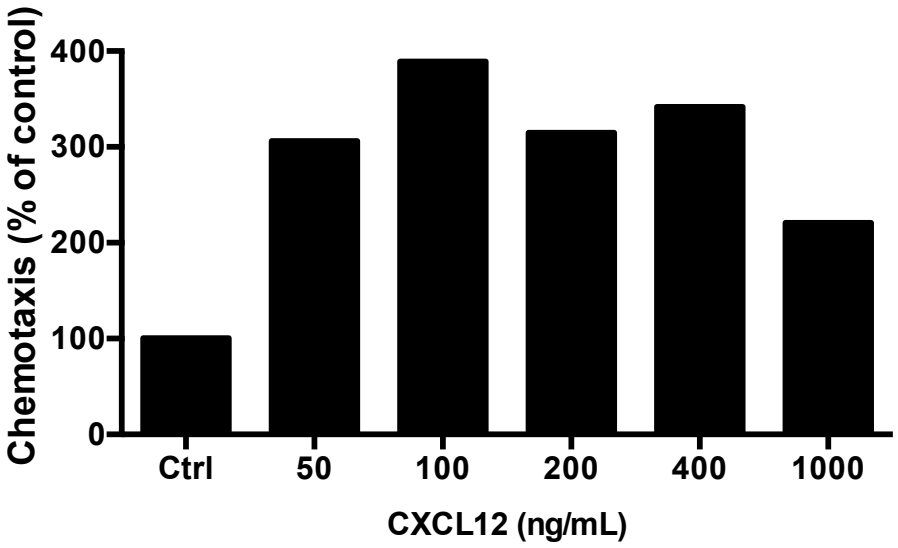
Chemotaxis (% of control)
400
300
200
100
0
Ctrl
50
100
200
400
1000
CXCL12 (ng/mL)

Figure 14

Figure 14. Determination of optimum CXCL12 dose for B-ALL chemotaxis. Bar graph represents chemotaxis of REH cells to escalating concentrations of CXCL12. X-axis represents various doses of CXCL12 and Y-axis represents percent chemotaxis with the control taken as 100 percent.

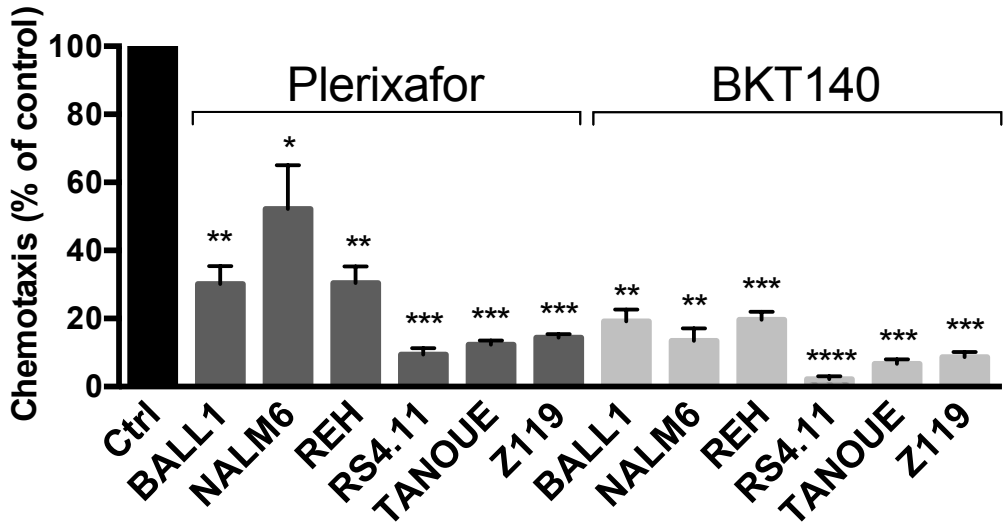
Chemotaxis (% of control)
100
80
60
40
20
0
Plerixafor
BKT140
**
*
**
***
***
***
**
**
***
****
***
***
Ctrl
BALL1
NALM6
REH
RS4.11
TANOUE
Z119
BALL1
NALM6
REH
RS4.11
TANOUE
Z119

Figure 15

Figure 15. CXCR4 inhibitors plerixafor (AMD3100) and BKT140 significantly reduce chemotaxis of B-ALL cell lines. B-ALL cells were incubated in medium alone (control) or medium containing (10μg/ml) plerixafor (AMD3100) or BKT140. The cells were allowed to undergo chemotaxis towards 100 ng/mL CXCL12 and then counted in flow cytometer for quantification. The bar diagrams represent the mean chemotaxis (± SEM) of 6 B-ALL cell lines in the presence or absence of CXCR4 inhibitors. Chemotaxis was significantly inhibited by both CXCR4 inhibitors (plerixafor/BKT140), with $*p < 0.05$; $**p < 0.01$; $***p < 0.001$ as indicated by the asterisks.

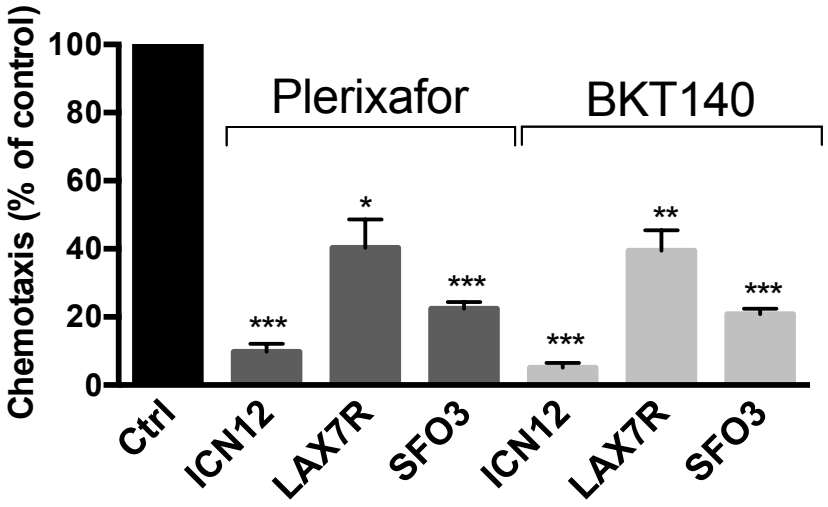
Chemotaxis (% of control)
100
80
60
40
20
0
Plerixafor
BKT140
*
**
***
***
***
***
Ctrl
ICN12
LAX7R
SFO3
ICN12
LAX7R
SFO3

Figure 16

Figure 16. CXCR4 inhibitors plerixafor (AMD3100) and BKT140 significantly reduce chemotaxis of xenograft expanded B-ALL cells. Xenograft expanded B-ALL cells were incubated in medium alone (control) or medium containing (10μg/ml) plerixafor (AMD3100) or BKT140. The cells were allowed to undergo chemotaxis towards 100 ng/mL CXCL12 and then counted in flow cytometer for quantification. The bar diagrams represent the mean chemotaxis (± SEM) of 3 B-ALL xenografts in the presence or absence of CXCR4 inhibitors. Chemotaxis was significantly inhibited by both CXCR4 inhibitors (plerixafor/BKT140), with $*p < 0.05$; $**p < 0.01$; $***p < 0.001$ as indicated by the asterisks.

As mentioned previously, ALL cells undergo a CXCR4 mediated in vitro process called Pseudoemperipolesis (PEP) to migrate under stromal cells. Figure 17 shows representative phase contrast microscopy images of B-ALL cell lines and SFO3 xenograft expanded primary cells undergoing PEP beneath 9-15C stromal cells. Cells that migrated below the mesenchymal marrow stromal cell line (9-15C) were counted by flow cytometry as previously explained(67). Significant inhibition of ALL cell migration under BMSCs was observed (Figure 18 & 19) for all cell lines and xenograft expanded primary cells tested in response to pre-incubation with 10μg/ml plerixafor and BKT140. For example, NALM6 cell line PEP was significantly reduced upon pre-treatment with 10μg/mL plerixafor or BKT140 to 61.4 ± 10.8% and 35.5 ± 5.5% (mean ± SEM, $p<0.05$) respectively as compared to control untreated cells. Similarly, SFO3 xenograft cell PEP was significantly decreased upon 10μg/mL plerixafor or BKT140 to 53.2 ± 4.08% and 53.8 ± 6.5% (mean ± SEM, $p<0.05$) respectively as compared to control untreated cells.

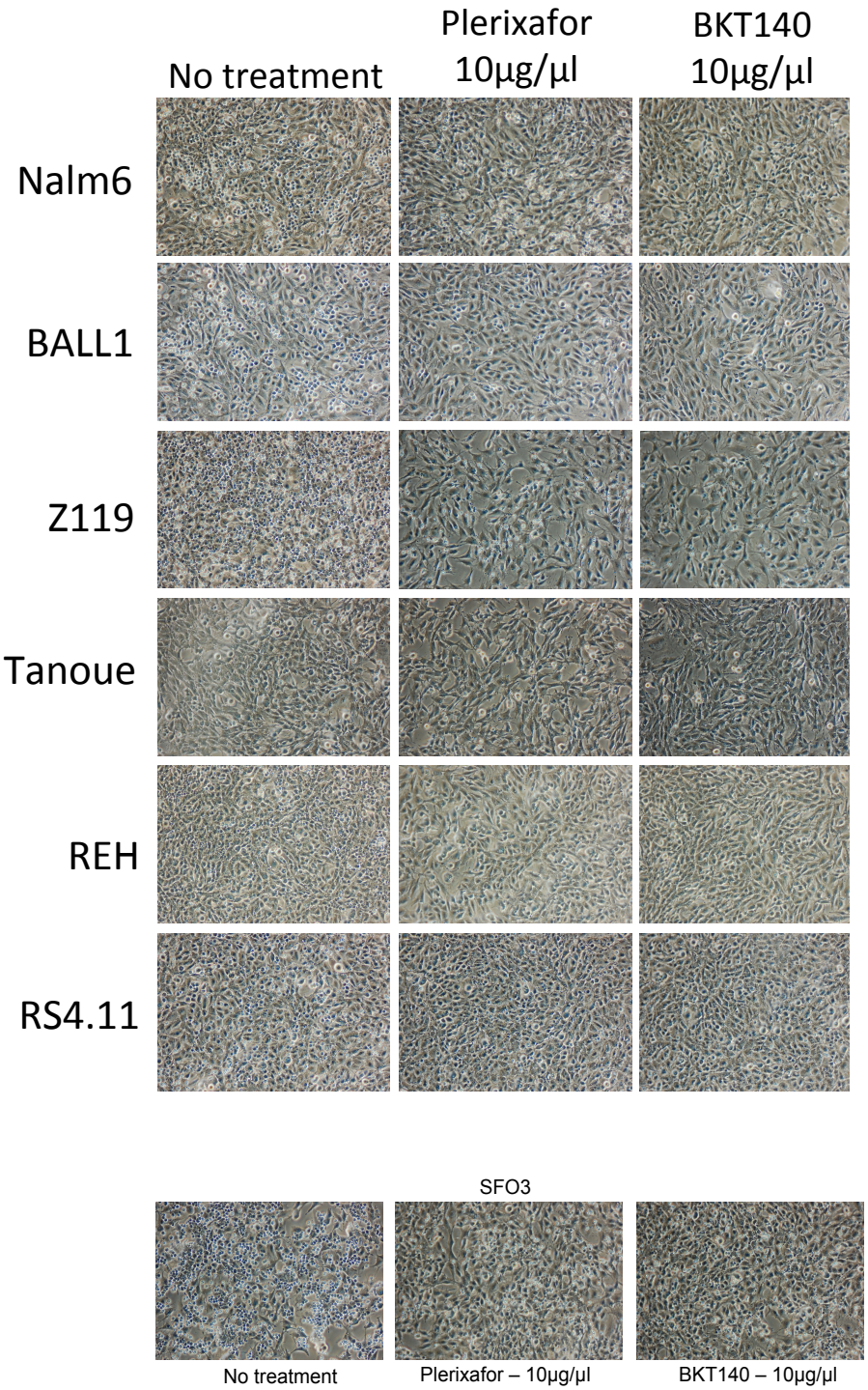
No treatment
Plerixafor 10µg/µl
BKT140 10µg/µl
Nalm6
BALL1
Z119
Tanoue
REH
RS4.11
SFO3
No treatment
Plerixafor – 10µg/µl
BKT140 – 10µg/µl

Figure 17

Figure 17. CXCR4 inhibitors plerixafor (AMD3100) and BKT140 significantly reduce Pseudoemperipolesis (PEP) of B-ALL cells. Representative phase contrast microscopy images show B-ALL cell lines and SFO3 xenograft expanded primary cells undergoing pseudoemperipolesis (PEP) in the presence (center and right-most column) or absence (left-most column) of CXCR4 inhibitors.

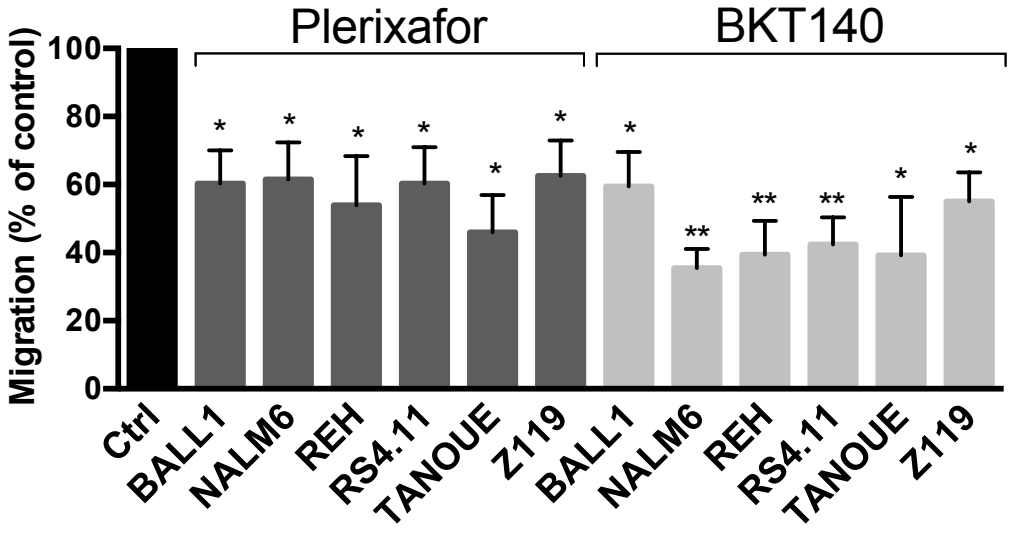
Plerixafor
BKT140
Migration (% of control)
100
80
60
40
20
0
*
*
*
*
*
*
*
**
**
**
*
*
Ctrl
BALL1
NALM6
REH
RS4.11
TANOUE
Z119
BALL1
NALM6
REH
RS4.11
TANOUE
Z119

Figure 18

Figure 18. CXCR4 inhibitors plerixafor (AMD3100) and BKT140 significantly reduce Pseudoemperipolesis of B-ALL cell lines. B-ALL cells were incubated in medium alone (control) or medium containing (10µg/ml) plerixafor (AMD3100) or BKT140. The cells were allowed to migrate beneath BMSCs and then counted in flow cytometer for quantification. The bar diagrams represent the mean PEP (± SEM) of 6 B-ALL cell lines in the presence or absence of CXCR4 inhibitors. PEP was significantly inhibited by both CXCR4 inhibitors (plerixafor/BKT140), with $*p < 0.05$; $**p < 0.01$; $***p < 0.001$ as indicated by the asterisks.

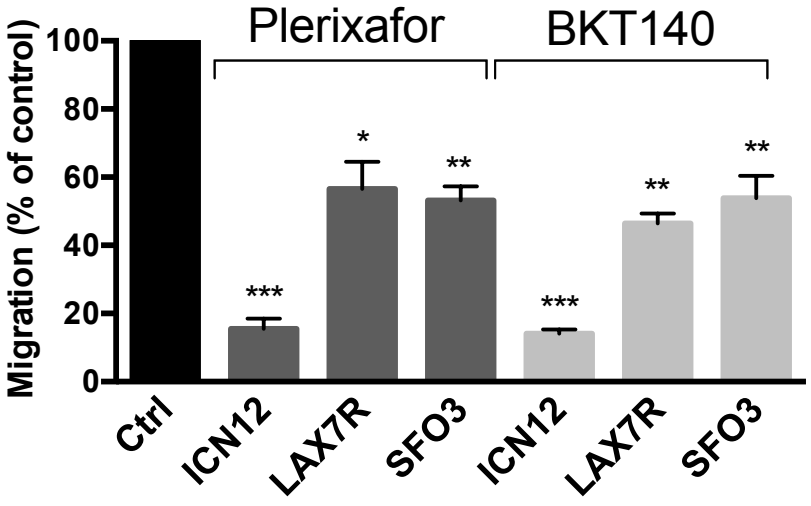
Plerixafor
BKT140
Migration (% of control)
100
80
60
40
20
0
***
*
**
***
**
**
Ctrl
ICN12
LAX7R
SFO3
ICN12
LAX7R
SFO3

Figure 19

Figure 19. CXCR4 inhibitors plerixafor (AMD3100) and BKT140 significantly reduce Pseudoemperipolesis of xenograft expanded primary B-ALL cells. Xenograft expanded primary B-ALL cells were incubated in medium alone (control) or medium containing (10μg/ml) plerixafor (AMD3100) or BKT140. The cells were allowed to migrate beneath BMSCs and then counted in flow cytometer for quantification. The bar diagrams represent the mean PEP (± SEM) of 3 xenograft expanded primary B-ALL cell lines in the presence or absence of CXCR4 inhibitors. PEP was significantly inhibited by both CXCR4 inhibitors (plerixafor/BKT140), with $*p < 0.05$; $**p < 0.01$; $***p < 0.001$ as indicated by the asterisks.

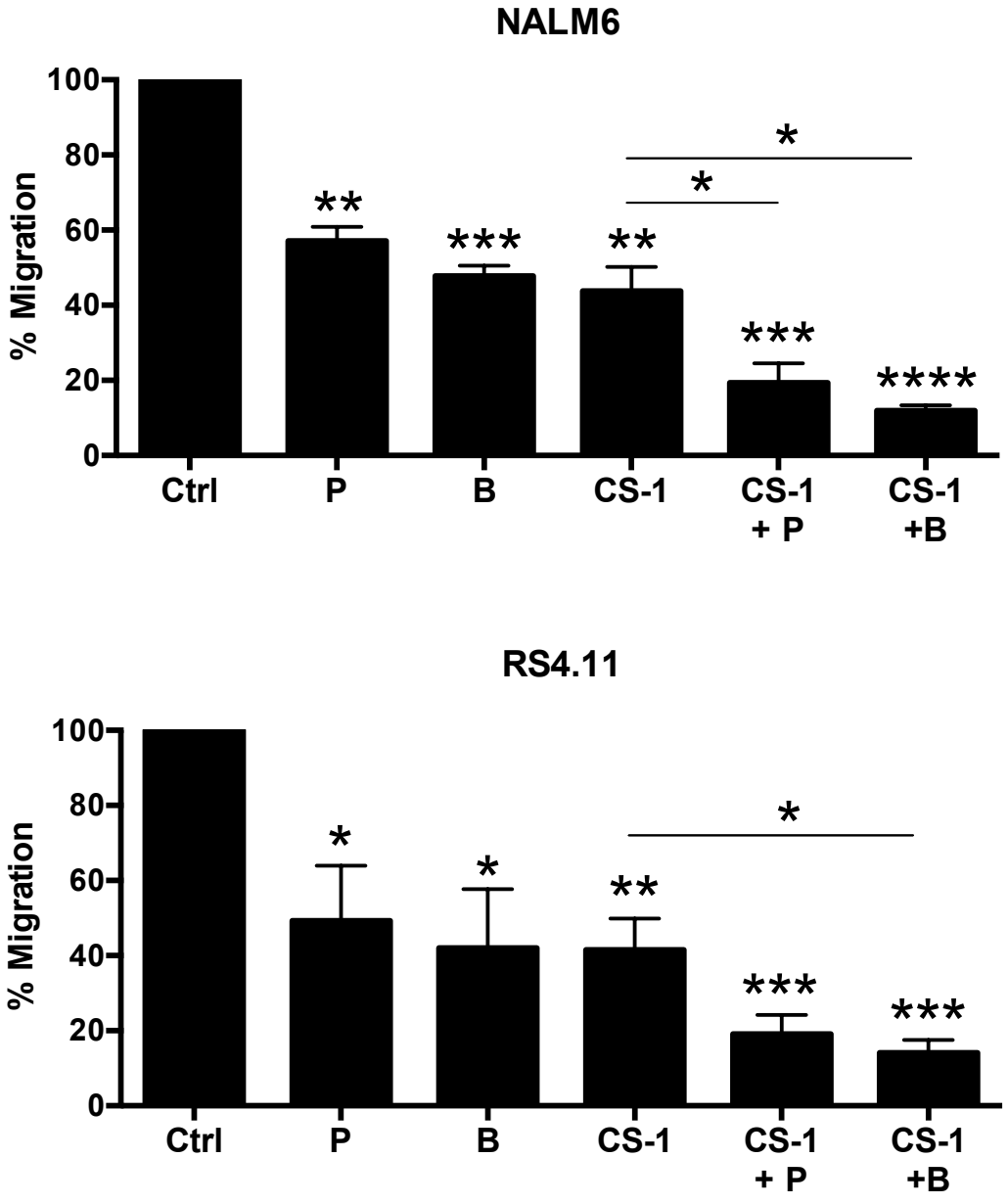
NALM6
% Migration
100
80
60
40
20
0
**
***
**
*
*
***
****
Ctrl
P
B
CS-1
CS-1 + P
CS-1 +B
RS4.11
% Migration
100
80
60
40
20
0
*
*
**
*
***
***
Ctrl
P
B
CS-1
CS-1 + P
CS-1 +B

Figure 20

Figure 20. Combination treatment with CXCR4 and CD49d antagonists inhibits B-ALL cell migration beneath BMSC (PEP) more effectively than single inhibitor treatment. NALM6 B-ALL cells were incubated in medium alone (control), or medium supplemented with plerixafor (10μg/mL), BKT140 (10μg/mL), CS1 (10μg/mL), or combinations of CS-1 with either CXCR4 antagonist, and then placed in BMSC co-cultures. After 4 hours of incubation, and then counted in flow cytometer for quantification. The bar diagram represents the mean PEP (± SEM) (Plerixafor/BKT140), with *$p < 0.05$; **$p < 0.01$; ***$p < 0.001$ as indicated by the asterisks.

The bone marrow microenvironment is a complex milieu of various cell types and secreted or surface-bound factors. In this dynamic setting, various molecules, apart from CXCR4, are involved in the processes of adhesion and migration. CD49D has been implicated in adhesion of ALL cells in various previous studies. B-ALL cells showed reduced levels of migration beneath stromal cells when treated with CD49D levels. Interestingly, the combination of CXCR4 and CD49D further significantly reduced migration of NALM6 and RS4.11 cells beneath bone marrow stromal cells (Figure 20).

CXCR4 Knock out inhibits adhesion and migration of ALL cells

In addition to the pharmacological model of inhibition we created a genetic deletion model by knocking out CXCR4 from ALL cell lines using the CRISPR Cas9 editing technology (Figure 21) for NALM6 and TANOUE. CXCR4 expression levels were tested at regular intervals in wild type and knock out cells to monitor maintenance of CXCR4 deletion over time (data not shown). Figure 23 shows representative histograms of NALM6 and TANOUE CXCR4 wild type and knockout cell lines.

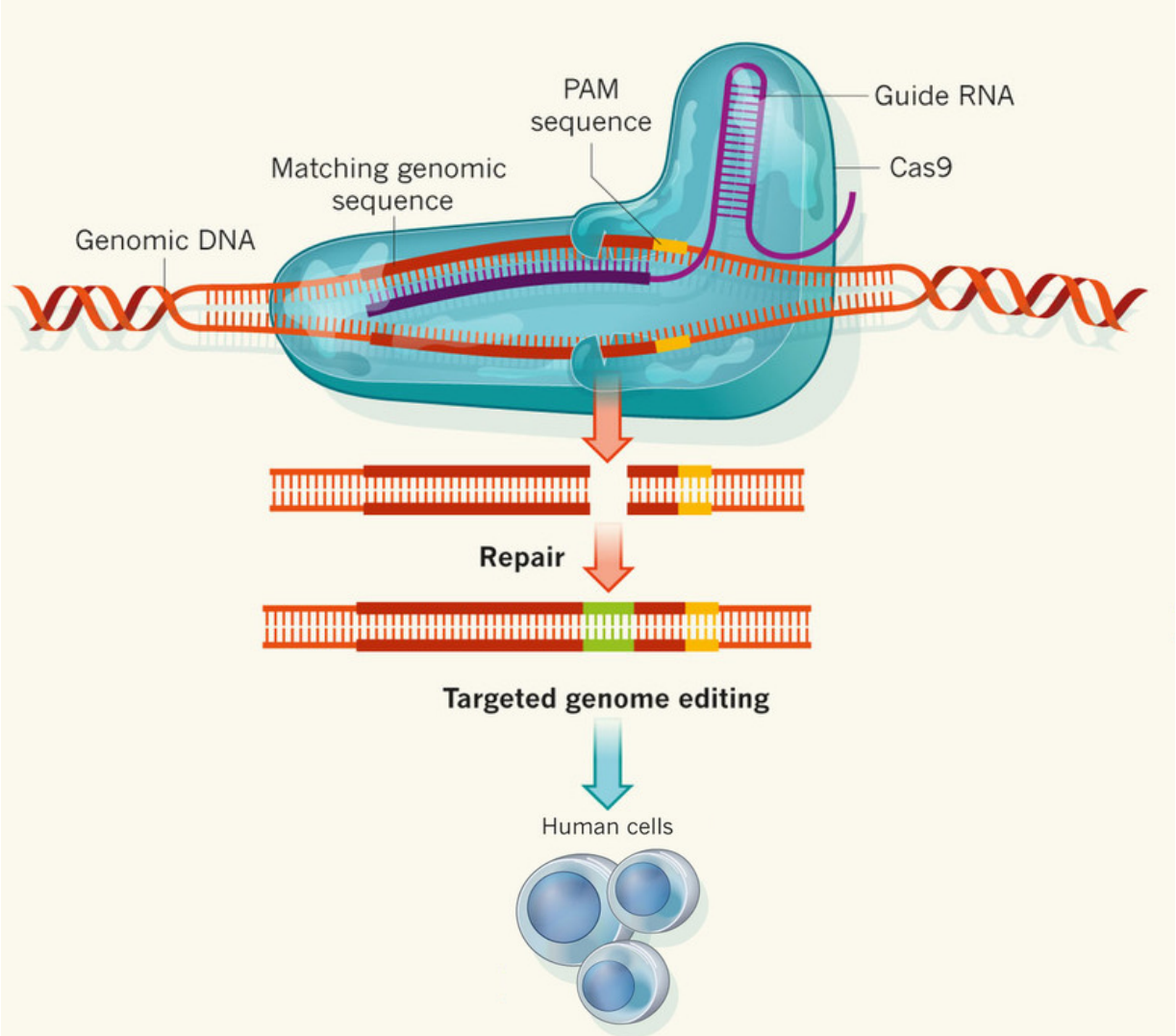
PAM
sequence
Guide RNA
Cas9
Matching genomic
sequence
Genomic DNA
Repair
Targeted genome editing
Human cells

Figure 21

Figure 21. The CRISPR-Cas9 gene editing technology (68). The CRISPR-Cas9 system functions as a part of defense system against invading DNA molecules for example viruses. The Cas9 enzyme is DNA endonuclease with two active sites that cleave the two strands of double-stranded DNA. The Cas9 enzyme is guided towards the target genomic site by an RNA molecule that is complementary to the target site, which is demarcated by the Protospacer Adjacent Motif (PAM) sequence. Consequently, the CRISPR-Cas9 system induces site-specific double stranded DNA breaks, which are repaired by the cells endogenous non-homologous end joining or homologous recombination.

Adapted with permission from

Charpentier, E., and J. A. Doudna. 2013. Biotechnology: Rewriting a genome. *Nature* 495: 50-51.

Table 1. Different parameters used to determine the ideal conditions for B-ALL cell electroporation.

Well	Voltage (V)	Width (millisecond)	Pulse
1	0	1	1
2	1400	20	1
3	1500	20	1
4	1600	20	1
5	1700	20	1
6	110	30	1
7	1200	30	1
8	1300	30	1
9	1400	30	1
10	1000	40	1
11	1100	40	1
12	1200	40	1
13	1100	20	2
14	1200	20	3
15	1200	20	4
16	1400	20	2
17	850	30	2
18	950	30	2
19	1050	30	2
20	1150	30	2
21	1300	10	3
22	1400	10	3
23	1500	10	3
24	1600	10	3

All knock out cell lines we established displayed significantly reduced chemotaxis and PEP as compared to their wild type counterparts corroborating the findings of the pharmacological inhibition of CXCR4. For example, chemotaxis and PEP of NALM6 CXCR4 KO cell line was 22.6 ± 12.5% and 41.8 ± 1.91 (mean ± SEM, $p<0.05$) respectively as compared to the wild type control (Figure 24). Similarly, chemotaxis to 100ng/mL CXCL12 and PEP beneath BMSCs for TANOUE CXCR4 KO was 10.3 ± 0.4% and 50.06 ± 2.5% respectively as compared to wild type control (Figure 24).

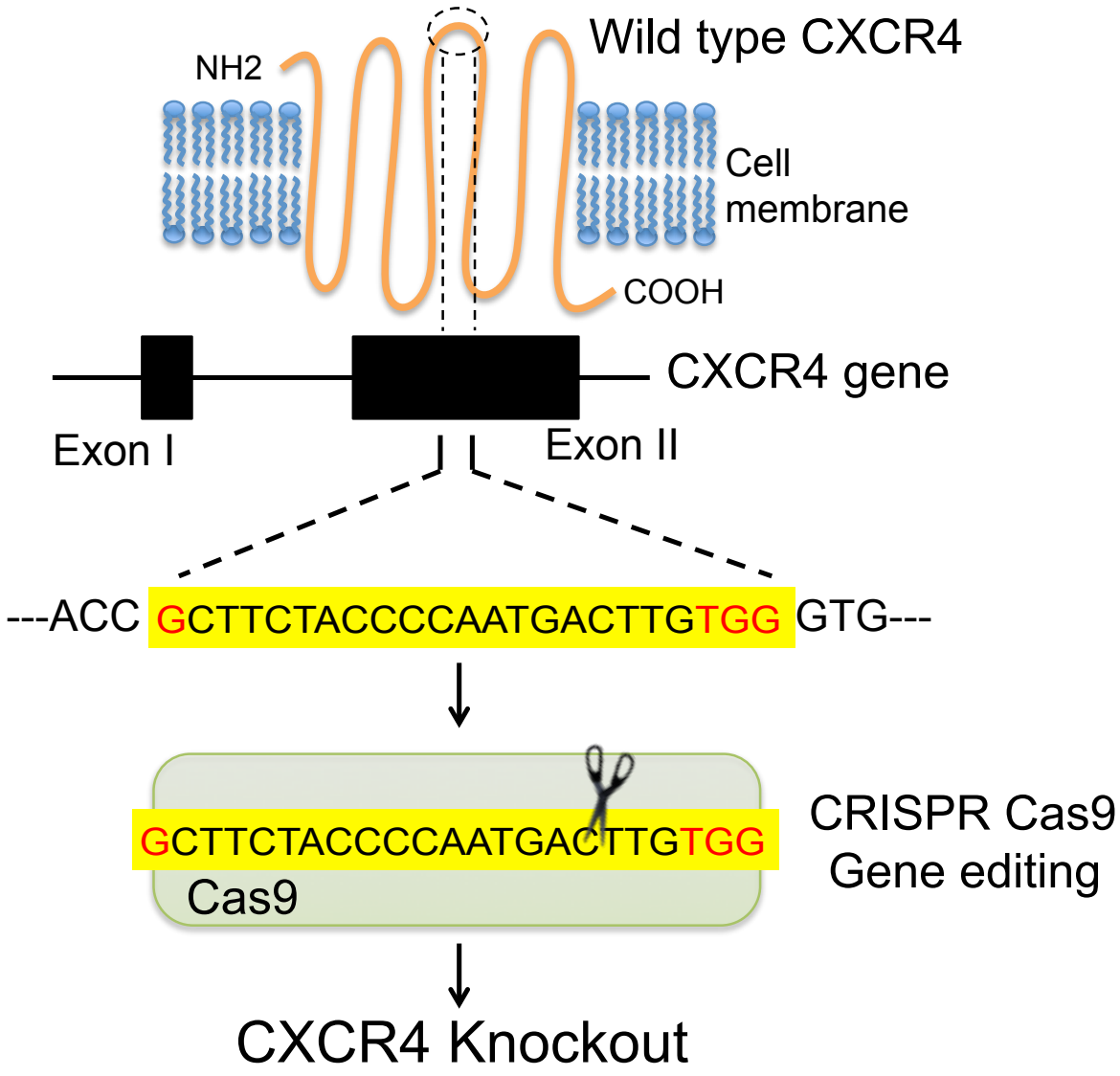
Wild type CXCR4
NH2
Cell membrane
COOH
CXCR4 gene
Exon I
Exon II
---ACC GCTTCTACCCCAATGACTTGTGG GTG---
GCTTCTACCCCAATGACTTGTGG
Cas9
CRISPR Cas9
Gene editing
CXCR4 Knockout

Figure 22

Figure 22. CXCR4 deletion from B-ALL using the CRISPR-Cas9 gene editing system. Figure depicts the mechanism of CXCR4 deletion through CRISPR-Cas9 gene editing system. The CRISPR Cas9 was directed towards the second extra cellular loop to introduce a frame-shift mutation resulting in lack of expression of the CXCR4 protein.

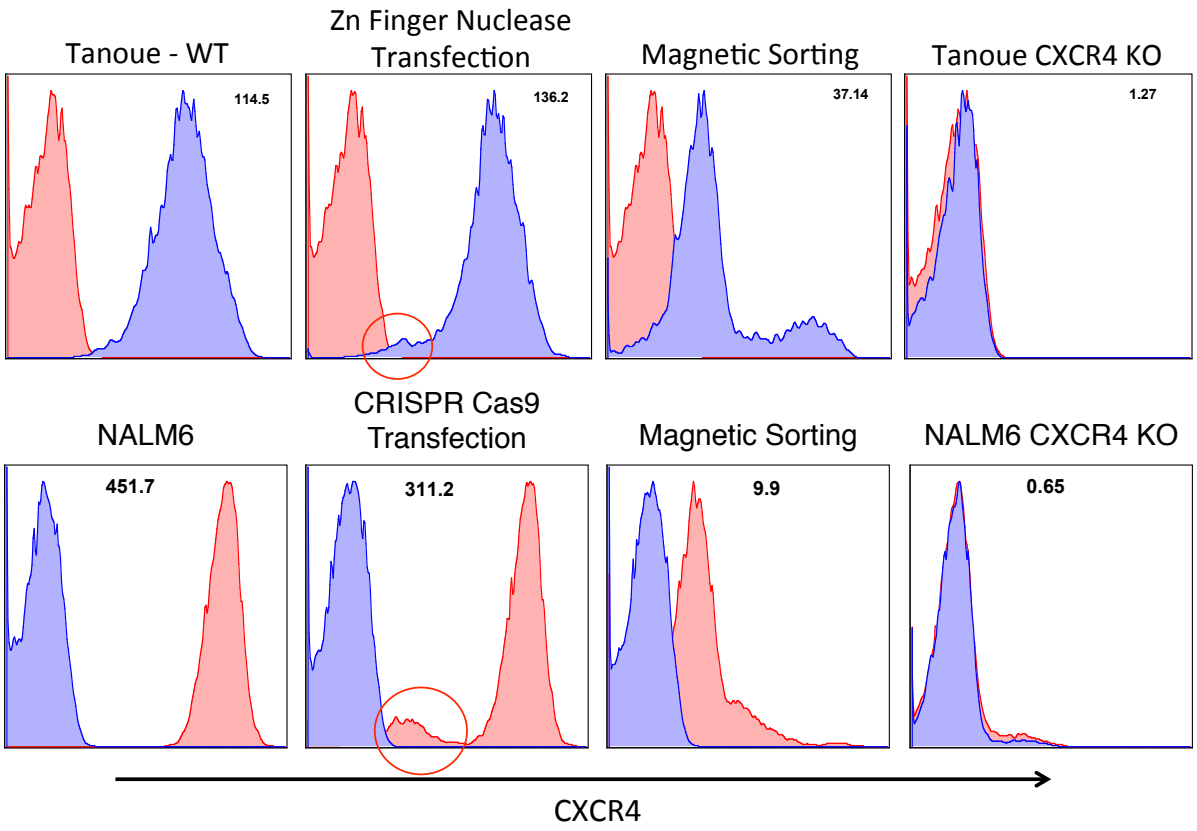
Tanoue - WT
Zn Finger Nuclease Transfection
Magnetic Sorting
Tanoue CXCR4 KO
114.5
136.2
37.14
1.27
NALM6
CRISPR Cas9 Transfection
Magnetic Sorting
NALM6 CXCR4 KO
451.7
311.2
9.9
0.65
CXCR4

Figure 23

Figure 23. CXCR4 deletion workflow from B-ALL cell lines. Histograms represent Mean Fluorescent intensity of CXCR4 at different steps in the generation of two CXCR4 knockout B-ALL cell lines, TANOUE (top) and NALM6 (bottom). The workflow shows histograms (left most) depicting expression of CXCR4 in wild type cells. Transfection of the CRISPR-Cas9 plasmid produces a small population of CXCR4 negative cells (circled in red), which was then sorted out using magnetic sorting to a pure population of CXCR4 negative TANOUE and NALM6 cells.

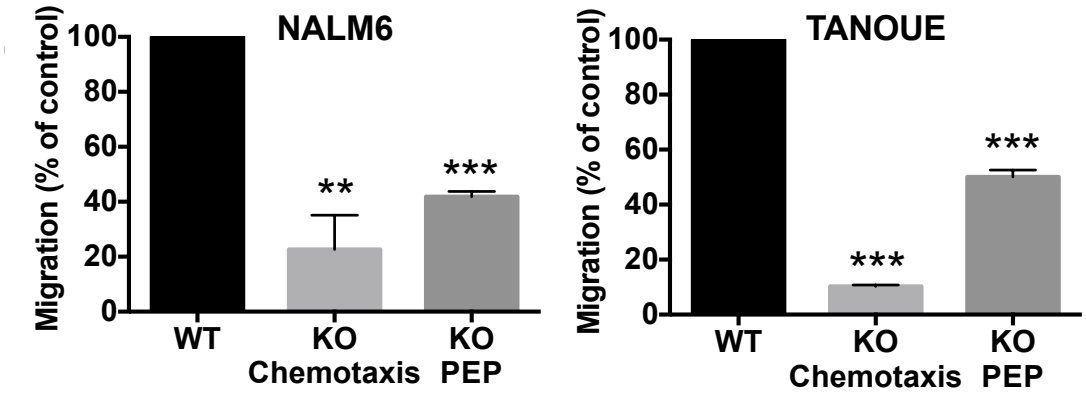
NALM6
Migration (% of control)
100
80
60
40
20
0
**
***
WT
KO Chemotaxis
KO PEP
TANOUE
Migration (% of control)
100
80
60
40
20
0
***
***
WT
KO Chemotaxis
KO PEP

Figure 24

Figure 24. CXCR4 gene deletion significantly decreases chemotaxis and PEP of B-ALL cell lines. NALM6 and TANOUE WT and KO cells (both untreated) were allowed to undergo chemotaxis towards 100 ng/mL CXCL12 or PEP beneath 9-15C Bone Marrow Stromal Cells and counted in flow cytometer for quantification. Bar diagrams representing mean chemotaxis/PEP (± SEM) show significant inhibition by both CXCR4 inhibitors (Plerixafor/BKT140), with $*p < 0.05$; $**p < 0.01$; $***p < 0.001$ as indicated by the asterisks.

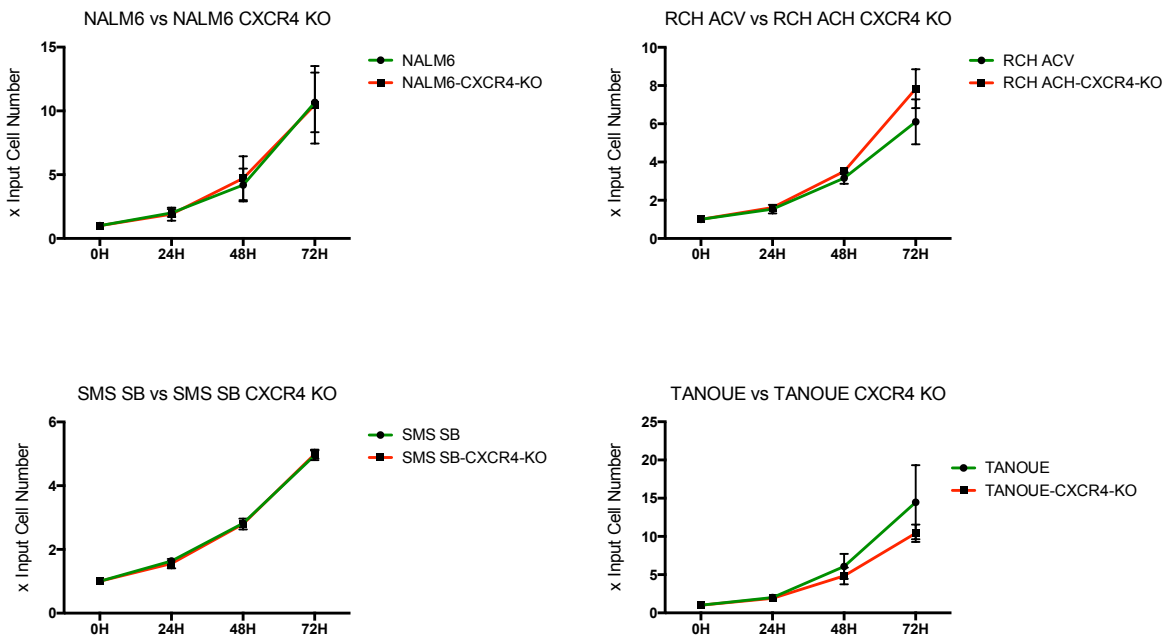
NALM6 vs NALM6 CXCR4 KO
x Input Cell Number
15
10
5
0
0H
24H
48H
72H
NALM6
NALM6-CXCR4-KO
RCH ACV vs RCH ACH CXCR4 KO
x Input Cell Number
10
8
6
4
2
0
0H
24H
48H
72H
RCH ACV
RCH ACH-CXCR4-KO
SMS SB vs SMS SB CXCR4 KO
x Input Cell Number
6
4
2
0
0H
24H
48H
72H
SMS SB
SMS SB-CXCR4-KO
TANOUE vs TANOUE CXCR4 KO
x Input Cell Number
25
20
15
10
5
0
0H
24H
48H
72H
TANOUE
TANOUE-CXCR4-KO

Figure 25

Figure 25. Growth rate comparison of wild type vs. knockout B-ALL cell lines. Graphs depict mean ± SEM of three independent growth assays. The cell number at time point 0 hours was taken as baseline and each time point thereafter (24, 48 and 72 hours) divided by 0 hours to obtain a times input cell number ratio which was plotted on graphs shown above.

CXCR4 Knockout does not affect growth rate of B-ALL cell lines

CXCL12 was first discovered as a Pre-B-Cell growth-stimulating factor(69). To determine the effect of CXCR4 knockout on B-ALL cell lines, we conducted a growth assay comparing the growth rates of wild type vs. knockout cell lines. Figure 25 shows results from three separate experiments. No significant difference in growth rates between wild type and knockout cell lines was observed indicating that malignant cells, at least the ones in culture, have adapted themselves to overcome CXCR4 dependent proliferation.

Bone marrow Stromal Cells provide Cell-Adhesion Mediated Drug Resistance to B-ALL Cells

Figures 26, 27 and 28 represent dose response curves for 4-Hydroperoxy Cyclophosphamide, Dexamethasone and Vincristine for all B-ALL cell lines. The dose response curves were used to determine IC50 concentrations at 48 hours for further experiments.

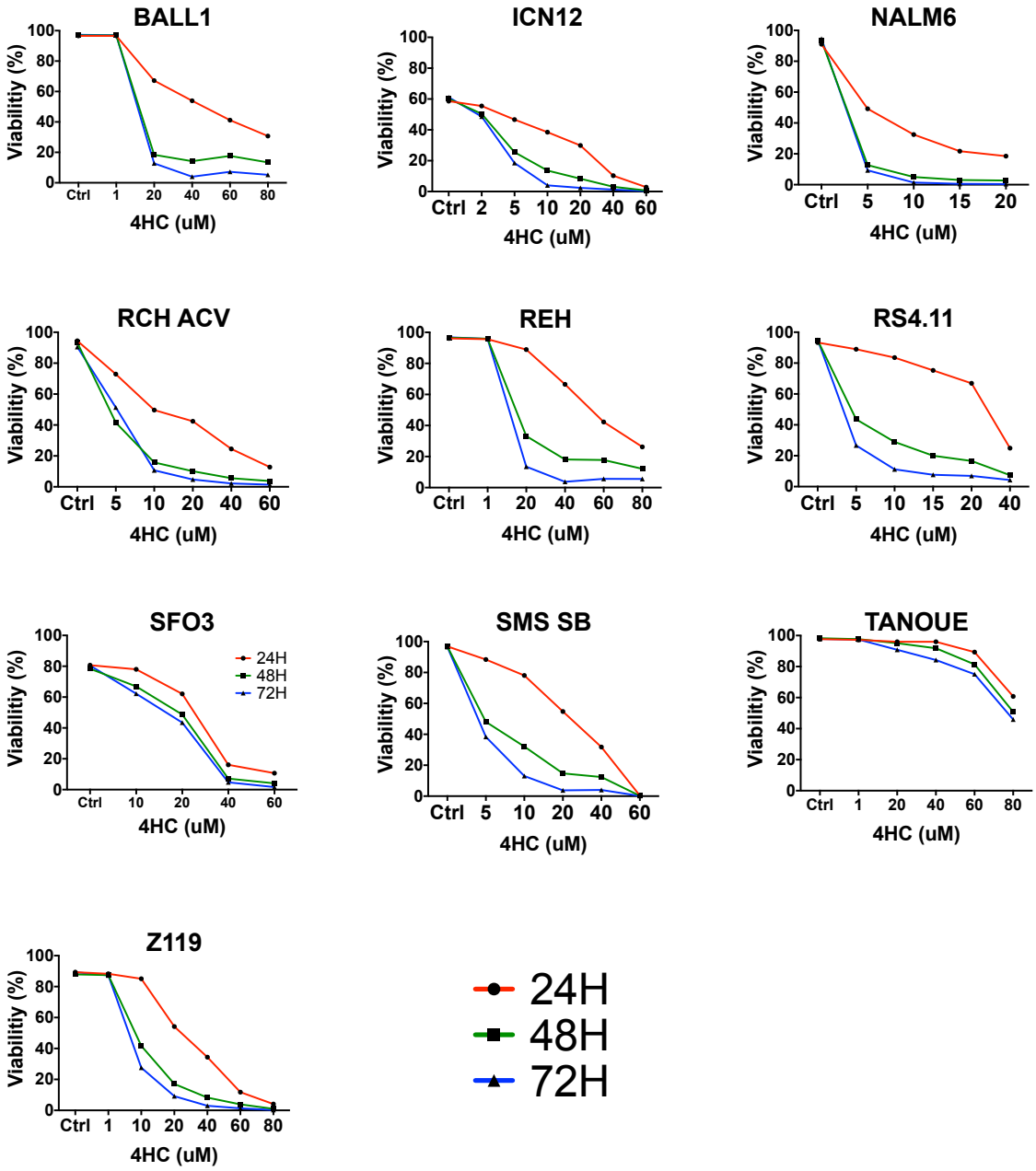
BALL1
ICN12
NALM6
RCH ACV
REH
RS4.11
SFO3
SMS SB
TANOUE
Z119
Viability (%)
4HC (uM)
24H
48H
72H

Figure 26

Figure 26. Dose determination of 4-Hydroperoxy Cyclophosphamide (4HC) in B-ALL cell lines. Graphs represent dose response curves of B-ALL cell lines treated with different doses of 4HC (x-axis). Viability (y-axis) was measured using Propidium Iodide/$DiOC_6$ staining at 24 (red line), 48 (green line) and 72 (blue line) hours.

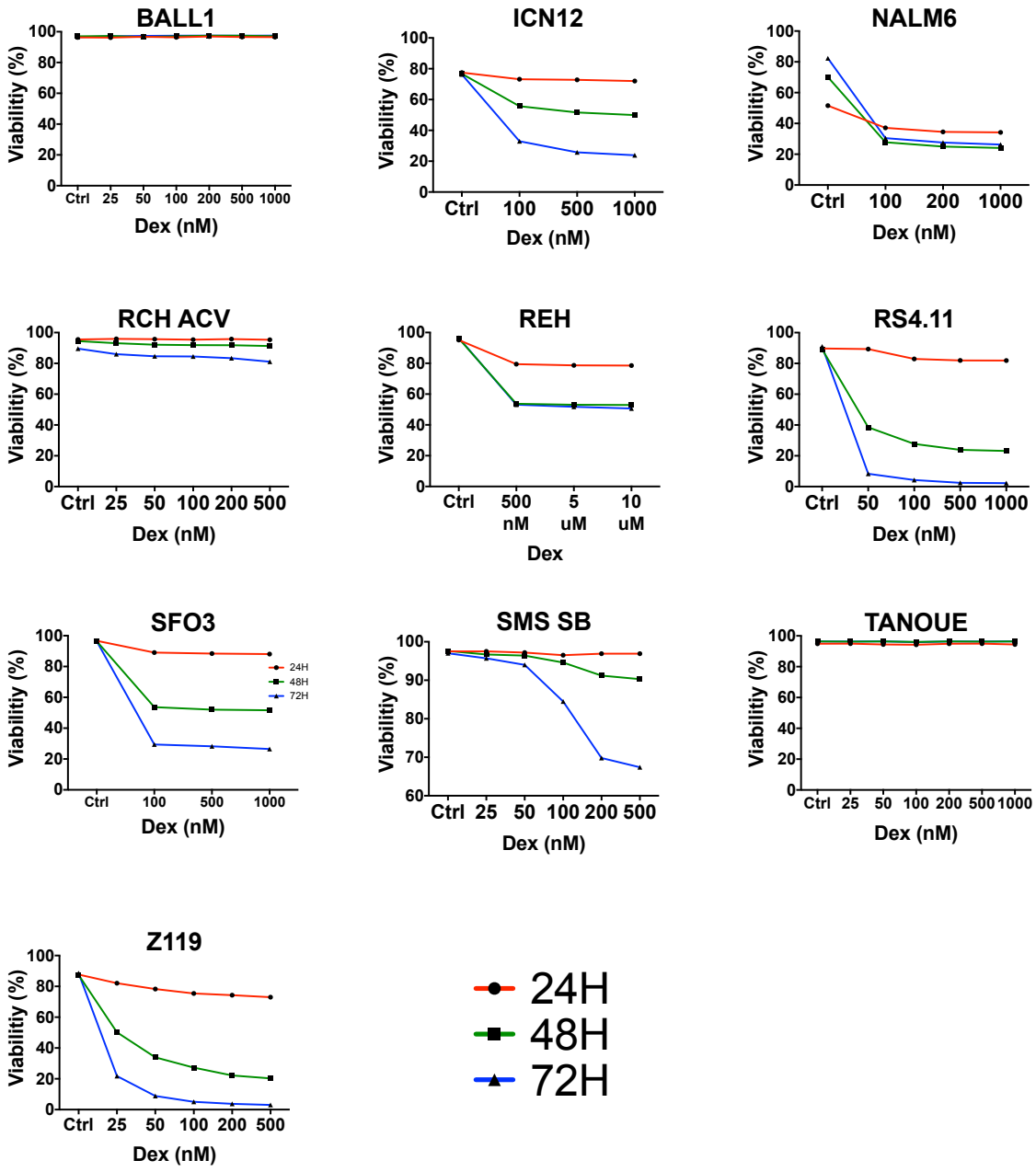
BALL1
Viability (%)
Ctrl 25 50 100 200 500 1000
Dex (nM)
ICN12
Viability (%)
Ctrl 100 500 1000
Dex (nM)
NALM6
Viability (%)
Ctrl 100 200 1000
Dex (nM)
RCH ACV
Viability (%)
Ctrl 25 50 100 200 500
Dex (nM)
REH
Viability (%)
Ctrl 500 nM 5 uM 10 uM
Dex
RS4.11
Viability (%)
Ctrl 50 100 500 1000
Dex (nM)
SFO3
Viability (%)
Ctrl 100 500 1000
Dex (nM)
24H
48H
72H
SMS SB
Viability (%)
Ctrl 25 50 100 200 500
Dex (nM)
TANOUE
Viability (%)
Ctrl 25 50 100 200 500 1000
Dex (nM)
Z119
Viability (%)
Ctrl 25 50 100 200 500
Dex (nM)
24H
48H
72H

Figure 27

Figure 27. Dose determination of Dexamethasone (Dex) in B-ALL cell lines. Graphs represent dose response curves of B-ALL cell lines treated with different doses of Dex (x-axis). Viability (y-axis) was measured using Propidium Iodide/$DiOC_6$ staining at 24 (red line), 48 (green line) and 72 (blue line) hours.

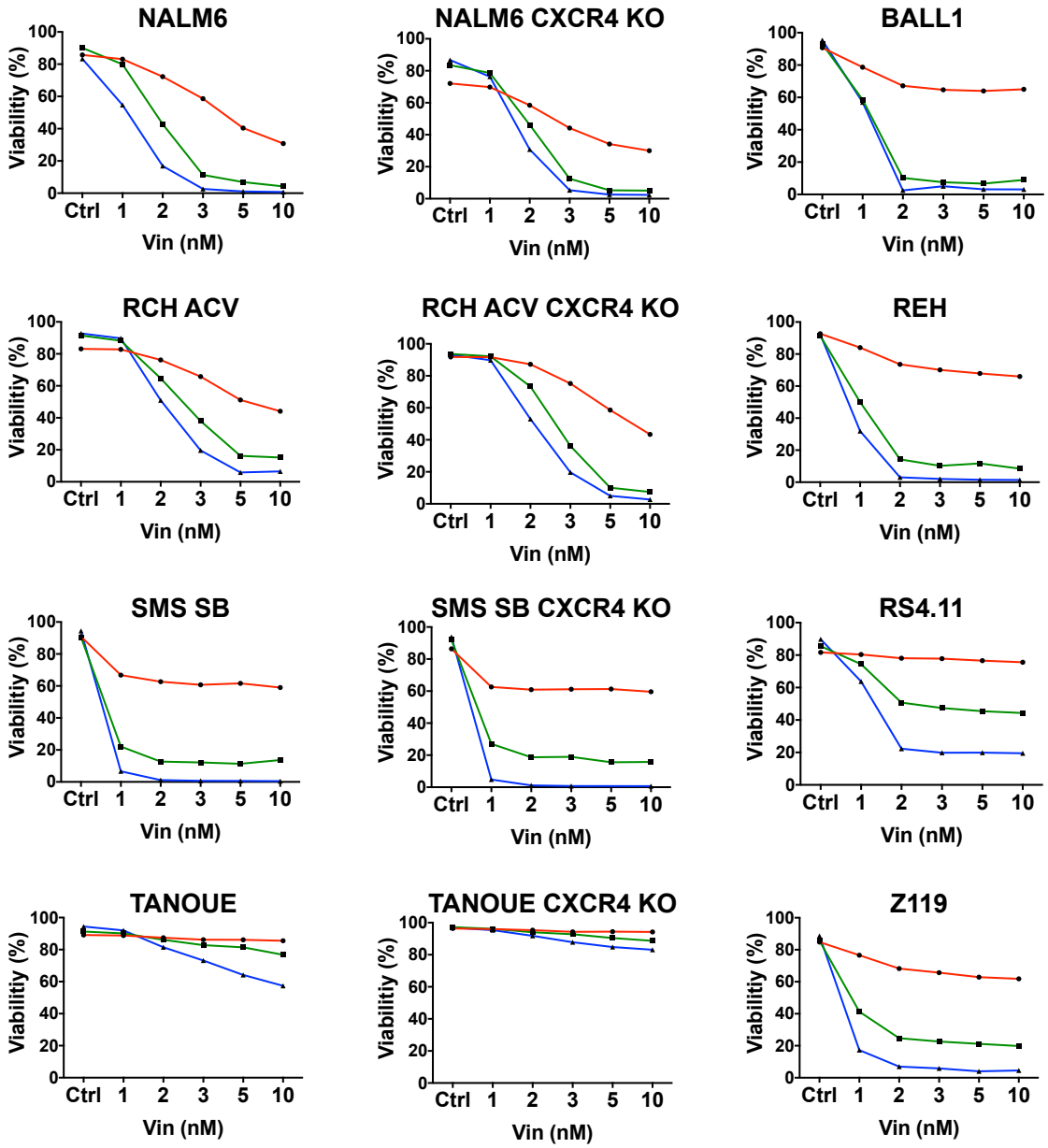
NALM6
NALM6 CXCR4 KO
BALL1
RCH ACV
RCH ACV CXCR4 KO
REH
SMS SB
SMS SB CXCR4 KO
RS4.11
TANOUE
TANOUE CXCR4 KO
Z119
Viability (%)
Vin (nM)
Ctrl 1 2 3 5 10
0 20 40 60 80 100

Figure 28

Figure 28. Dose determination of Vincristine (Vin) in B-ALL cell lines. Graphs represent dose response curves of B-ALL cell lines treated with different doses of Vin (x-axis). Viability (y-axis) was measured using Propidium Iodide/$DiOC_6$ staining at 24 (red line), 48 (green line) and 72 (blue line) hours.

Vincristine

Control 2nM 3nM 5nM 10nM

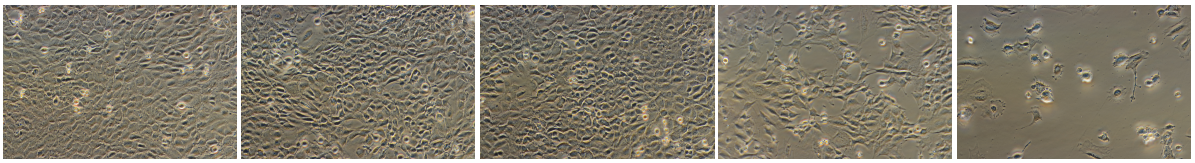

Dexamethasone

Control 25nM 100nM 200nM 500nM

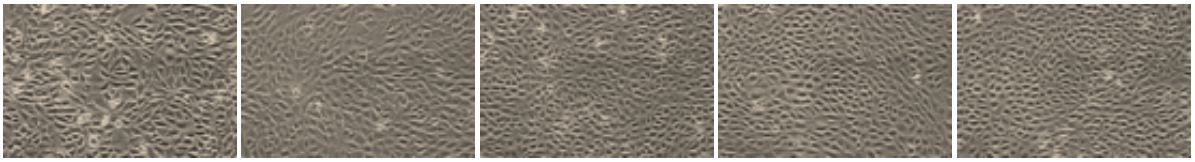

Figure 29

Figure 29. Effect of chemotherapy drugs on BMSCs. Phase contrast microscopy images represent growth of 9-15C murine BMSC cell line after 48 hours of treatment with difference concentrations of Vincristine and Dexamethasone.

To determine whether the chemotherapeutic drugs have any adverse effects on the bone marrow stromal cells being used, the stromal cell line was treated with indicated concentrations of Dexamethasone and Vincristine before conducting chemo-sensitization assays. As stated earlier, the concentration range of Vincristine for B-ALL cell lines is 2-3 nM and 50-100 nM for Dexamethasone. It was observed that IC_{50} concentrations for both drugs for B-ALL cells did not affect the 9-15C cell line. Vincristine did, however have an effect at concentrations of 5nM and above.

4-Hydroperoxy Cyclophosphamide (4HC) was not tested on the stromal cells because 4HC treatment includes incubation of B-ALL cells for 45 minutes and then change of media. Due to this the stromal cells are not exposed to the drug.

To determine the effect of chemotherapeutic drugs on the B-ALL cells that had undergone PEP, we measured viability of a drug treated co-culture well. The well was thoroughly washed and supernatant discarded. The stromal layer with the migrated B-ALL cells was then trypsinized and viability measured using PI/$DiOC_6$ staining. Figure 29 depicts the gating strategy for this experiment. Briefly, a well with drug treated B-ALL cell line alone was taken as a gating template and all cells, alive and apoptotic, were gated around to get a lymphocyte gate. This gate was then applied to the drug treated co-culture. Since stromal cells

are much larger than B-ALL cells, they were outside this lymphocyte gate. The cells inside this lymphocyte gate were then analyzed for percentage of viable cells.

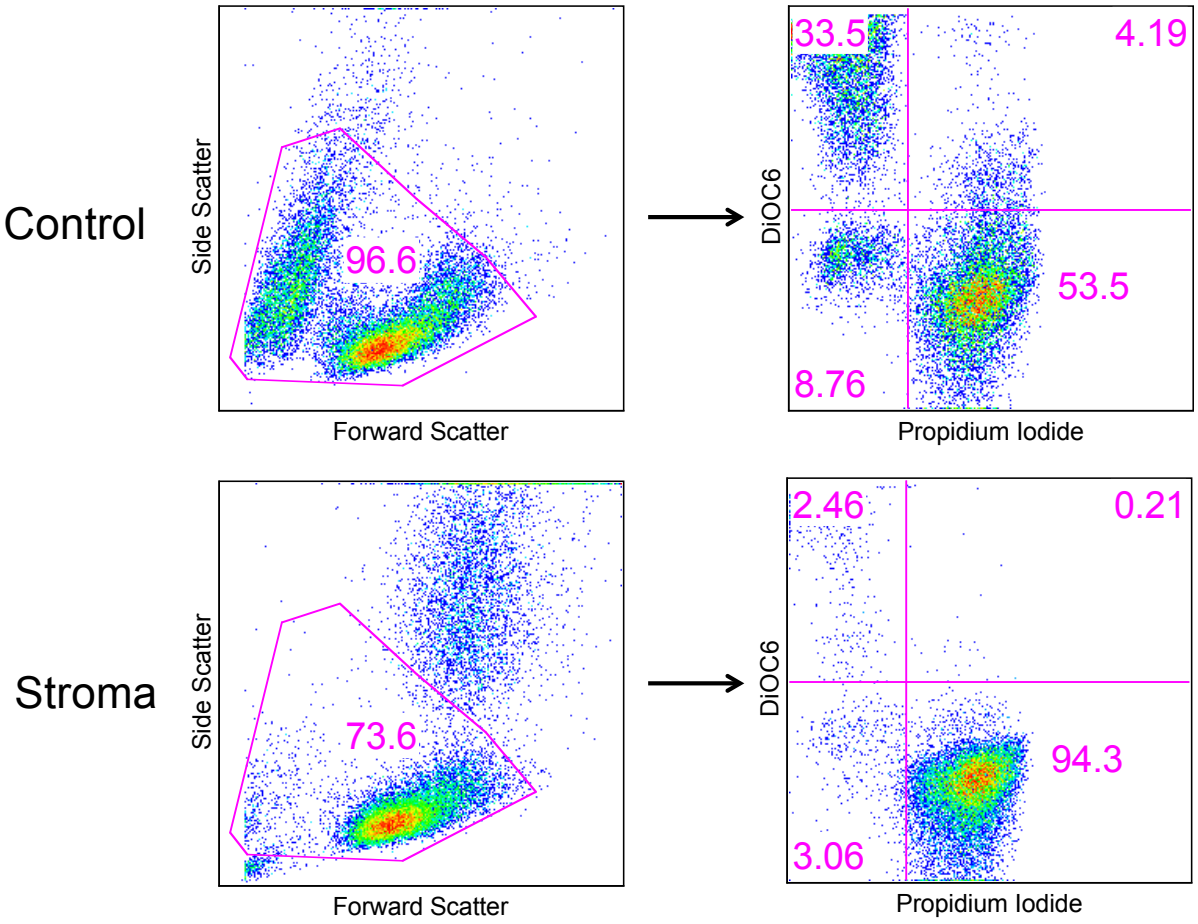
Control
Side Scatter
96.6
Forward Scatter
33.5
4.19
53.5
8.76
DiOC6
Propidium Iodide
Stroma
Side Scatter
73.6
Forward Scatter
2.46
0.21
94.3
3.06
DiOC6
Propidium Iodide

Figure 30

Figure 30. Gating strategy for viability measurement of B-ALL cells migrated beneath BMSCs. A lymphocyte gate that includes viable and apoptotic cells for drug treated NALM6 cells alone was generated (top left dot plot) and applied to the drug treated NALM6-BMSC co-culture well (bottom left dot plot) and PI/$DiOC_6$ staining assessed for cells within this gate (right hand side dot plots).

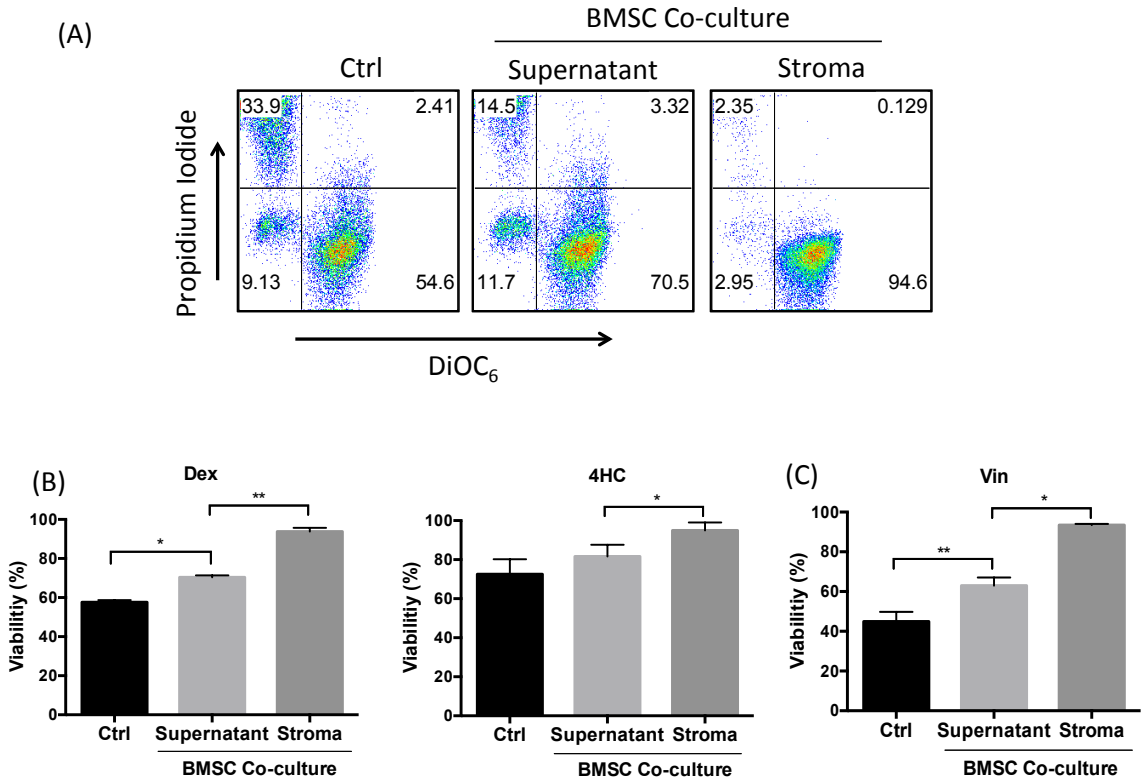
(A)
BMSC Co-culture
Ctrl
Supernatant
Stroma
Propidium Iodide
33.9
2.41
9.13
54.6
14.5
3.32
11.7
70.5
2.35
0.129
2.95
94.6
DiOC6
(B)
Dex
4HC
(C)
Vin
Viability (%)
Ctrl
Supernatant
Stroma
BMSC Co-culture

Figure 31

Figure 31. Bone Marrow Stromal Cell (BMSC) co-culture overcomes drug-induced cytotoxicity of B-ALL cell line. (A) Dot plots show representative experiment depicting viability of drug (Dex) treated NALM6 cells in the presence and absence of BMSC co-culture. In the NALM6-BMSC co-culture sample, viability of NALM6 cells in supernatant and those that migrated beneath the stroma was measured separately. (B) Bar graphs show mean of three separate experiments illustrated in contour plots (A). In addition to Dex treatment (left-hand graph), the experiment was also performed with 2.5μM 4-HydroperoxyCyclophosphamide (4HC) and Vincristine in the presence and absence (control) of BMSC co-culture. Bar diagrams represent mean drug induced cytotoxicity (± SEM) of three separate experiments. Viability was measured using PI/$DiOC_6$ staining at 48H and asterisks indicate significant differences in cytotoxicity (*$p < 0.05$; **$p < 0.01$).

To test the effect of Bone Marrow Stromal Cells on drug induced cytotoxicity, NALM6 cells were treated with Dexamethasone (Dex), 4-HydroperoxyCyclophosphamide (4HC), Vincristine (Vin) with and without co-culture with 9-15C stromal cell line and viability measured using PI/DiOC6. Figure 30 shows representative dot plots of Dex treated NALM6 cells in the presence and absence of 9-15C stromal cell line. Co-culture of NALM6 cells with mesenchymal marrow stromal cell line (9-15C) significantly increased viability to 70.3 ± 1.04% as compared to 57.6 ± 1.08% from treatment with Dex alone (mean ± SEM, $p<0.05$). Similarly, mesenchymal marrow stromal cell line (9-15C) significantly increased viability of NALM6 to 63 ± 4.1% as compared to 44.9 ± 4.8% from treatment with Vin alone (mean ± SEM, $p<0.05$). A similar trend was observed with 4HC treatment where the viability for NALM6 cells with 4HC treatment alone was 72.5 ± 4.46% and was increased to 81.67 ± 3.45% with BMSC co-culture (mean ± SEM, p=not significant). However, only a modest rescue was observed in the supernatant of the co-culture. As stated earlier, B-ALL cells undergo Pseudoemperipolesis and reside under BMSCs, to analyze drug induced cytotoxicity in those cells the BMSC layer was trypsinized and viability measured (gating strategy depicted in Figure 29). Cells that had undergone PEP and were beneath the stromal cells were highly resistant to Dex, 4HC and Vin with viability of 93.7 ± 1.9%, 94.9 ± 2.3%, 93.4 ± 0.5% (mean ± SEM, $p<0.05$)

respectively as compared to the NALM6 cells in the supernatant (Figure 30).

CXCR4 inhibition or deletion overcomes BMSC derived drug resistance

To test the effect of inhibition of chemokine receptor CXCR4 on BMSC derived chemotherapy resistance, NALM6 cells were pre-treated with, 10μg/ml Plerixafor or 10μg/ml BKT140 before Dex, 4HC or Vin drug treatment. The addition of Plerixafor or BKT140 to the Dex-NALM6-BMSC co-culture significantly decreased the viability of NALM6 cells to 57.9 ± 3.2% and 54.2 ± 3.2% respectively as compared to the Dex-NALM6-BMSC co-culture alone (72.38 ± 0.25%, mean ± SEM, $p<0.05$) (Figure 4A). Similarly, Plerixafor/BKT140 addition to the Vin-NALM6-BMSC co-culture sensitized cells to Vin treatment increasing cytotoxicity to 33.8 ± 2.08% and 33.5 ± 3.1% viable cells respectively as compared to Vin-NALM6-BMSC alone (58.5 ± 1.6%, mean ± SEM, $p<0.05$). Lastly, Plerixafor/BKT140 addition to the 4HC-NALM6-BMSC co-culture increased cytotoxicity to 66.03 ± 5.1% and 67.1 ± 1.2% viable cells respectively as compared to 4HC-NALM6-BMSC alone (82.9 ± 1%, mean ± SEM, $p<0.05$) (Figure 4A). This reversal of acquired resistance of NALM6 after the addition of CXCR4 inhibitors outlines the critical role that CXCR4 plays in making the cells resistant to chemotherapy. Similar

results obtained with Dex treated ICN12 xenograft and REH and Z119 cell lines indicating that this is not a cell line phenomenon (Figure 31).

To further dissect the mechanism by which the BMSCs provide leukemia cells with resistance, we replaced the BMSCs in the co-culture cytotoxicity experiment above with recombinant CXCL12 (Figure 4B). It was observed that CXCL12 alone also rescued NALM6 cells from chemotherapy-induced cytotoxicity (66.7 ± 0.8%) as compared to Dex treatment alone (56.7 ± 2.3%, mean ± SEM, $p<0.05$). The addition of 10μg/ml Plerixafor or BKT140 abolished this rescue (56.9 ± 2.7 and 52.6 ± 3.9% respectively) as compared to Dex alone (56.73 ± 2.31%, mean ± SEM, $p<0.05$). Similar results were observed with Vincristine, corroborating the findings of the previous experiments and indicating the CXCR4 is one of the critical mechanisms used by NALM6 for chemo-resistance.

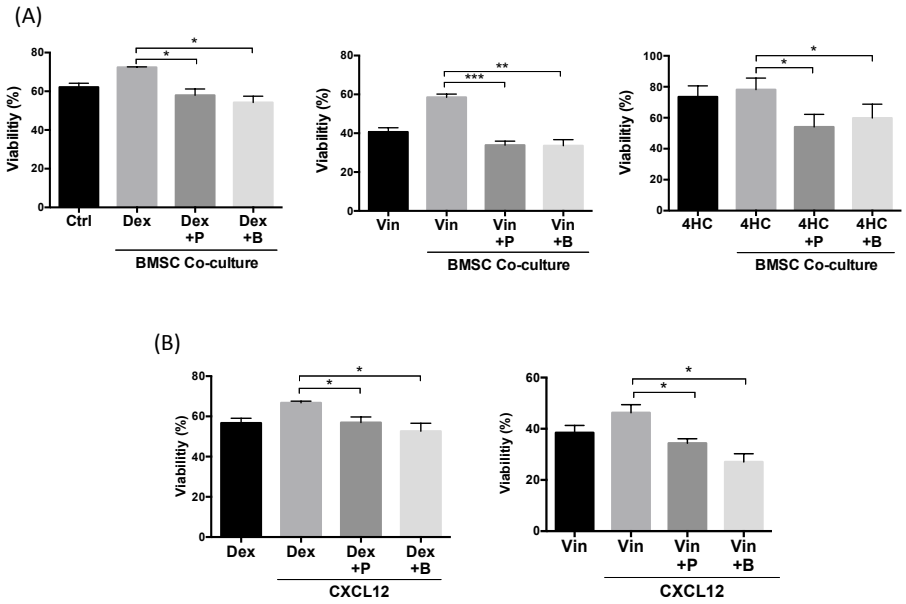
(A)
Viability (%)
Ctrl
Dex
Dex +P
Dex +B
BMSC Co-culture
Vin
Vin +P
Vin +B
4HC
4HC +P
4HC +B
(B)
CXCL12

(C)

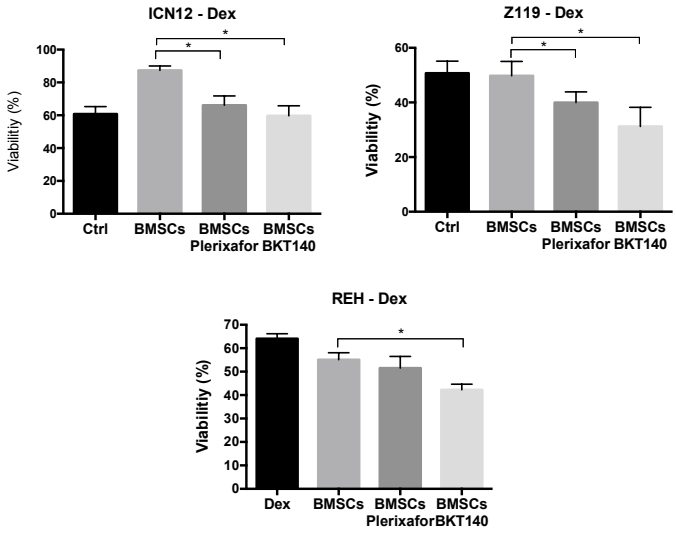
ICN12 - Dex
Z119 - Dex
REH - Dex
Viability (%)
Ctrl
BMSCs
BMSCs Plerixafor
BMSCs BKT140
Dex

Figure 32

Figure 32. <u>CXCR4 inhibitors sensitize NALM6 cells to chemotherapy.</u> (A) Bar graphs depict viability of NALM6 cells in supernatant, 48H after treatment with 100 nM Dexamethasone (Dex), 2nM Vincristine (Vin) and 2.5μM 4-Hydroperoxy Cyclophosphamide (4HC) in the presence and absence (control) of BMSC co-culture. Additionally, before plating on stromal cells, NALM6 cells were incubated in medium alone or medium containing (10μg/ml) Plerixafor (AMD3100) or BKT140. (B) Viability of NALM6 cells was analyzed 48H after treatment with 100 nM Dex or 2nM Vin in the presence and absence (control) of CXCR4 ligand CXCL12. Additionally, before the addition of CXCL12, NALM6 cells were incubated in medium alone or medium containing (10μg/ml) Plerixafor (AMD3100) or BKT140. (C) Bar graphs depict viability of ICN12, REH and Z119 cells in supernatant, 48H after treatment with 100 nM Dexamethasone (Dex) in the presence and absence (control) of BMSC co-culture. Additionally, before plating on stroma, cells were incubated in medium alone or medium containing (10μg/ml) Plerixafor (AMD3100) or BKT140. Bar diagrams represent mean drug induced cytotoxicity (± SEM) of three separate experiments. Viability was measured using PI/$DiOC_6$ staining at 48H and asterisks indicate significant differences in cytotoxicity ($*p < 0.05$).

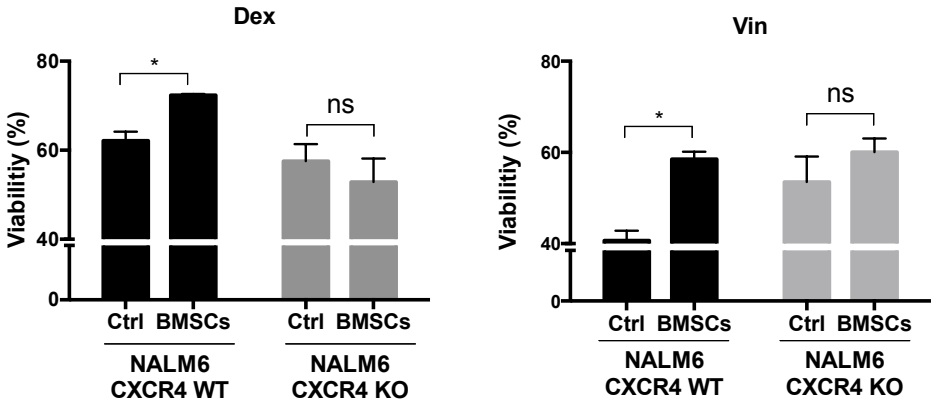
Dex
Viability (%)
80
60
40
0
*
ns
Ctrl
BMSCs
Ctrl
BMSCs
NALM6
CXCR4 WT
NALM6
CXCR4 KO
Vin
Viability (%)
80
60
40
0
*
ns
Ctrl
BMSCs
Ctrl
BMSCs
NALM6
CXCR4 WT
NALM6
CXCR4 KO

Figure 33

Figure 33. CXCR4 deletion abolishes BMSC derived rescue of drug treated NALM6 cells. NALM6 CXCR4 Wild type (WT) (black bars) and NALM6 CXCR4 Knockout (KO) (grey bars) were treated with 100 nM Dex (left hand side graph) or 2nM Vin (right hand side graph) in the presence and absence (control) of BMSC co-culture and viability measured for cells in the supernatant. Bar diagrams representing mean chemotaxis/PEP (± SEM) show significant inhibition by both CXCR4 inhibitors (Plerixafor/BKT140), with $*p < 0.05$; $**p < 0.01$; $***p < 0.001$ as indicated by the asterisks.

To further corroborate the findings of pharmacological inhibition of CXCR4 in the co-culture setting, NALM6 CXC4 KO cells were treated with Dexamethasone and Vincristine in the presence and absence of BMSCs (Figure 32). Unlike wild type NALM6 cells, Dex or Vin treated NALM6 CXCR4 KO cell line showed no significant difference in cytotoxicity in the absence or presence of BMSCs (57.5 ± 3.8% vs. 52.8 ± 5.2% for Dex and 53.5 ± 5.5% vs. 60.06 ± 2.9% for Vin, respectively, mean ± SEM, p=not significant). The failure of BMSCs to rescue NALM6 CXCR4 KO from Dex induced cytotoxicity indicates the importance of CXCR4 in acquired chemo-resistance.

CXCR4 deletion decreases leukemia burden, bone marrow infiltration and increases survival in leukemic mice

To test the effect of CXCR4 deletion in vivo, nine non-irradiated NSG mice per group were injected with GFP positive NALM6 WT or NALM6 CXCR4 KO cells and bioluminescent Intensity (BLI) measured at day 6, 10, 14 and 17 (Figure 33). Mice injected with NALM6 CXCR4 KO had significantly less BLI signal than NALM6 WT throughout the course of the disease ($p<0.001$ on day 6, $p<0.05$ on day 10, $p<0.05$ on day 14, and $p<0.001$ on day 17). In three representative mice per group sacrificed on day 17, flow cytometry demonstrated that mice injected with NALM6 CXCR4 KO cells had less leukemic infiltration in bone marrow than NALM6 WT (mean ± SEM, 30.3% ± 4.4% vs. 2.8% ± 1.4%,

$p<0.005$). Staining by CXCR4 12G5 antibody revealed the lack of CXCR4 expression in mice injected with NALM6 CXCR4 KO (mean fluorescent intensity/isotype, 2.1 ± 0.1) compared to NALM6 WT (120.1 ± 1.0, $p<0.001$). The proportion of circulating leukemic cells was also measured in three representative mice from each group on day 17 and living mice (five mice per each group) on days 20 and 24. Mice injected with NALM6 CXCR4 KO cells had significantly lower circulating leukemic cells than NALM6 WT (0.27% ± 0.05% vs. 0.02% ± 0.01%, $p<0.05$ on day 17; 0.78% ± 0.13% vs. 0.05%±0.004%, $p<0.05$ on day 20; 1.2% ± 0.34% vs. 0.1% ± 0.02%, $p<0.05$ on day 24). These differences in leukemia progression translated into significant prolongation of survival in mice injected with NALM6 CXCR4 KO cells (median survival, 34 days vs. 27.5 days; $p<0.005$).

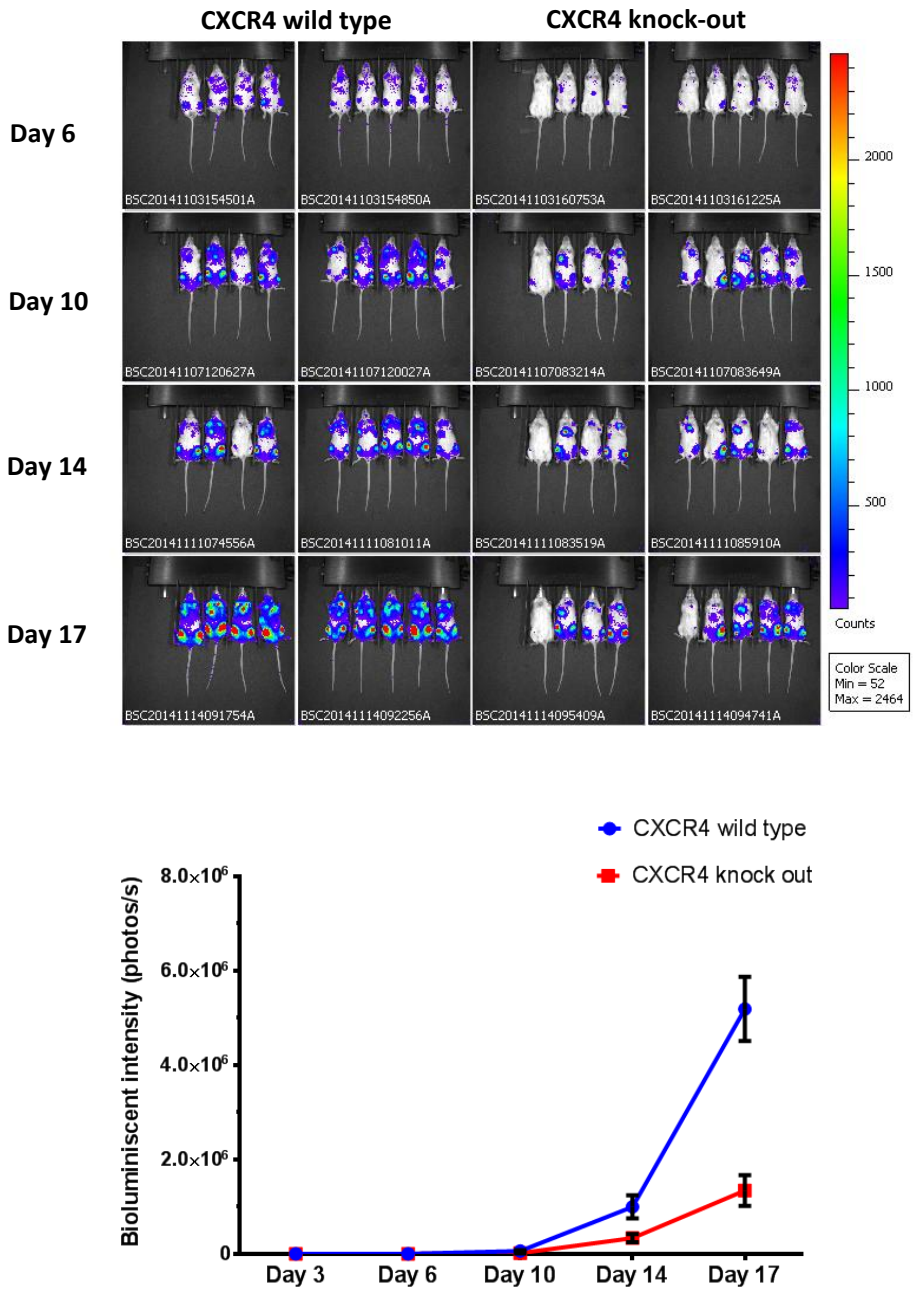
CXCR4 wild type
CXCR4 knock-out
Day 6
Day 10
Day 14
Day 17
BSC20141103154501A
BSC20141103154850A
BSC20141103160753A
BSC20141103161225A
BSC20141107120627A
BSC20141107120027A
BSC20141107083214A
BSC20141107083649A
BSC20141111074556A
BSC20141111081011A
BSC20141111083519A
BSC20141111085910A
BSC20141114091754A
BSC20141114092256A
BSC20141114095409A
BSC20141114094741A
2000
1500
1000
500
Counts
Color Scale
Min = 52
Max = 2464
CXCR4 wild type
CXCR4 knock out
Bioluminiscent intensity (photos/s)
8.0x10^6
6.0x10^6
4.0x10^6
2.0x10^6
0
Day 3
Day 6
Day 10
Day 14
Day 17

Figure 34

Figure 34. Bioluminescent intensity of mice injected with GFP positive NALM6 CXCR4 Knockout or Wild type cells. Nine mice per group were injected with GFP positive NALM6 CXCR4 Wild Type (WT) or NALM6 CXCR4 Knock out (KO) cells and Bioluminescent Imaging (BLI) measured for all mice during the course of the experiment (on days 6, 10, 14 and 17). Graph depicts quantification of BLI (photons/second) for mice injected with NALM6 CXCR4 WT (blue line) vs. NALM6 CXCR4 KO (red line) ($p<0.001$).

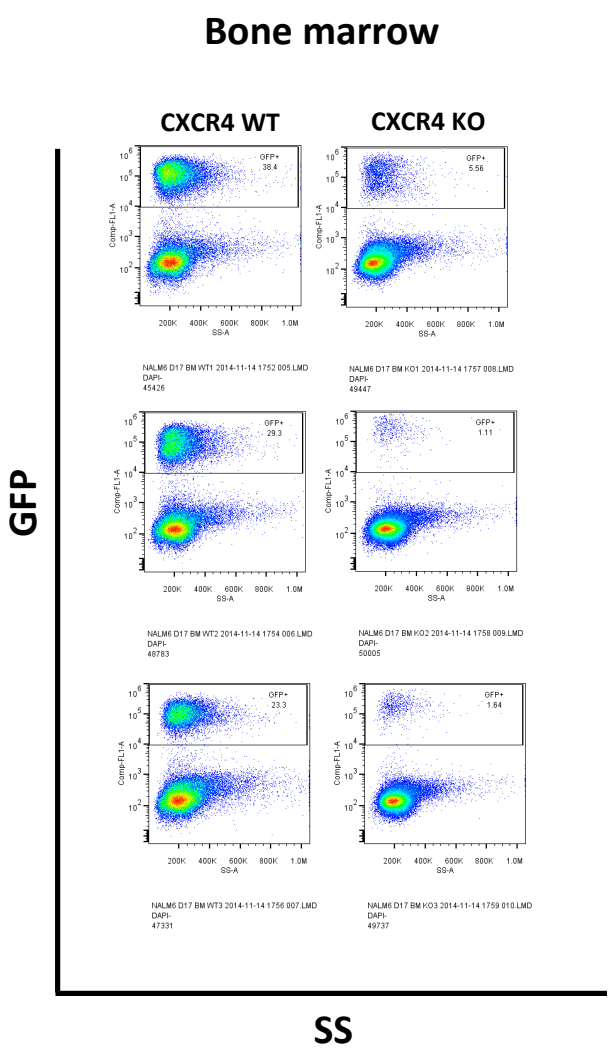
Bone marrow
CXCR4 WT
CXCR4 KO
GFP
SS
GFP+
38.4
GFP+
5.56
GFP+
29.3
GFP+
1.11
GFP+
23.3
GFP+
1.64
Comp-FL1-A
SS-A
200K
400K
600K
800K
1.0M
NALM6 D17 BM WT1 2014-11-14 1752 005.LMD
DAPI-
45426
NALM6 D17 BM KO1 2014-11-14 1757 008.LMD
DAPI-
49447
NALM6 D17 BM WT2 2014-11-14 1754 006.LMD
DAPI-
48783
NALM6 D17 BM KO2 2014-11-14 1758 009.LMD
DAPI-
50005
NALM6 D17 BM WT3 2014-11-14 1756 007.LMD
DAPI-
47331
NALM6 D17 BM KO3 2014-11-14 1759 010.LMD
DAPI-
49737

Figure 35

Figure 35. CXCR4 deletion reduces bone marrow infiltration of leukemic cells *in vivo*. Dot plots show cell counts of GFP positive wild type (left column) or CXCR4 knockout (right column) NALM6 cells from bone marrow aspirates of three representative mice sacrificed on day 17 of the experiment. X-axis represents side scatter and Y-axis represents GFP expression. GFP expressing cells are gate.

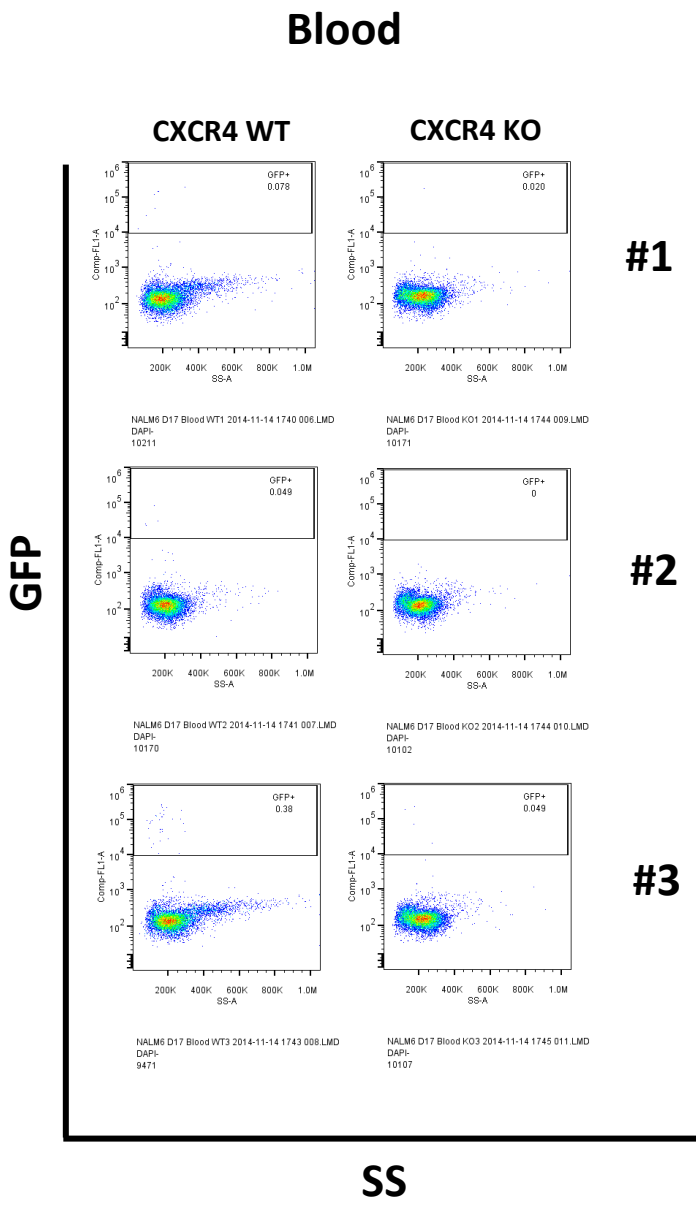
Blood
CXCR4 WT
CXCR4 KO
#1
#2
#3
GFP
SS
GFP+
0.078
GFP+
0.020
GFP+
0.049
GFP+
0
GFP+
0.38
GFP+
0.049
Comp-FL1-A
SS-A
200K
400K
600K
800K
1.0M
NALM6 D17 Blood WT1 2014-11-14 1740 006.LMD
DAPI-
10211
NALM6 D17 Blood KO1 2014-11-14 1744 009.LMD
DAPI-
10171
NALM6 D17 Blood WT2 2014-11-14 1741 007.LMD
DAPI-
10170
NALM6 D17 Blood KO2 2014-11-14 1744 010.LMD
DAPI-
10102
NALM6 D17 Blood WT3 2014-11-14 1743 008.LMD
DAPI-
9471
NALM6 D17 Blood KO3 2014-11-14 1745 011.LMD
DAPI-
10107

Figure 36

Figure 36. CXCR4 deletion decreases blood counts of leukemic cells *in vivo*. Dot plots show cell counts of GFP positive wild type (left column) or CXCR4 knockout (right column) NALM6 cells from blood of three representative mice sacrificed on day 17 of the experiment. X-axis represents side scatter and Y-axis represents GFP expression. GFP expressing cells are gate.

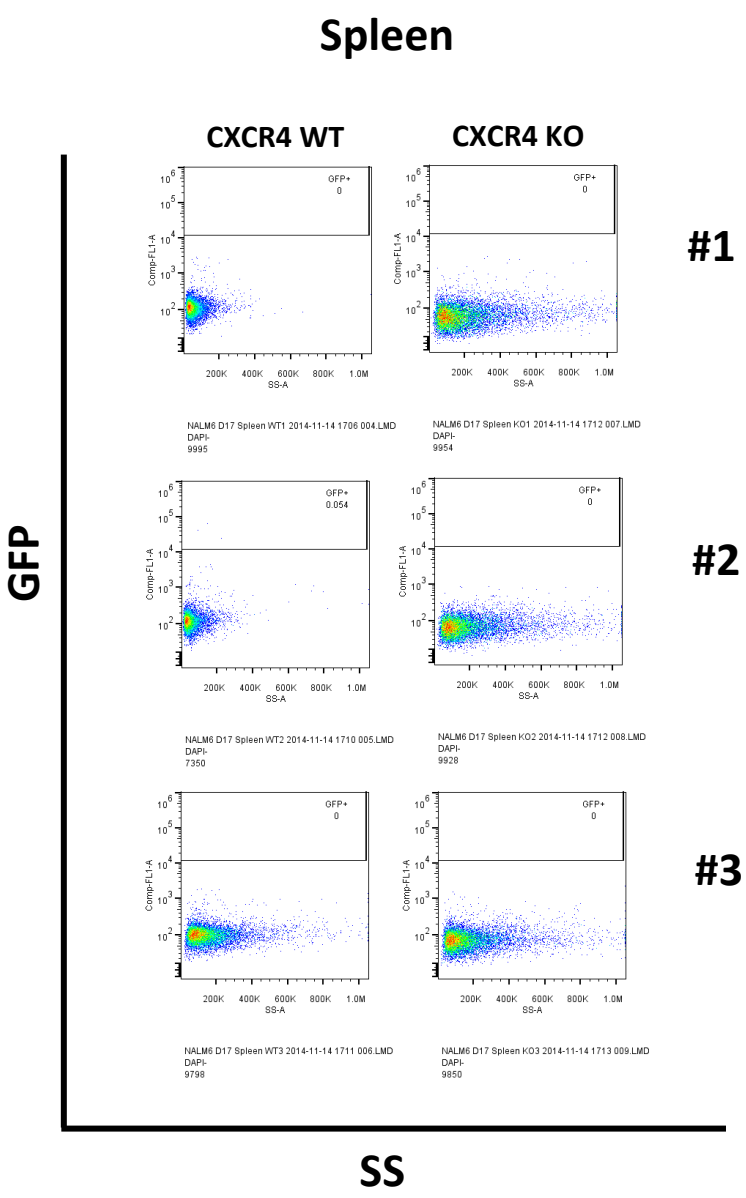
Spleen
CXCR4 WT
CXCR4 KO
#1
#2
#3
GFP
SS
GFP+
0
0.054
Comp-FL1-A
SS-A
200K
400K
600K
800K
1.0M
NALM6 D17 Spleen WT1 2014-11-14 1706 004.LMD
DAPI-
9995
NALM6 D17 Spleen KO1 2014-11-14 1712 007.LMD
DAPI-
9954
NALM6 D17 Spleen WT2 2014-11-14 1710 005.LMD
DAPI-
7350
NALM6 D17 Spleen KO2 2014-11-14 1712 008.LMD
DAPI-
9928
NALM6 D17 Spleen WT3 2014-11-14 1711 006.LMD
DAPI-
9798
NALM6 D17 Spleen KO3 2014-11-14 1713 009.LMD
DAPI-
9850

Figure 37

Figure 37. Leukemic cell count of the spleen of mice injected with CXCR4 WT or KO cells. Dot plots show cell counts of GFP positive wild type (left column) or CXCR4 knockout (right column) NALM6 cells from spleen of three representative mice sacrificed on day 17 of the experiment. X-axis represents side scatter and Y-axis represents GFP expression. GFP expressing cells are gate.

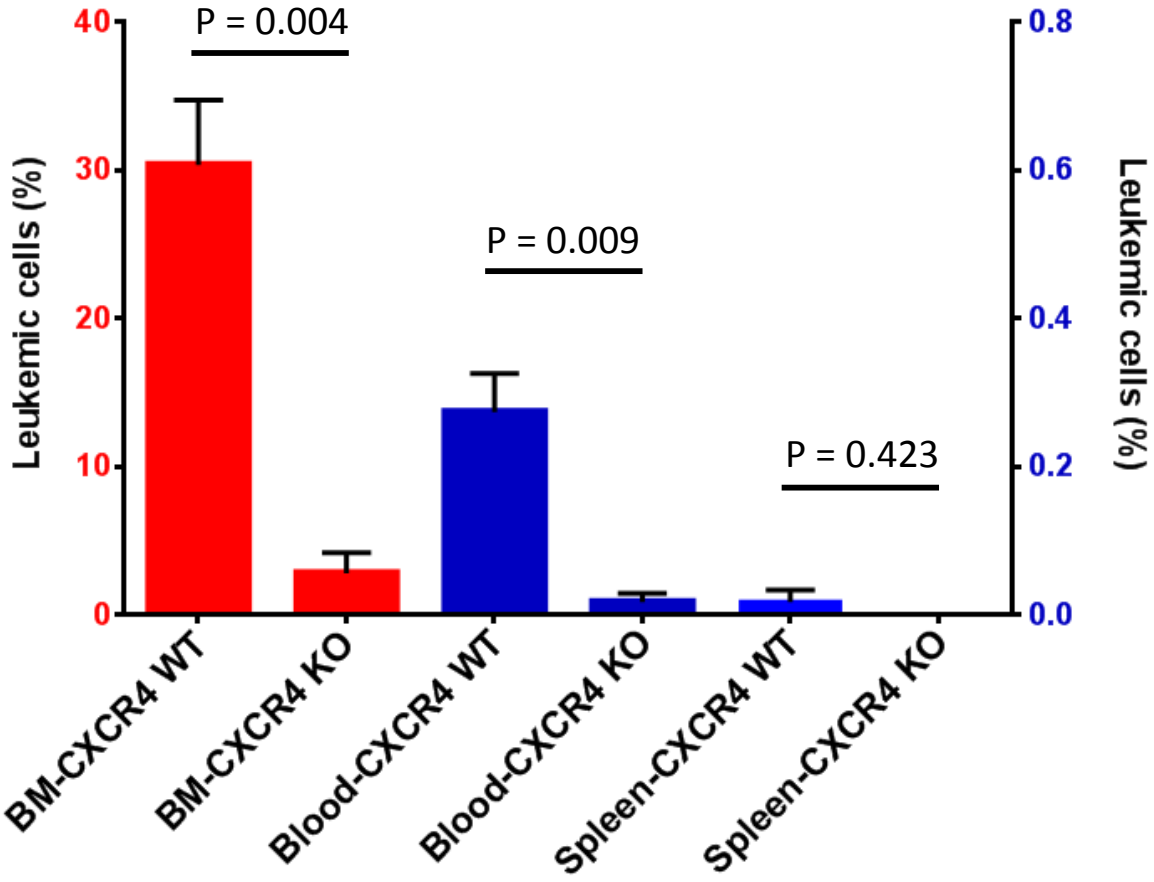
P = 0.004
P = 0.009
P = 0.423
Leukemic cells (%)
Leukemic cells (%)
40
30
20
10
0
0.8
0.6
0.4
0.2
0.0
BM-CXCR4 WT
BM-CXCR4 KO
Blood-CXCR4 WT
Blood-CXCR4 KO
Spleen-CXCR4 WT
Spleen-CXCR4 KO

Figure 38

Figure 38. CXCR4 deletion significantly decreases disease burden *in vivo*. Bone marrow and blood of three mice per group were analyzed on day 17 for GFP positive leukemia cells using flow cytometer. Bar graph shows quantification of number of GFP positive leukemia cells in the bone marrow (red bars) or the blood (blue bars).

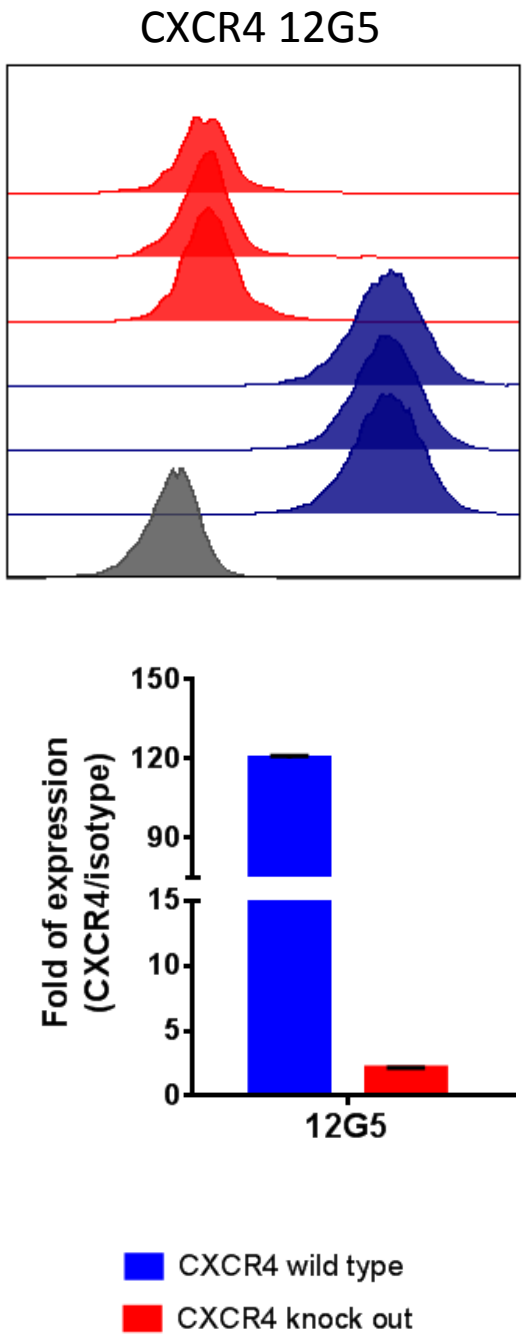
CXCR4 12G5
Fold of expression (CXCR4/isotype)
150
120
90
15
10
5
0
12G5
CXCR4 wild type
CXCR4 knock out

Figure 39

Figure 39. CXCR4 Knockout cells maintain lack of CXCR4 expression *in vivo*. CXCR4 expression was measured at day 17 using 12G5 antibodies in mice injected with NALM6 CXCR4 wild type and knockout cells. The upper figure shows histograms of three representative mice. The grey histogram represents isotype control, the red histograms represent leukemia cells from mice injected with CXCR4 knockout cells and blue histograms show leukemia cells from mice injected with CXCR4 wild type. The bar graph represents quantification of the CXCR4 levels showing lack of expression of CXCR4 in mice injected with NALM6 CXCR4 knockout cells.

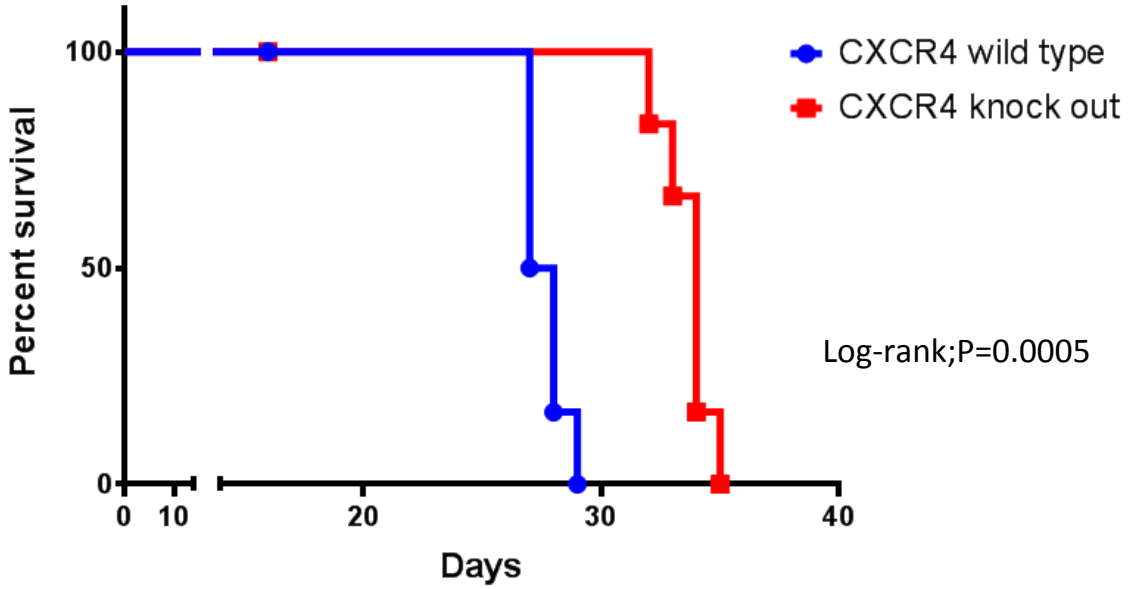

Median survival		Hazard Ratio (logrank)		
CXCR4 wild type	27.50	Ratio (and its reciprocal)	4.196	0.2383
CXCR4 knock out	34.00	95% CI of ratio	6.330 to 111.7	0.008954 to 0.1580

Figure 40

Figure 40. CXCR4 deletion significantly increases survival of B-ALL mice. Kaplan-Meier survival curve shows the survival of mice injected with NALM6 CXCR4 WT (blue line) vs. NALM6 CXCR4 KO (red line) ($p<0.05$).

CXCR4 expression does not correlate with overall and relapse free survival in Pre-B-ALL patients

In contrast to previous studies, we did not observe any significant correlation between CXCR4 or CD49D expression and outcome. However, in both univariate and multivariate analysis, we noted a correlation between high relative numbers of bone marrow blasts and survival (both overall and relapse free) (Tables 3, 4 and 5).

Table 2. Clinical and laboratory characteristics of patients analyzed

Characteristics	Value
No. of patients	137
Sex, no.	
Male	77
Female	60
Median age, y (range)	50 (18, 80)
Median % of CXCR4 blasts (range)	81.1 (1.7, 100)
Median CXCR4, MFIR (range)	25.9 (0, 1023.5)
Median % of cd49d blasts (range)	99.9 (76.5, 100)
Median cd49d, MFIR (range)	106.3 (0, 4290.9)
BCR ABL status, n (%)	
Ph +	50 (36.5)
Ph -	87 (63.5)
Median BM blast percentage (range)	86 (1, 99)
Median PB blast percentage (range)	19 (0, 96)
Median WBC count, × 10^9L (range)	9.9 (0.4, 629.4)
Median LDH level, U/L (range)	913.5 (197, 28015)
Median platelet count, × 10^9L (range)	31.5 (0, 337)
Median time to follow up, mo (range)	
Relapse	24
Therapy	
AUG BFM	28
HCMAD	6
HCMAD + Dasatinib	10
HCMAD + Imatinib	1
HCVAD	4
HCVAD + Dasatinib	7
HCVAD + Inotuzomab	25
HCVAD + Ofatumumab	22
HCVAD + Ponatinib	32

Table 3. Univariate Cox proportional hazards models for Overall Survival

covariate	HR	95% CI		p-value	N_dead	N_total
Age_at_Start	1.00	0.99	1.02	0.60	39	137
log(CD49)	0.97	0.71	1.33	0.85	35	120
log(CXCR4)	1.04	0.84	1.30	0.71	35	120
log(WBC)	1.00	0.83	1.20	0.99	39	135
BM_blast	1.02	1.00	1.05	**0.03**	39	134
log(PB blast)	0.97	0.80	1.17	0.73	37	131
Hgb	0.91	0.75	1.11	0.36	38	132
log(PLT)	0.69	0.50	0.97	**0.03**	38	132
LDH	1.00	1.00	1.00	0.51	36	128
Alb	0.41	0.22	0.78	**0.01**	35	125
BCR_ABL= Ph+ (vs. negative)	0.82	0.42	1.63	0.58	39	137

Table 4. Multivariate cox proportional hazards models for Overall Survival

Variable	HR	95% CI		p-value
BM_Blast	1.02	1.00	1.05	0.05
Alb	0.35	0.16	0.73	0.01
log(CXCR4)	0.85	0.66	1.08	0.18
log(CD49)	0.88	0.59	1.31	0.52

Table 5. Univariate cox proportional hazards model for relapse-free survival among 129 patients who have achieved CR, CRp or PR

covariate	HR	95% CI		p-value	Event	Total
Age_at_Start	1.00	0.98	1.01	0.68	40	129
log(CD49)	1.22	0.89	1.67	0.22	36	112
log(CXCR4)	1.13	0.92	1.39	0.25	36	112
log(WBC)	1.08	0.91	1.28	0.40	40	127
BM_blast	1.02	1.00	1.04	**0.03**	40	126
log(PB blast)	1.03	0.85	1.25	0.74	39	124
Hgb	0.95	0.77	1.16	0.61	39	124
log(PLT)	0.72	0.51	1.01	0.06	39	124
LDH	1.00	1.00	1.00	0.57	37	120
Alb	0.54	0.28	1.05	0.07	36	117
BCR_ABL= Ph+ (vs. negative)	0.93	0.49	1.78	0.83	40	129

Table 6. Multivariable cox proportional hazards model for CR duration among patients who have achieved CR, CRp or PR (N=110, N_event=36)

Variable	HR	95% CI		P-value
BM_Blast	1.02	1.00	1.05	0.08
log(CXCR4)	1.03	0.83	1.28	0.79
log(CD49)	1.20	0.85	1.71	0.30

Table 7. Univariate logistic regression models for response (CR, CR or PR)

Variable	Odds Ratio	95% CI		P-value
Age_at_Start	0.98	0.94	1.02	0.29
log(CD49)	1.24	0.72	2.13	0.44
log(CXCR4)	1.22	0.80	1.87	0.35
log(WBC)	1.10	0.72	1.66	0.67
BM_blast	1.00	0.96	1.04	0.92
log(PB blast)	1.10	0.70	1.71	0.69
Hgb	1.10	0.68	1.79	0.70
log(PLT)	1.40	0.68	2.90	0.36
LDH	1.00	1.00	1.00	0.50
Alb	2.09	0.48	9.10	0.33
BCR_ABL= Ph+ (vs. negative)	4.29	0.51	35.91	0.18

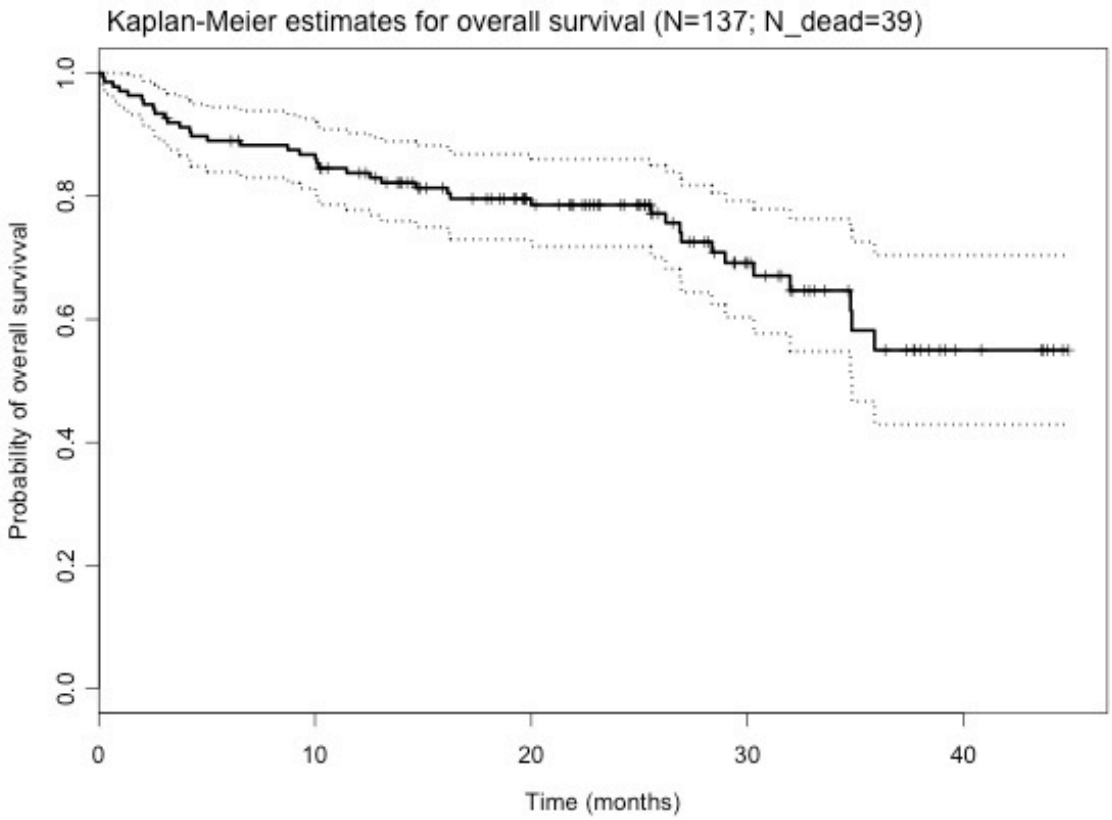
Kaplan-Meier estimates for overall survival (N=137; N_dead=39)
Probability of overall survivval
0.0
0.2
0.4
0.6
0.8
1.0
0
10
20
30
40
Time (months)

Figure 41

Figure 41. Kaplan Meier curves for overall survival. Graph depicts Kaplan Meier curve for overall survival in patients diagnosed with Pre-B-cell Acute Lymphoblastic Leukemia.

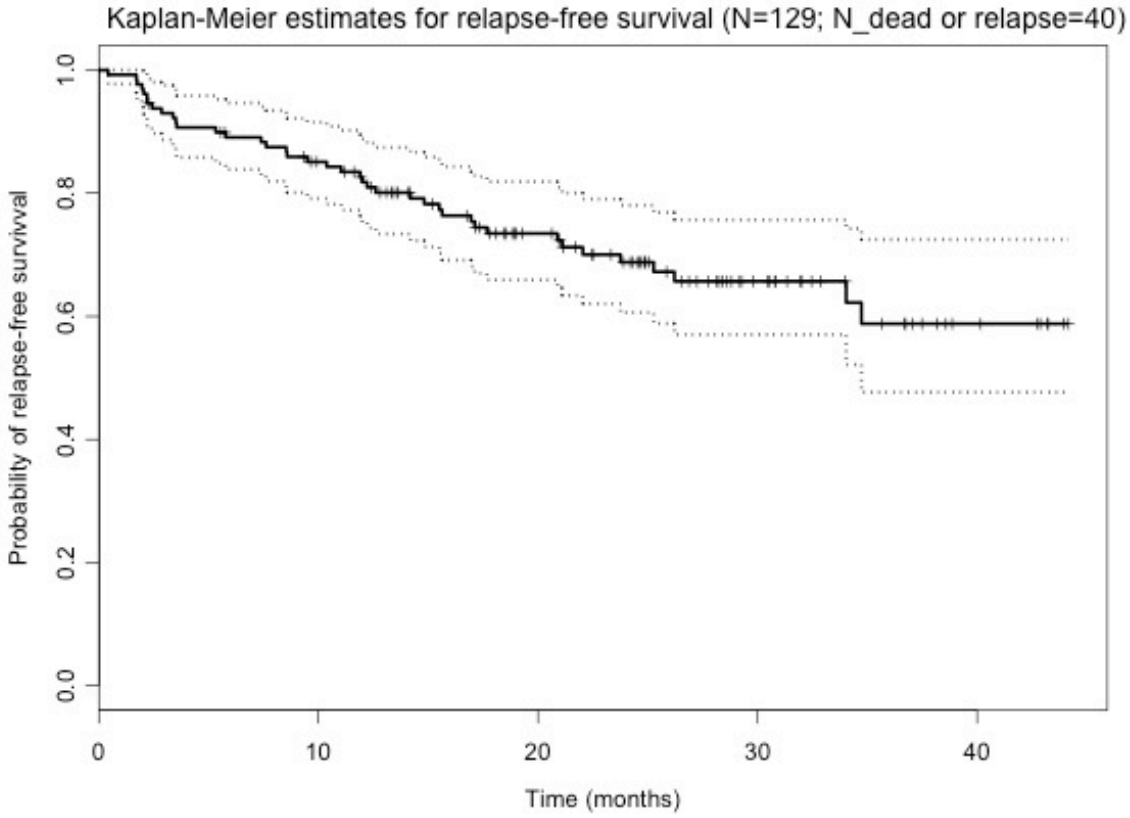
Kaplan-Meier estimates for relapse-free survival (N=129; N_dead or relapse=40)
Probability of relapse-free survivval
0.0
0.2
0.4
0.6
0.8
1.0
0
10
20
30
40
Time (months)

Figure 42

Figure 42. Kaplan Meier curves for relapse free survival. Graph depicts Kaplan Meier curve for relapse free survival in patients diagnosed with Pre-B-cell Acute Lymphoblastic Leukemia.

Chapter 4

~ *Discussion* ~

The clinical significance of inhibition of the CXCL12/CXCR4 pathway spans various diseases including metastasis(70), arthritis(71), WHIM syndrome(72), HIV entry to CD4 positive T-Cells(73) and leukemia migration and dissemination. Highly specific inhibitors of this pathway were first developed to inhibit HIV entry into CD4 positive T cells(64, 74, 75). High levels of CXCR4 surface expression have been associated with inferior prognosis in ALL patients(57, 59) and in our study we show evidence that CXCR4 could serve as an effective target worth exploring in B-Cell Acute Lymphoblastic Leukemia. It has been previously demonstrated that Bone Marrow Stromal Cells protect leukemia cells from chemotherapy using various secreted and surface bound factors. In this study, we demonstrate that CXCR4 is one of the central mechanisms used by stromal cells to provide chemo-resistance to B-ALL cells.

We observed that all B-ALL cell lines and xenografts tested positive for CXCR4 irrespective of their maturation stage. The absence of other chemokine receptors indicates that CXCR4 is possibly one of the most important chemokine receptor present in B-ALL cells. This is also corroborated by the lethal phenotype of both CXCR4 and SDF1 deficient mice showing defective B-Cell development. Xenografts showed markedly lower CXCR4 expression than cell lines but the presence and activity of CXCR4 was evidenced by the functional responses to CXCR4 activation and inhibition stimuli. The xenograft cells displayed significant chemotaxis and extensive PEP beneath BMSCs and these responses were

significantly decreased upon CXCR4 inhibition. The low CXCR4 surface expression was possibly due to co-culture conditions in which xenografts are routinely maintained. Upon CXCL12 binding, CXCR4 has been reported to undergo endocytosis and internalization to vesicles from where it is recycled to the cell surface. Constitutive secretion of CXCL12 by the stromal cell layer might cause internalization of the CXCR4 receptor thereby reducing surface expression. Indeed, when xenograft cells were taken off stroma, CXCR4 expression increased as compared to the co-culture setting. Similar observations were made by Van den Berk et al (59) in B-ALL patients, they showed significantly lower CXCR4 expression in leukemic bone marrow cells than of the peripheral blood. This possibly serves the purpose of homeostatic regulation, where CXCR4 expression is down regulated in BM and up-regulated in peripheral blood to maintain equilibrium between BM homing and egress. Lai et al (76) reported that sustained CXCR4 signaling enhancement in vivo resulted in diminished peripheral blood reconstitution, likely due to the prevention of release of hematopoietic cells from the bone marrow(76). This phenomenon could also explain high levels of CXCR4 in cell lines, since they are continuously cultured in the absence of stromal cells. Indeed, B-ALL cell lines displayed lower CXCR4 levels upon BMSC co-culture exposure. An additional chemokine receptor of interest was the second CXCL12 receptor CXCR7, which has been previously known to be a decoy receptor acting as a sink for

CXCL12(77). However, all cell lines tested negative for CXCR7, ruling out any involvement in B-ALL pathogenesis.

It has been shown in previous studies that in human B-cells derived from bone marrow that CXCR4 expression level does not correlate with responsiveness to CXCL12(78). As mentioned above, the internalization of CXCR4 is the major factor in play. Indeed, Tarasova et al demonstrated that CXCR4 undergoes spontaneous ligand independent internalization and gets sorted into endosomes(79). Additionally, it has been demonstrated that in leukocytes the internalization and recycling of CXCR4 is a rapid process that takes place in response to various stimuli. Additionally, B cells have a large intracellular pool of CXCR4(80). Considering the above information, it is clear that quantification of CXCR4 surface expression at a singular time point does not represent the entirety of functional CXCR4 present in the cell which is possibly why the surface expression on cells does not correlate with functional responses like chemotaxis and pseudoemperipolesis.

CXCR4 inhibitor pre-treatment significantly reduced chemotaxis to CXCL12 and PEP under BMSCs for all xenografts and cell lines tested. It was observed that exposure to CXCR4 inhibitors induced a more robust decrease in chemotaxis than in PEP. The chemotaxis assay is conducted in Transwell chambers with only CXCL12 in the lower chamber and blockade of CXCR4 disrupts this linear interaction. Essentially, in our

setting, the chemotaxis assay is a quantification of the movement of the cells in response to a single chemokine attractant. On the other hand, the PEP co-culture is a dynamic setting with several factors other than CXCR4 involved. Indeed, in addition to migration, adhesion processes start to play a role in the co-culture and although CXCR4 is possibly the main chemotactic factor for B-ALL, several other adhesion molecules are expressed by them. One such factor is CD49D (or VLA-4)(28) and it was observed in our experiments that a combination of CXCR4 and CD49D inhibitors significantly decreased PEP as compared to CXCR4 or CD49D inhibitors alone.

Besides inhibition of CXCR4 function, CXCR4 antagonists also can induce signaling after binding to its target, CXCR4. Plerixafor and ALX40-4C have been characterized as weak partial agonist, whereas the polyphemusin derivative peptide inhibitor BTK140 was characterized as an inverse CXCR4 agonist(81). Signaling responses induced by stimulation of CXCR4 with high concentrations of plerixafor and ALX40-4C were less robust than those seen with its natural ligand, CXCL12, and hence plerixafor and ALX40-4C were characterized as peak partial CXCR4 agonist(81). The agonistic activity of plerixafor and ALX40-4C raise concern that some of the activity seen with CXCR4 antagonists may be due to agonistic activity, rather than blockade of CXCR4 function. Along the same lines, preclinical work with BMS-936564/MDX-1338, a therapeutic anti-human CXCR4 monoclonal antibody, revealed that this

CXCR4 antagonist also induced downstream signaling. The authors compared BMS-936564 with plerixafor in preclinical assays and noted marked differences; while BMS-936564 induced target cell apoptosis, plerixafor did not, suggesting that antibody binding to CXCR4 drives a signal to induce apoptosis that is independent from inhibition of CXCL12 binding(82). These differences in inhibitor-induced signaling raise the question whether some of the anti-leukemia activity seen in prior studies may be related agonistic activity of the CXCR4 antagonist. Therefore, we compared pharmacologic and genetic functional deletion of CXCR4 in preclinical models of B-ALL.

It has been previously shown that the microenvironment protects leukemia cells from drug-induced cytotoxicity. More importantly, we analyzed the cells that had undergone PEP to reside under the stromal cell layer, mimicking leukemia cells in the bone marrow. The viability of these cells was unaffected by drug treatment and similar to control cells without any drug, revealing the high degree of chemo-protection stroma provides to leukemia cells. This observation highlights the importance of new therapeutic agents that not only inhibit cells from homing to the bone marrow, but also promote egress of leukemia cells already in these niches. This has been evidenced by the fact that Plerixafor has already been approved as a stem cell mobilizer in Non-hodgkins lymphoma and multiple myeloma(60).

In addition to being an effective mobilizer of CXCR4 positive cells from bone marrow niches, CXCR4 antagonists have also been shown to sensitize leukemia cells to conventional chemotherapy in CLL(83) and AML(84). Our experiments demonstrate that CXCR4 is an effective target in ALL as well. Plerixafor and BKT140 sensitized ALL cell lines to cytotoxicity induced by Dexamethasone, Vincristine and Cyclophosphamide. The addition of CXCR4 inhibitors to conventional chemotherapy thus becomes a dual treatment strategy wherein CXCR4 inhibition not only drives leukemia cells out of their protective niches but also makes cells more sensitive to chemotherapy treatment.

To corroborate our findings in the pharmacological inhibition of CXCR4 we generated a CXCR4 genetic deletion model and observed the similar deficient chemotaxis and PEP. CXCR4 knockout B-ALL cells displayed no difference in the growth rates as compared to the wild type cells even though CXCL12 was first identified as a pre-B-cell growth stimulating factor. This indicates to the possibility that B-ALL cells have potentially gained independence from CXCR4 signaling for their proliferation. Additionally, CXCR4 knockout cells were not rescued from drug-induced cytotoxicity by stromal cell co-culture like the CXCR4 wild type counterparts indicating the essential role of the CXCL12/CXCR4 axis in chemo-resistance of B-ALL cells. This also indicates that B-ALL cells depend on CXCR4 for their survival but not proliferation. This also corroborates with the fact that CXCR4 knockout cell lines maintain

CXCR4 negative status in spite of long-term culture. If CXCR4 positive cell lines had a proliferative edge as compared to wild type cells, the miniscule number of CXCR4 positive cells would potentially outgrow the knockout cells over times. This was also observed in our *in vivo* experiments where mice injected with knockout cells, showed CXCR4 negative cells throughout the course of the experiment.

To understand the role CXCR4 plays in B-ALL engraftment, progression and survival, NALM6-CXCR4-KO and NALM6-WT cells were introduced into NSG mice and disease progression monitored. It was observed that CXCR4 deletion significantly reduced leukemia burden and progression supporting the conventional role of CXCL12 as a pre-B cell growth factor and the role of CXCL12/CXCR4 in B-cell lymphopoiesis. Significantly reduced bone marrow infiltration/retention in mice that were injected with CXCR4 knockout cells as compared to the wild type counterparts validated our in vitro PEP experiments. Most importantly, the mice injected with CXCR4 Knockout cells survived significantly longer than the mice injected with CXCR4 Wild type cells, highlighting the importance of this axis in leukemia prognosis.

Previously, studies have reported that higher CXCR4 expression is associated with worse outcome in patients with B-ALL(57, 59). In contrast, our analyses in the patient data set did not reveal a correlation between CXCR4 expression and patient outcome. However, it was

observed that the patient set was also not correlated with established prognostic markers such as LDH. Additionally, as mentioned earlier the entirety of CXCR4 expression and function is not represented by a one time quantification. All patient samples had CXCR4 measured in bone marrow aspirates at diagnosis using flow cytometry. It has been previously demonstrated that B-ALL cells express higher levels of CXCR4 in peripheral blood and lower levels in the bone marrow due to internalization of CXCR4. Ten patients were found in our study with CXCR4 measured in both bone marrow and peripheral blood. Indeed, barring one patient, nine patients had CXCR4 levels lower in the bone marrow. However, no significance was achieved due to low patient numbers.

On the other hand, worse patient outcome was associated with bone marrow blast percentage. Since it has been established in previous studies that CXCR4 antagonists successfully mobilize B-ALL cells from the bone marrow(45, 85, 86), the inclusion of CXCR4 antagonists could be of potential therapeutic value.

In summary, our study validates the role of CXCR4 in the pathogenesis of B-ALL by demonstrating its effect on migration, adhesion and survival of leukemia cells. We show that this mechanism could help overcome the current clinical challenge of minimal residual disease and its impending outcome of relapse. In addition to inhibiting

chemotaxis and pseudoemperipolesis, CXCR4 inhibitors sensitize B-ALL cells to chemotherapy, providing a dual mechanism wherein not only do they mobilize leukemia cells out of the bone marrow, they also sensitize these cells to chemotherapy.

Conclusions

CXCR4 inhibitors Plerixafor (small molecule) and BKT140 (peptide) interfere with CXCR4 activation, signaling and bone marrow homing of leukemia cells. Adhesion of B-ALL cells to bone marrow stromal cell (BMSC) through CXCR4/CXCL12 protects leukemia cells from cytotoxic drugs, and causes cell adhesion-mediated drug resistance (CAM-DR). Due to the critical role of the CXCR4/CXCL12 axis in B-ALL cell adhesion to bone marrow stromal cells (BMSC), we hypothesize that targeting CXCR4 will attenuate CAM-DR in B-ALL.

All tested B-ALL cell lines and xenograft-expanded primary cells were found to be positive for surface expression of CXCR4. Pre-treatment with Plerixafor/BKT140 significantly inhibited the spontaneous migration of B-ALL cells beneath BMSCs *in vitro* (Pseudoemperipolesis/PEP). B-ALL cell line and xenograft expanded primary B-ALL cell chemotaxis towards CXCL12 was also abrogated by pre-incubation with Plerixafor or BKT140. In order to better dissect CXCR4 function in B-ALL, we established two CXCR4 knock out cell lines, TANOUE-CXCR4-KO and NALM6-CXCR4-KO, using CRISPR Cas9 technology. Chemotaxis to CXCL12 and PEP beneath BMSCs was significantly decreased for CXCR4 knockout cells in comparison to wild type controls without any drug treatment.

We showed that co-culture with BMSCs rescued B-ALL cells in the supernatant from Dexamethasone (DEX), Vincristine (VIN) or Cyclophosphamide (4HC) induced cytotoxicity. Furthermore, B-ALL cells residing under the BMSC layer (as a result of PEP) were highly resistant to Dex/4HC/Vin treatment. Targeting CXCR4 significantly inhibited B-ALL chemotaxis towards CXCL12 gradient and PEP beneath BMSCs. Consequently, chemo-sensitivity assays performed with a combination of DEX/4HC/Vin and CXCR4 inhibitor showed enhanced cytotoxicity as compared to DEX/4HC/Vin alone. BMSCs rescued NALM6 from DEX induced cytotoxicity but failed to rescue NALM6 CXCR4 KO, indicating that CXCR4 is the central mechanism used by stromal cells to provide drug resistance to ALL cells.

We extended our experiments to *in vivo* studies. 9 non-irradiated NSG mice per group were injected with GFP+ NALM6 WT or NALM6 CXCR4 KO cells and bioluminescent Intensity (BLI) measured at day 6, 10, 14 and 17. Mice injected with NALM6 CXCR4 KO had significantly less BLI signal than NALM6 WT throughout the course of the disease. In 3 representative mice per group sacrificed on day 17, flow cytometry demonstrated that NALM6 CXCR4 KO injected mice had less leukemic infiltration in bone marrow than NALM6 WT. Staining by CXCR4 12G5 antibodies revealed the lack of CXCR4 expression in mice injected with NALM6 CXCR4 KO compared to NALM6 WT. The proportion of circulating

leukemic cells was also measured in 3 representative mice from each group on day 17 and living mice (5 mice per each group) on days 20 and 24. NALM6 CXCR4 KO injected mice had significantly lower circulating leukemic cells than NALM6 WT. These differences in leukemia progression resulted in significant prolongation of survival in NALM6 CXCR4 KO injected mice. Collectively, these findings provide a rationale for clinical targeting of CXCR4 in patients with B-ALL.

Future Directions

Determination of CXCR7 expression

Corroborating data reported by Honczarenko et al (1999)(78), the present study does not demonstrate a correlation between CXCR4 expression and CXCL12 responsiveness. As the alternate decoy receptor that sequesters CXCL12 away from CXCR4, the expression and function of CXCR7 could be one way to regulate functionality of CXCR4.

Conflicting data have been reported regarding expression of CXCR7 in B cells where some studies report high expression of the receptor (Infantino et al 2006)(87) and other studies demonstrating complete lack of the CXCR7 protein (88). The availability of quality antibodies to detect the surface expression of CXCR7 is a major challenge. Similar observations have been made with other cancers, for example, conflicting data has been reported about expression of CXCR7 in breast cancer. This presents a challenge to identifying a robust negative control.

Furthermore, plerixafor has been reported to have agonistic activity towards CXCR7 and shows activation of G-protein independent β-arrestin signaling leading to MAPK activation(89).

Identification of appropriate negative/positive controls and determination of CXCR7 expression is crucial to the understanding of the dynamics of CXCR4 function.

Elucidation of the CXCR4 signaling mechanism

As demonstrated by the chemotaxis and pseudoemperipolesis experiments, expression of CXCR4 is crucial in B-ALL cell migration. Additionally, according to chemo-sensitivity experiments conducted with CXCL12 in place of BMSC co-culture (Figure 31), CXCR4 is also involved in providing B-ALL cells resistance to chemotherapy.

CXCR4 has been shown to activate various signaling cascades, however it is not yet fully understood which signaling regulators is responsible for migration and resistance to chemotherapy. In order to identify novel targets and stratify patients that are resistant to CXCR4 inhibitors, it is essential better understand the key regulators downstream of CXCR4 that are crucial for providing chemotherapy resistance to B-ALL cells.

Addition of chemotherapy to in vivo experiments

Our *in vivo* experiments demonstrated a significant increase in survival of mice injected with B-ALL cells lacking CXCR4 expression as compared to mice injected with wild type CXCR4 cells. Additionally, leukemia burden, bone marrow infiltration and circulating leukemia cells

were significantly lower in mice injected with CXCR4 knockout cells throughout the course of the experiment.

The addition of a chemotherapy treatment regimen to the *in vivo* experiment could further widen the gap between the survival times of mice injected with CXCR4 knockout and wild type cells. This could serve as additional evidence that could lead to the clinical testing of CXCR4 inhibitors as chemo-sensitizers in B-ALL.

BIBLIOGRAPHY

1. Pui, C.-H., M. V. Relling, and J. R. Downing. 2004. Acute lymphoblastic leukemia. *New England Journal of Medicine* 350: 1535-1548.

2. Faderl, S., S. Jeha, and H. M. Kantarjian. 2003. The biology and therapy of adult acute lymphoblastic leukemia. *Cancer* 98: 1337-1354.

3. Pui, C.-H., and W. E. Evans. 2006. Treatment of Acute Lymphoblastic Leukemia. *New England Journal of Medicine* 354: 166-178.

4. Siegel, R., J. Ma, Z. Zou, and A. Jemal. 2014. Cancer statistics, 2014. *CA: a cancer journal for clinicians* 64: 9-29.

5. Foà, R., S. Chiaretti, A. Guarini, and A. Vitale. 2009. Adult acute lymphoblastic leukemia. *Revista Brasileira de Hematologia e Hemoterapia* 31: 41-47.

6. Murphy, S. L., J. Xu, and K. D. Kochanek. 2013. Deaths: final data for 2010. *National vital statistics reports : from the Centers for Disease Control and Prevention, National Center for Health Statistics, National Vital Statistics System* 61: 1-117.

7. Bhojwani, D., and C.-H. Pui. 2013. Relapsed childhood acute lymphoblastic leukaemia. *The lancet oncology* 14: e205-e217.

8. Peled, A., I. Petit, O. Kollet, M. Magid, T. Ponomaryov, T. Byk, A. Nagler, H. Ben-Hur, A. Many, L. Shultz, O. Lider, R. Alon, D. Zipori, and T. Lapidot. 1999. Dependence of human stem cell engraftment and repopulation of NOD/SCID mice on CXCR4. *Science (New York, N.Y.)* 283: 845-848.

9. Bleul, C. C., R. C. Fuhlbrigge, J. M. Casasnovas, A. Aiuti, and T. A. Springer. 1996. A highly efficacious lymphocyte chemoattractant, stromal cell-derived factor 1 (SDF-1). *The Journal of experimental medicine* 184: 1101-1109.

10. Bradstock, K., V. Makrynikola, A. Bianchi, W. Shen, J. Hewson, and D. Gottlieb. 2000. Effects of the chemokine stromal cell-derived factor-1 on the migration and localization of precursor-B acute lymphoblastic leukemia cells within bone marrow stromal layers. *Leukemia* 14: 882-888.

11. Osmond, D., S. Rico‐Vargas, H. Valenzona, L. Fauteux, L. Liu, R. Janani, L. Lu, and K. Jacobsen. 1994. Apoptosis and macrophage‐mediated cell deletion in the regulation of B lymphopoiesis in mouse bone marrow. *Immunological reviews* 142: 209-230.

12. Witte, P. L., M. Robinson, A. Henley, M. G. Low, D. L. Stiers, S. Perkins, R. A. Fleischman, and P. W. Kincade. 1987. Relationships between B‐lineage lymphocytes and stromal cells in long‐term bone marrow cultures. *European journal of immunology* 17: 1473-1484.

13. Manabe, A., E. Coustan-Smith, F. G. Behm, S. C. Raimondi, and D. Campana. 1992. Bone marrow-derived stromal cells prevent apoptotic cell death in B-lineage acute lymphoblastic leukemia. *Blood* 79: 2370-2377.

14. Brüggemann, M., T. Raff, and M. Kneba. 2012. Has MRD monitoring superseded other prognostic factors in adult ALL? *Blood* 120: 4470-4481.

15. Burger, J. A., and A. Burkle. 2007. The CXCR4 chemokine receptor in acute and chronic leukaemia: a marrow homing receptor and potential therapeutic target. *British journal of haematology* 137: 288-296.

16. Ma, Q., D. Jones, P. R. Borghesani, R. A. Segal, T. Nagasawa, T. Kishimoto, R. T. Bronson, and T. A. Springer. 1998. Impaired B-lymphopoiesis, myelopoiesis, and

derailed cerebellar neuron migration in CXCR4- and SDF-1-deficient mice. *Proceedings of the National Academy of Sciences of the United States of America* 95: 9448-9453.

17. Nagasawa, T., S. Hirota, K. Tachibana, N. Takakura, S.-i. Nishikawa, Y. Kitamura, N. Yoshida, H. Kikutani, and T. Kishimoto. 1996. Defects of B-cell lymphopoiesis and bone-marrow myelopoiesis in mice lacking the CXC chemokine PBSF/SDF-1.

18. Nagasawa, T. 2006. Microenvironmental niches in the bone marrow required for B-cell development. *Nature Reviews Immunology* 6: 107-116.

19. Ma, Q., D. Jones, and T. A. Springer. 1999. The chemokine receptor CXCR4 is required for the retention of B lineage and granulocytic precursors within the bone marrow microenvironment. *Immunity* 10: 463-471.

20. Sugiyama, T., H. Kohara, M. Noda, and T. Nagasawa. 2006. Maintenance of the hematopoietic stem cell pool by CXCL12-CXCR4 chemokine signaling in bone marrow stromal cell niches. *Immunity* 25: 977-988.

21. Bradstock, K. F., V. Makrynikola, A. Bianchi, W. Shen, J. Hewson, and D. J. Gottlieb. 2000. Effects of the chemokine stromal cell-derived factor-1 on the migration and localization of precursor-B acute lymphoblastic leukemia cells within bone marrow stromal layers [In Process Citation]. *Leukemia* 14: 882-888.

22. Spiegel, A., O. Kollet, A. Peled, L. Abel, A. Nagler, B. Bielorai, G. Rechavi, J. Vormoor, and T. Lapidot. 2004. Unique SDF-1-induced activation of human precursor-B ALL cells as a result of altered CXCR4 expression and signaling. *Blood* 103: 2900-2907.

23. Sipkins, D. A., X. Wei, J. W. Wu, J. M. Runnels, D. Cote, T. K. Means, A. D. Luster, D. T. Scadden, and C. P. Lin. 2005. In vivo imaging of specialized bone marrow endothelial microdomains for tumour engraftment. *Nature* 435: 969-973.

24. Conter, V., C. R. Bartram, M. G. Valsecchi, A. Schrauder, R. Panzer-Grumayer, A. Moricke, M. Arico, M. Zimmermann, G. Mann, G. De Rossi, M. Stanulla, F. Locatelli, G. Basso, F. Niggli, E. Barisone, G. Henze, W. D. Ludwig, O. A. Haas, G. Cazzaniga, R. Koehler, D. Silvestri, J. Bradtke, R. Parasole, R. Beier, J. J. van Dongen, A. Biondi, and M. Schrappe. 2010. Molecular response to treatment redefines all prognostic factors in children and adolescents with B-cell precursor acute lymphoblastic leukemia: results in 3184 patients of the AIEOP-BFM ALL 2000 study. *Blood* 115: 3206-3214.

25. Shen, W., L. J. Bendall, D. J. Gottlieb, and K. F. Bradstock. 2001. The chemokine receptor CXCR4 enhances integrin-mediated in vitro adhesion and facilitates engraftment of leukemic precursor-B cells in the bone marrow. *Experimental hematology* 29: 1439-1447.

26. Burger, J. A., A. Spoo, A. Dwenger, M. Burger, and D. Behringer. 2003. CXCR4 chemokine receptors (CD184) and alpha4beta1 integrins mediate spontaneous migration of human CD34+ progenitors and acute myeloid leukaemia cells beneath marrow stromal cells (pseudoemperipolesis). *British journal of haematology* 122: 579-589.

27. Burger, J. A., M. Burger, and T. J. Kipps. 1999. Chronic lymphocytic leukemia B cells express functional CXCR4 chemokine receptors that mediate spontaneous migration beneath bone marrow stromal cells. *Blood* 94: 3658-3667.

28. Filshie, R., D. Gottlieb, and K. Bradstock. 1998. VLA‐4 is involved in the engraftment of the human pre‐B acute lymphoblastic leukaemia cell line NALM‐6 in SCID mice. *British journal of haematology* 102: 1292-1300.

29. Corcione, A., N. Arduino, E. Ferretti, A. Pistorio, M. Spinelli, L. Ottonello, F. Dallegri, G. Basso, and V. Pistoia. 2006. Chemokine receptor expression and function in childhood acute lymphoblastic leukemia of B-lineage. *Leukemia research* 30: 365-372.

30. Bendall, L. J., R. Baraz, J. Juarez, W. Shen, and K. F. Bradstock. 2005. Defective p38 mitogen-activated protein kinase signaling impairs chemotaxic but not proliferative responses to stromal-derived factor-1alpha in acute lymphoblastic leukemia. *Cancer research* 65: 3290-3298.

31. Juarez, J., K. F. Bradstock, D. J. Gottlieb, and L. J. Bendall. 2003. Effects of inhibitors of the chemokine receptor CXCR4 on acute lymphoblastic leukemia cells in vitro. *Leukemia* 17: 1294-1300.

32. Caruz, A., M. Samsom, J. M. Alonso, J. Alcami, F. Baleux, J. L. Virelizier, M. Parmentier, and F. Arenzana-Seisdedos. 1998. Genomic organization and promoter characterization of human CXCR4 gene. *FEBS letters* 426: 271-278.

33. Loetscher, M., T. Geiser, T. O'Reilly, R. Zwahlen, M. Baggiolini, and B. Moser. 1994. Cloning of a human seven-transmembrane domain receptor, LESTR, that is highly expressed in leukocytes. *The Journal of biological chemistry* 269: 232-237.

34. Feng, Y., C. C. Broder, P. E. Kennedy, and E. A. Berger. 1996. HIV-1 entry cofactor: functional cDNA cloning of a seven-transmembrane, G protein-coupled receptor. *Science (New York, N.Y.)* 272: 872-877.

35. De Clercq, E. 2003. The bicyclam AMD3100 story. *Nature reviews. Drug discovery* 2: 581-587.

36. Crump, M. P., J. H. Gong, P. Loetscher, K. Rajarathnam, A. Amara, F. Arenzana‐Seisdedos, J. L. Virelizier, M. Baggiolini, B. D. Sykes, and I. Clark‐Lewis. 1997. Solution structure and basis for functional activity of stromal cell‐derived factor‐1; dissociation of CXCR4 activation from binding and inhibition of HIV‐1. *The EMBO journal* 16: 6996-7007.

37. Doranz, B. J., M. J. Orsini, J. D. Turner, T. L. Hoffman, J. F. Berson, J. A. Hoxie, S. C. Peiper, L. F. Brass, and R. W. Doms. 1999. Identification of CXCR4 domains that support coreceptor and chemokine receptor functions. *Journal of virology* 73: 2752-2761.

38. Zlotnik, A., and O. Yoshie. 2000. Chemokines: a new classification system and their role in immunity. *Immunity* 12: 121-127.

39. Nagasawa, T., H. Kikutani, and T. Kishimoto. 1994. Molecular cloning and structure of a pre-B-cell growth-stimulating factor. *Proceedings of the National Academy of Sciences of the United States of America* 91: 2305-2309.

40. Shirozu, M., T. Nakano, J. Inazawa, K. Tashiro, H. Tada, T. Shinohara, and T. Honjo. 1995. Structure and chromosomal localization of the human stromal cell-derived factor 1 (SDF1) gene. *Genomics* 28: 495-500.

41. Yu, L., J. Cecil, S. B. Peng, J. Schrementi, S. Kovacevic, D. Paul, E. W. Su, and J. Wang. 2006. Identification and expression of novel isoforms of human stromal cell-derived factor 1. *Gene* 374: 174-179.

42. D'Apuzzo, M., A. Rolink, M. Loetscher, J. A. Hoxie, I. Clark-Lewis, F. Melchers, M. Baggiolini, and B. Moser. 1997. The chemokine SDF-1, stromal cell-derived factor 1,

attracts early stage B cell precursors via the chemokine receptor CXCR4. *European journal of immunology* 27: 1788-1793.

43. Wright, D. E., E. P. Bowman, A. J. Wagers, E. C. Butcher, and I. L. Weissman. 2002. Hematopoietic stem cells are uniquely selective in their migratory response to chemokines. *The Journal of experimental medicine* 195: 1145-1154.

44. Peled, A., V. Grabovsky, L. Habler, J. Sandbank, F. Arenzana-Seisdedos, I. Petit, H. Ben-Hur, T. Lapidot, and R. Alon. 1999. The chemokine SDF-1 stimulates integrin-mediated arrest of CD34(+) cells on vascular endothelium under shear flow. *The Journal of clinical investigation* 104: 1199-1211.

45. Aiuti, A., I. J. Webb, C. Bleul, T. Springer, and J. C. Gutierrez-Ramos. 1997. The chemokine SDF-1 is a chemoattractant for human CD34+ hematopoietic progenitor cells and provides a new mechanism to explain the mobilization of CD34+ progenitors to peripheral blood. *The Journal of experimental medicine* 185: 111-120.

46. Zou, Y. R., A. H. Kottmann, M. Kuroda, I. Taniuchi, and D. R. Littman. 1998. Function of the chemokine receptor CXCR4 in haematopoiesis and in cerebellar development. *Nature* 393: 595-599.

47. Burns, J. M., B. C. Summers, Y. Wang, A. Melikian, R. Berahovich, Z. Miao, M. E. Penfold, M. J. Sunshine, D. R. Littman, C. J. Kuo, K. Wei, B. E. McMaster, K. Wright, M. C. Howard, and T. J. Schall. 2006. A novel chemokine receptor for SDF-1 and I-TAC involved in cell survival, cell adhesion, and tumor development. *The Journal of experimental medicine* 203: 2201-2213.

48. Balabanian, K., B. Lagane, S. Infantino, K. Y. Chow, J. Harriague, B. Moepps, F. Arenzana-Seisdedos, M. Thelen, and F. Bachelerie. 2005. The chemokine SDF-

1/CXCL12 binds to and signals through the orphan receptor RDC1 in T lymphocytes. *The Journal of biological chemistry* 280: 35760-35766.

49. de Lourdes Perim, A., M. K. Amarante, R. L. Guembarovski, C. E. de Oliveira, and M. A. Watanabe. 2015. CXCL12/CXCR4 axis in the pathogenesis of acute lymphoblastic leukemia (ALL): a possible therapeutic target. *Cellular and molecular life sciences : CMLS* 72: 1715-1723.

50. Busillo, J. M., and J. L. Benovic. 2007. Regulation of CXCR4 signaling. *Biochimica et biophysica acta* 1768: 952-963.

51. Ratajczak, M. Z., E. Zuba-Surma, M. Kucia, R. Reca, W. Wojakowski, and J. Ratajczak. 2006. The pleiotropic effects of the SDF-1-CXCR4 axis in organogenesis, regeneration and tumorigenesis. *Leukemia* 20: 1915-1924.

52. Busillo, J. M., and J. L. Benovic. 2007. Regulation of CXCR4 signaling. *Biochimica et Biophysica Acta (BBA) - Biomembranes* 1768: 952-963.

53. Teicher, B. A., and S. P. Fricker. 2010. CXCL12 (SDF-1)/CXCR4 pathway in cancer. *Clinical cancer research : an official journal of the American Association for Cancer Research* 16: 2927-2931.

54. Shimizu, N., Y. Soda, K. Kanbe, H. Y. Liu, R. Mukai, T. Kitamura, and H. Hoshino. 2000. A putative G protein-coupled receptor, RDC1, is a novel coreceptor for human and simian immunodeficiency viruses. *Journal of virology* 74: 619-626.

55. Wurth, R., A. Bajetto, J. K. Harrison, F. Barbieri, and T. Florio. 2014. CXCL12 Modulation of CXCR4 and CXCR7 activity in human glioblastoma stem-like cells and regulation of the tumor microenvironment. *Frontiers in cellular neuroscience* 8.

56. Shah, N., L. Oseth, and T. W. LeBien. 1998. Development of a model for evaluating the interaction between human pre-B acute lymphoblastic leukemic cells and the bone marrow stromal cell microenvironment. *Blood* 92: 3817-3828.

57. Konoplev, S., J. L. Jorgensen, D. A. Thomas, E. Lin, J. Burger, H. M. Kantarjian, M. Andreeff, L. J. Medeiros, and M. Konopleva. 2011. Phosphorylated CXCR4 is associated with poor survival in adults with B-acute lymphoblastic leukemia. *Cancer* 117: 4689-4695.

58. Crazzolara, R., A. Kreczy, G. Mann, A. Heitger, G. Eibl, F. M. Fink, R. Mohle, and B. Meister. 2001. High expression of the chemokine receptor CXCR4 predicts extramedullary organ infiltration in childhood acute lymphoblastic leukaemia. *British journal of haematology* 115: 545-553.

59. van den Berk, L. C., A. van der Veer, M. E. Willemse, M. J. Theeuwes, M. W. Luijendijk, W. H. Tong, I. M. van der Sluis, R. Pieters, and M. L. den Boer. 2014. Disturbed CXCR4/CXCL12 axis in paediatric precursor B-cell acute lymphoblastic leukaemia. *British journal of haematology* 166: 240-249.

60. Brave, M., A. Farrell, S. Ching Lin, T. Ocheltree, S. Pope Miksinski, S. L. Lee, H. Saber, J. Fourie, C. Tornoe, B. Booth, W. Yuan, K. He, R. Justice, and R. Pazdur. 2010. FDA review summary: Mozobil in combination with granulocyte colony-stimulating factor to mobilize hematopoietic stem cells to the peripheral blood for collection and subsequent autologous transplantation. *Oncology* 78: 282-288.

61. Welschinger, R., F. Liedtke, J. Basnett, A. Dela Pena, J. G. Juarez, K. F. Bradstock, and L. J. Bendall. 2013. Plerixafor (AMD3100) induces prolonged mobilization of acute

lymphoblastic leukemia cells and increases the proportion of cycling cells in the blood in mice. *Experimental hematology* 41: 293-302.e291.

62. Uy, G. L., M. P. Rettig, I. H. Motabi, K. McFarland, K. M. Trinkaus, L. M. Hladnik, S. Kulkarni, C. N. Abboud, A. F. Cashen, K. E. Stockerl-Goldstein, R. Vij, P. Westervelt, and J. F. DiPersio. 2012. A phase 1/2 study of chemosensitization with the CXCR4 antagonist plerixafor in relapsed or refractory acute myeloid leukemia. *Blood* 119: 3917-3924.

63. Broxmeyer, H. E., C. M. Orschell, D. W. Clapp, G. Hangoc, S. Cooper, P. A. Plett, W. C. Liles, X. Li, B. Graham-Evans, T. B. Campbell, G. Calandra, G. Bridger, D. C. Dale, and E. F. Srour. 2005. Rapid mobilization of murine and human hematopoietic stem and progenitor cells with AMD3100, a CXCR4 antagonist. *The Journal of experimental medicine* 201: 1307-1318.

64. Schols, D., J. A. Este, G. Henson, and E. De Clercq. 1997. Bicyclams, a class of potent anti-HIV agents, are targeted at the HIV coreceptor fusin/CXCR-4. *Antiviral research* 35: 147-156.

65. Hatse, S., K. Princen, G. Bridger, E. De Clercq, and D. Schols. 2002. Chemokine receptor inhibition by AMD3100 is strictly confined to CXCR4. *FEBS letters* 527: 255-262.

66. Hendrix, C. W., C. Flexner, R. T. MacFarland, C. Giandomenico, E. J. Fuchs, E. Redpath, G. Bridger, and G. W. Henson. 2000. Pharmacokinetics and safety of AMD-3100, a novel antagonist of the CXCR-4 chemokine receptor, in human volunteers. *Antimicrobial agents and chemotherapy* 44: 1667-1673.

67. Hoellenriegel, J., S. A. Meadows, M. Sivina, W. G. Wierda, H. Kantarjian, M. J. Keating, N. Giese, S. O'Brien, A. Yu, L. L. Miller, B. J. Lannutti, and J. A. Burger. 2011. The

phosphoinositide 3'-kinase delta inhibitor, CAL-101, inhibits B-cell receptor signaling and chemokine networks in chronic lymphocytic leukemia. *Blood* 118: 3603-3612.

68. Charpentier, E., and J. A. Doudna. 2013. Biotechnology: Rewriting a genome. *Nature* 495: 50-51.

69. Nagasawa, T., T. Nakajima, K. Tachibana, H. Iizasa, C. C. Bleul, O. Yoshie, K. Matsushima, N. Yoshida, T. A. Springer, and T. Kishimoto. 1996. Molecular cloning and characterization of a murine pre-B-cell growth-stimulating factor/stromal cell-derived factor 1 receptor, a murine homolog of the human immunodeficiency virus 1 entry coreceptor fusin. *Proceedings of the National Academy of Sciences of the United States of America* 93: 14726-14729.

70. Muller, A., B. Homey, H. Soto, N. Ge, D. Catron, M. E. Buchanan, T. McClanahan, E. Murphy, W. Yuan, S. N. Wagner, J. L. Barrera, A. Mohar, E. Verastegui, and A. Zlotnik. 2001. Involvement of chemokine receptors in breast cancer metastasis. *Nature* 410: 50-56.

71. Villalvilla, A., R. Gomez, J. A. Roman-Blas, R. Largo, and G. Herrero-Beaumont. 2014. SDF-1 signaling: a promising target in rheumatic diseases. *Expert opinion on therapeutic targets* 18: 1077-1087.

72. Al Ustwani, O., R. Kurzrock, and M. Wetzler. 2014. Genetics on a WHIM. *British journal of haematology* 164: 15-23.

73. Bleul, C. C., M. Farzan, H. Choe, C. Parolin, I. Clark-Lewis, J. Sodroski, and T. A. Springer. 1996. The lymphocyte chemoattractant SDF-1 is a ligand for LESTR/fusin and blocks HIV-1 entry.

74. Murakami, T., T. Nakajima, Y. Koyanagi, K. Tachibana, N. Fujii, H. Tamamura, N. Yoshida, M. Waki, A. Matsumoto, O. Yoshie, T. Kishimoto, N. Yamamoto, and T. Nagasawa. 1997. A small molecule CXCR4 inhibitor that blocks T cell line-tropic HIV-1 infection. *The Journal of experimental medicine* 186: 1389-1393.

75. Doranz, B. J., K. Grovit-Ferbas, M. P. Sharron, S. H. Mao, M. B. Goetz, E. S. Daar, R. W. Doms, and W. A. O'Brien. 1997. A small-molecule inhibitor directed against the chemokine receptor CXCR4 prevents its use as an HIV-1 coreceptor. *The Journal of experimental medicine* 186: 1395-1400.

76. Lai, C. Y., S. Yamazaki, M. Okabe, S. Suzuki, Y. Maeyama, Y. Iimura, M. Onodera, S. Kakuta, Y. Iwakura, and M. Nojima. 2014. Stage‐Specific Roles for Cxcr4 Signaling in Murine Hematopoietic Stem/Progenitor Cells in the Process of Bone Marrow Repopulation. *Stem cells (Dayton, Ohio)* 32: 1929-1942.

77. Naumann, U., E. Cameroni, M. Pruenster, H. Mahabaleshwar, E. Raz, H. G. Zerwes, A. Rot, and M. Thelen. 2010. CXCR7 functions as a scavenger for CXCL12 and CXCL11. *PloS one* 5: e9175.

78. Honczarenko, M., R. S. Douglas, C. Mathias, B. Lee, M. Z. Ratajczak, and L. E. Silberstein. 1999. SDF-1 responsiveness does not correlate with CXCR4 expression levels of developing human bone marrow B cells. *Blood* 94: 2990-2998.

79. Tarasova, N. I., R. H. Stauber, and C. J. Michejda. 1998. Spontaneous and ligand-induced trafficking of CXC-chemokine receptor 4. *The Journal of biological chemistry* 273: 15883-15886.

80. Forster, R., E. Kremmer, A. Schubel, D. Breitfeld, A. Kleinschmidt, C. Nerl, G. Bernhardt, and M. Lipp. 1998. Intracellular and surface expression of the HIV-1

coreceptor CXCR4/fusin on various leukocyte subsets: rapid internalization and recycling upon activation. *Journal of immunology (Baltimore, Md. : 1950)* 160: 1522-1531.

81. Zhang, W. B., J. M. Navenot, B. Haribabu, H. Tamamura, K. Hiramatu, A. Omagari, G. Pei, J. P. Manfredi, N. Fujii, J. R. Broach, and S. C. Peiper. 2002. A point mutation that confers constitutive activity to CXCR4 reveals that T140 is an inverse agonist and that AMD3100 and ALX40-4C are weak partial agonists. *The Journal of biological chemistry* 277: 24515-24521.

82. Kuhne, M. R., T. Mulvey, B. Belanger, S. Chen, C. Pan, C. Chong, F. Cao, W. Niekro, T. Kempe, K. A. Henning, L. J. Cohen, A. J. Korman, and P. M. Cardarelli. 2013. BMS-936564/MDX-1338: a fully human anti-CXCR4 antibody induces apoptosis in vitro and shows antitumor activity in vivo in hematologic malignancies. *Clinical cancer research : an official journal of the American Association for Cancer Research* 19: 357-366.

83. Burger, M., T. Hartmann, M. Krome, J. Rawluk, H. Tamamura, N. Fujii, T. J. Kipps, and J. A. Burger. 2005. Small peptide inhibitors of the CXCR4 chemokine receptor (CD184) antagonize the activation, migration, and antiapoptotic responses of CXCL12 in chronic lymphocytic leukemia B cells. *Blood* 106: 1824-1830.

84. Nervi, B., P. Ramirez, M. P. Rettig, G. L. Uy, M. S. Holt, J. K. Ritchey, J. L. Prior, D. Piwnica-Worms, G. Bridger, T. J. Ley, and J. F. DiPersio. 2009. Chemosensitization of acute myeloid leukemia (AML) following mobilization by the CXCR4 antagonist AMD3100. *Blood* 113: 6206-6214.

85. Liles, W. C., H. E. Broxmeyer, E. Rodger, B. Wood, K. Hubel, S. Cooper, G. Hangoc, G. J. Bridger, G. W. Henson, G. Calandra, and D. C. Dale. 2003. Mobilization of

hematopoietic progenitor cells in healthy volunteers by AMD3100, a CXCR4 antagonist. *Blood* 102: 2728-2730.

86. Devine, S. M., N. Flomenberg, D. H. Vesole, J. Liesveld, D. Weisdorf, K. Badel, G. Calandra, and J. F. DiPersio. 2004. Rapid mobilization of CD34+ cells following administration of the CXCR4 antagonist AMD3100 to patients with multiple myeloma and non-Hodgkin's lymphoma. *Journal of clinical oncology : official journal of the American Society of Clinical Oncology* 22: 1095-1102.

87. Infantino, S., B. Moepps, and M. Thelen. 2006. Expression and regulation of the orphan receptor RDC1 and its putative ligand in human dendritic and B cells. *Journal of immunology (Baltimore, Md. : 1950)* 176: 2197-2207.

88. Berahovich, R. D., B. A. Zabel, M. E. Penfold, S. Lewén, Y. Wang, Z. Miao, L. Gan, J. Pereda, J. Dias, and I. I. Slukvin. 2010. CXCR7 protein is not expressed on human or mouse leukocytes. *The Journal of Immunology* 185: 5130-5139.

89. Torossian, F., A. Anginot, A. Chabanon, D. Clay, B. Guerton, C. Desterke, L. Boutin, S. Marullo, M. G. Scott, J. J. Lataillade, and M. C. Le Bousse-Kerdiles. 2014. CXCR7 participates in CXCL12-induced CD34+ cell cycling through beta-arrestin-dependent Akt activation. *Blood* 123: 191-202.

Shubhchintan Randhawa was born in Chandigarh, India on May 29, 1986, the daughter of Rajinder Kaur Dhadda and Jaspinder Singh Randhawa. After completing her high school at Vivek High School, Chandigarh, India in 2004, she entered University of Hertfordshire in Hatfield, UK. She received the degree of Bachelor of Science (Honors) with a major in biotechnology from Hertfordshire in May, 2008. She entered University of Leicester and received the degree of Master of Science with distinction in the major of Cancer Cell & Molecular Biology. In May of 2010 she entered The University of Texas Graduate School of Biomedical Sciences at Houston.

Permanent address:

14851 Fir Knoll Way

Cypress, Texas 77429